

https://dspace.org/

A proxy precipitation record for the Central Namib Desert using 13C analysis on Acacia erioloba

Mac Conachie, Kayla Storm

2022
https://hdl.handle.net/10539/36971

Downloaded from a DSpace repository. https://dspace.org/



University of the Witwatersrand

School of Geography, Archaeology and Environmental Studies

A proxy precipitation record for the Central Namib Desert using $\delta^{13}C$ analysis on *Acacia erioloba*

A dissertation submitted to the Faculty of Science, University of the Witwatersrand, Johannesburg, in fulfilment of the requirements for the degree of Master of Science.

Kayla Storm Mac Conachie

723404

August 2022

DECLARATION

I declare that this thesis is my own, unaided work, unless where specified otherwise. It is being submitted for the Degree of Master of Science at the University of the Witwatersrand, Johannesburg. It has not been submitted before for any degree or examination at any other University.



Kayla Storm Mac Conachie

1st day of August 2022

Abstract

Namibia is one of the most arid countries in sub-Saharan Africa and aridity in the region is being exacerbated by climate change. Past climate reconstructions allow for deductions to be made regarding climate patterns and cycles; this facilitates more accurate future climate projections. There are few reliable meteorological or historical climate records for Namibia. While some long-term palaeoclimate records have been produced from proxies such as speleothems and hyrax middens, these offer relatively coarse temporal resolution. Dendroclimatological investigations can produce high-resolution palaeoclimate reconstructions, with precise radiocarbon dating. Therefore, a very high level of calibration between tree rings and climatic data can be achieved. This research project uses the stable-carbon isotope approach and ^{14}C dating on two *Acacia* (*Vachellia*) *erioloba* trees, (namely Husab-1 and 2) to test whether a proxy precipitation chronology for the Erongo region in central Namibia could be produced. Radiocarbon dates on the trees indicate that Husab-1 and 2 grew during the Little Ice Age (LIA) and the beginning of the modern era until the mid-20th Century CE. $\delta^{13}C$ analyses suggest that there was marked rainfall variability during this period, which is consistent with other palaeoenvironmental research for the Namib region, and other regions within the Summer Rainfall Zone (SRZ) of southern Africa. Although errors in the age model resulted in inaccuracies, a proxy precipitation record was produced. Comparisons between the Husab chronology and paleoenvironmental records, such as the Dante Cave speleothem records, and slack water deposits found along the Khan River, highlighted climatic variability within Namibia during the LIA. Furthermore, statistically significant relationships between Sea Surface Temperature (SST) anomalies, the Southern Annular Mode (SAM), and the proxy precipitation chronology indicate that these may have been key drivers for precipitation variability in the central Namib Desert during the past 600 years.

Acknowledgements

This research project is dedicated to my father Gary Mac Conachie, and my stepfather Mardo Maguire who sadly passed away during my Master of Science degree.

Dad, without you I would not have chosen the path that led me to pursue this degree. It was your love for nature, geography and wildlife that sparked my passion, and I hope that I made you proud. You are forever in my heart; I love you so much and miss you, always.

Mards, you were always there when I needed anything! Thank you for always taking care of me and my mom and thank you for loving me as if I was your own daughter. You are so loved and fiercely missed every day.

First and foremost, huge thanks must go to my supervisors Prof. Stephan Woodborne and Prof. Jennifer Fitchett. Stephan, thank you for your expertise and guidance in a field in which I had no previous experience. Thank you for allowing me to use your tree samples and for making this project a reality. Jen, without your encouragement, understanding and patience I would definitely not have made it this far! You put the 'super' in supervisor. I appreciate you more than you could ever know.

Thank you to the NRF for awarding me the DST-NRF innovation master's scholarship that provided the funding for this research project. Thanks also to the University of the Witwatersrand Postgraduate Merit Award, and later the Writing Fellowship, for further funding my studies.

Thanks must go to iThemba LABS for all radiocarbon analyses, and use of their laboratory facilities and equipment. Thank you to Dr. Grant Hall and the University of

Pretoria Mammal Research Institute for guiding me and allowing me to use the lab facilities and equipment needed for various stages of this project. Thanks also to the Rössing Uranium Mine for kindly sharing their rainfall data from Pointbill station for use in this project.

Thank you to all my friends and family who have assisted me in one way or another during this journey. Julia, thank you for all the zoom calls and assistance that you gave me all the way from the Northern Hemisphere. Your knowledge of QGIS was extremely valuable, and I would not have been able to complete this dissertation without your help, encouragement, and your amazing friendship.

Nicole Robertson, thank you for your invaluable lab assistance, sample preparation, endless weighing and, of course, your company and counsel during the last two years. Kiah, your willingness to help me get through the last few months means more to me than you know! Thank you for being there for me and helping me find the willpower to make it to the finish line.

Mom, you have been my rock and my pillar of strength throughout this journey and my life. Thank you for raising me to be the strong and capable person that I have become. Without you, I would not have overcome the many obstacles along my path. Your love and guidance have led me to this moment, and I am eternally grateful for you. Love you!

Last but certainly not least, to my partner, Chris, thank you for being patient with me throughout this journey, for the endless cups of coffee, and always coming to the rescue when something (inevitably) goes wrong with my PC. Thanks for putting up with the extremely stressed, emotional, and anxious version of me for the past two years. I’m so looking forward to the next chapter of my life with you.

Table of Contents

Abstract iii

Acknowledgements iv

Table of Contents vi

List of Figures x

List of Tables xv

List of Acronyms xvi

CHAPTER 1: INTRODUCTION 1

1.1 Background 1

1.2 Rationale 6

1.3 Aims and Objectives 7

1.4 Structure of dissertation 7

CHAPTER 2: LITERATURE REVIEW 10

2.1 Introduction 10

2.2 Background to palaeoclimatic resources in southern Africa 12

2.3 Dendroclimatology 14

2.3.1 Global developments 14

2.3.2 Key issues and debates 23

2.4 Dendroclimatological research in southern Africa 25

2.5 Palaeoenvironmental research in southern Africa 29

2.6 Palaeoclimate research in the Namib Desert 33

2.7 Summary of climate variability over the past millennium in Namibia 35
2.8 Conclusions 36
CHAPTER 3: STUDY SITE 38
3.1 Environmental Setting 38
3.2 Climate 39
3.3 Geomorphology 45
3.4 Flora and Fauna 47
3.5 Conclusion 53
CHAPTER 4: MATERIALS AND METHODS 54
4.1 Introduction 54
4.2 Acquisition of tree specimens 56
4.3 Sampling and subsampling 56
4.4 Sample preparation 58
4.4.1 Soxhlet extraction process 58
4.4.2 α-cellulose reduction process: 60
4.4.3 Weighing samples 62
4.5 Stable carbon isotope analysis 63
4.6 AMS radiocarbon dating 64
4.7 Corrections 65
4.8 Contemporary meteorological data 65
4.9 Statistical analyses 66
CHAPTER 5: RESULTS 68
5.1 Introduction 68

5.2 Radiocarbon dates 68
5.2.1 Husab-1 68
5.2.2 Husab-2 69
5.3 Age model 70
5.4 Age constrained stable carbon isotope analysis 73
5.5 Meteorological data 78
5.6 Comparisons between the tree record and climate forcing 82
5.6.1 Southern Oscillation Index 82
5.6.2 Indian Ocean Dipole 83
5.6.3 Southern Annular Mode 84
5.6.4 Sea Surface Temperatures 85
5.7 Conclusion 86
CHAPTER 6: DISCUSSION 87
6.1 Introduction 87
6.2 Climate during the last millennium in Namibia 88
6.3 Climate during the last millennium in southern Africa 95
6.4 Long term dendroclimatic studies in southern Africa 99
6.5 The Husab isotopic time series 101
6.6 Synoptic Drivers 106
6.7 Climate Forcing and the Husab isotope record 109
6.8 Limitations 115
6.8.1 Sampling technique 115
6.8.2 Errors in the radiocarbon dates 116
6.8.3 Comparisons to meteorological data 117
CHAPTER 7: CONCLUSIONS 118

7.1 Introduction 118

7.2 Synthesis 118

7.3 Achievement of study aims 119

7.4 Directions for future work 122

REFERENCES 123

APPENDICES I

8 APPENDIX 1: HUSAB-1 ISOTOPE DATA I

9 APPENDIX 2: HUSAB-2 ISOTOPE DATA II

List of Figures

Figure 1: Fractionation in trees (own figure). 5

Figure 2: Köppen-Geiger Climate classification maps for Southern Africa (a) 1980-2016, and (b) 2071-2100 (Beck *et al*., 2018). 11

Figure 3: Graph indicating the number of publications over time (1980-2019) which use specific keywords related to dendrochronology (Pearl *et al*., 2020: 3). 16

Figure 4: Locations and number of published tree ring chronologies over the period 60-year period 1960-2019. Points represent ITRDB (International Tree-Ring Data Bank) sites collected in each 20-year period. Shaded areas represent the number of publications per country in each 20-year period determined by the authors' affiliated institution (Pearl *et al*., 2020: 925). 17

Figure 5: Trends in carbon isotope research derived from a search for ("tree rings" AND "carbon isotopes") in the title, abstract, or keywords of scientific literature using Scopus (Shestakova and Martinez-Sancho, 2021: 2). 21

Figure 6:The number of, and different kinds of proxies used in published Quaternary palaeoenvironmental studies for southern Africa from 1950-2017 (Knight and Fitchett, 2019: 39). 30

Figure 7:Spatial extent of published palaeoenvironmental studies in southern Africa (adapted from Fitchett *et al*., 2017: 281). 31

Figure 8: Map showing locations of dendroclimatic and dendrochronological studies in southern Africa and Namibia (Own figure). 35

Figure 9: The African continent, indicating the location of Namibia and the location of study site:22°34'24.20"S, 15°0'21.42"E (Data source: Atlas of Namibia Project, 2002). 39

Figure 10: Average annual rainfall in Central Namibia (Data source: Atlas of Namibia Project, 2002). 41
Figure 11: (A) Southern African synoptics which promote rainfall in Namibia: Angola Low (AL), Coastal Low (CL), Cold Front (CF), Intertropical Convergence Zone (ITCZ), Tropical Temperate Trough (TTT), West Coast Trough (WCT), Westerly Wave Low (WWL), Zaire/Congo Air Boundary (ZAB) and the major pressure systems: Continental High Pressure (CHP), South Atlantic High pressure (SAHP), and the South Indian Ocean High Pressure (SIPH). (B) The Namibian Coastline (Eckardt *et al*., 2013: 2). 42
Figure 12: Approximate number of fog days in Central Namibia (Data source: Atlas of Namibia Project, 2002). 44
Figure 13: Average annual temperatures in Central Namibia (Data source; Atlas of Namibia Project, 2002). 45
Figure 14: Surface geological map with study site marked as a yellow star (Chudasama *et al*., 2019: 16). 47
Figure 15: Natural regions of Namibia (Info-Namibia, 2021). 48
Figure 16: Biomes of Namibia (a) adapted from Irish (1994: 553) and (b) adapted from Mendelsohn *et al*. (2002: 98). 49
Figure 17: The main controls on carbon isotope fractionation (McCarroll and Loader, 2004: 774). 55
Figure 18: Radial sections Husab-1 and 2 (own photo). 57
Figure 19a (left) and b (right): indicating the sub-sampling process (own photo). 57
Figure 20: A close-up of the radial section of Husab-2 (own photo). 57
Figure 21: Showing specialised test tubes and carousel used in the Soxhlet extraction process (own photo). 58

Figure 22: Diagram of the Soxhlet extractor setup microbalance housed at the University of Pretoria Stable isotope laboratory, Mammal research institute (own photo). 59
Figure 23: Photo of the samples in water bath during the α-cellulose reduction process (own photo). 60
Figure 24: (a) and (b) illustrating samples in the process of α-cellulose reduction and (c) when the process was complete (own photos). 61
Figure 25: The Mettler Toledo microbalance housed at the University of Pretoria Stable isotope laboratory, Mammal research institute (Robertson, 2021). 62
Figure 26: (a) indicating the tin capsule used for weighing, and (b) after it is moulded into a ball (own photos). 63
Figure 27: (a) The CHNSO 1100 series elemental analyser and (b) Delta-V stable light isotope mass spectrometer (Robertson, 2021). 64
Figure 28: Calibrated intercept ranges (1-sigma) (Tables 6 and 7) are represented as the purple and green vertical bands. The thin horizontal lines of the same colours represent the age model, which is a linear relationship between sample number and calendar age commencing with '0' representing the bark of the tree. Husab-1 is represented in purple, and Husab-2 is represented in green. 72
Figure 29: $\delta^{13}C$ (‰ VPDB) isotopic time series for Husab-1(purple) and Husab-2 (green) representing a proxy rainfall scale with wetter periods at the top and drier periods at the bottom of the graph. 75
Figure 30: Relatively wet and dry years for Husab-1 (purple) and Husab-2 (green) between ~1400 and ~1970 cal yr CE. Wet years are above, and dry years are represented below the axis line. 78

Figure 31: Composite Figure including rainfall data from the CHIRPS PENTAD gridded dataset (blue bars) and the Pointbill Station dataset (green bars) at the bottom with SAM (Orange), IOD (Blue), SOI (Yellow), and SST (Green) graphs for the period 1980-2020. 81

Figure 32: Comparison between $\delta^{13}C$ isotope values and the SOI (1871-1974) with $\delta^{13}C$ in blue and SOI in green. 82

Figure 33: Comparison between $\delta^{13}C$ and the IOD (1870-1974) with $\delta^{13}C$ in blue and IOD in red. 83

Figure 34: Comparison between $\delta^{13}C$ and the SAM index (1460-1974) with $\delta^{13}C$ in blue and SAM in purple. 84

Figure 35: Comparison between $\delta^{13}C$ and SST anomalies (1665-1974) with $\delta^{13}C$ in blue and SST in orange. 85

Figure 36: Slack water deposits which occurred during the LIA (Heine and Völkel 2011: 11). 91

Figure 37: Historical precipitation data compiled by Grodek *et al*. (2020). Wet periods are indicated by the blue bars (3= extremely wet) and dry periods are in orange (-3 = extremely dry). The green line represents rainfall (mm) for Windhoek (Ministry of Agriculture, Water and Forestry, (MAWF), Namibia) (Adapted from Grodek *et al*., 2020). 94

Figure 38: Palaeoclimate reconstruction for the SRZW and SRZE, blue indicates wetter conditions while yellow represents drier conditions (above or below the mean) for the period 1500-1900 (Hannaford and Beck, 2021: 15). 96

Figure 39: Annually resolved rainfall reconstructions for southern Africa SRZ (1850-1900) (Nash *et al*., 2019: 469). 97

Figure 40: Comparison between Husab-1 (blue line), Husab-2 (green line) and the DP1 speleothem record with $\delta^{18}O$ in red and $\delta^{13}C$ in black (Voarintsoa *et al*., 2017). 102

Figure 41: Comparison between Windhoek rainfall (mm) in grey (adapted from Grodek *et al*., 2020; MAWF) and Husab-1 (blue) and Husab-2 (green) isotope record between 1835-2015. 105

Figure 42: Synoptic climate systems of southern Africa (Saarinen *et al*., 2022: 17). 107

Figure 43: Composite figure showing the SAM index (purple), SST anomaly (orange) and Husab isotope record (Here Husab 1 and 2 were averaged to form one record) (dark blue). 111

List of Tables

Table 1: Early dendrochronological research (Adapted from Speer, 2010: 30-31). .. 15

Table 2: Tree species used in dendroclimatic reconstructions in southern Africa 29

Table 3:Dendrochronological studies from Namibia (adapted from Shikangalah, 2020: 0195-0196). 34

Table 4: Vegetation types in Namibia (adapted from Mendelsohn *et al*., 2002: 99).. 50

Table 5: Endemic plant species found within the project area of the Rössing uranium mine recorded 2003-2006. Endemism rating: '3' means that it is only found in central Namib, '2' if the plant is found in the central Namib and one other region, and '1' if the plant is also found in several other regions in Namibia (Pallet *et al*., 2008, Appendix F) 51

Table 6: AMS radiocarbon dates for Husab-1 and associated calibrated calendar dates (* asterisk symbol indicates pMC value)..... 69

Table 7: AMS radiocarbon dates for Husab-2 and associated calibrated calendar dates (* asterisk symbol indicates pMC value)..... 70

Table 8: List of approximate relatively wet and dry years according to rainfall proxy for Husab-1 and 2 (extremely dry years are noted with an Asterix*)..... 77

Table 9: Summary of Spearman's Rank Correlation analyses for rainfall data for the study site and forcing datasets (see chapter 4, section 4.9 for datasets used). 80

Table 10: Wet and dry periods (Grab and Zumturn, 2018) and flood years identified by Stengel (1964) for Namibia. 93

List of Acronyms

ABF	Angola Benguela Front
AL	Angola Low
AMC	Abbabis Metamorphic Complex
AMS	Accelerator Mass Spectrometry
CAB	Congo Air Boundary
Catm	Concentration of CO2 in the atmosphere
CF	Cold Front
CHIRPS	Climate Hazards Group InfraRed Precipitation with Station data
CHP	Central High Pressure
Ci	The intrinsic concentration of CO2 within plant cells
CL	Coastal Low
CMIP	Coupled Modelling Inter-Comparison Project
COL	Cut off Low
ENSO	El Niño Southern Oscillation
GEE	Google Earth Engine
IOD	Indian Ocean Dipole
ITCZ	Intertropical Convergence Zone
ITRDB	International Tree-Ring Data Bank
LIA	Little Ice Age
LTRR	The University of Arizona Laboratory of Tree Ring Research
MAWF	Ministry of Agriculture, Water and Forestry
MCA	Medieval Climate Anomaly
MLC	Mid-latitude Cyclone
pMC	Percent Modern Carbon
PMIP	Palaeoclimate Modelling Inter-Comparison Project
RUBISCO	Ribulose-1,5-bisphosphate carboxylase-oxygenase
SAHP	South Atlantic High Pressure
SAM	Southern Annular Mode
SIHP	South Indian High Pressure
SOI	Southern Oscillation Index
SRZ	Summer Rainfall Zone
SRZE	Summer Rainfall Zone East
SRZW	Summer Rainfall Zone West
SST	Sea Surface Temperatures
TRWI	Tree Ring Width Index
TTT	Tropical Temperate Trough
VPDB	Vienna-Pee Dee Belemnite
WCT	West Coast Trough
WRZ	Winter Rainfall Zone
WWL	Westerly Wave Low
ZAB	Zaire Aire Boundary

CHAPTER 1: INTRODUCTION

1.1 Background

Changes in the southern African hydroclimate, and resultant impacts on water availability, are of key concern to ecosystems, water accessibility and the economy under climate change (Nhemachena *et al*., 2020). Droughts and extreme climatic events can have devastating environmental, economic, and social consequences (Inman *et al*., 2020). Under future climate projections, Namibia is projected to become hotter and drier, with increased rainfall variability (Angula and Kaundjua, 2016; IPCC, 2021). The vulnerability of the country to water stress is likely to increase (Spear *et al*., 2018) and changes in the climate will adversely impact agricultural yields, resulting in decreased household food security and increased poverty (Angula and Kaundjua, 2016). More research into the nature and rate of climate change in Namibia is required to facilitate improved adaptive and risk management strategies for the country (Reid *et al*., 2008; Shikangalah, 2020). This chapter highlights the need for palaeoclimate research in the central Namib Desert, related to the paucity of published high-resolution palaeoclimate research in the region, and it presents an overview of the background and context in which this research project is situated.

Namibia is one of the most arid countries in sub-Saharan Africa and the aridity in the region is exacerbated by climate change (Reid *et al*., 2007, 2008). Water is a fundamental resource for arid regions, even without climate change (Macdonald *et al*., 2009; Inman *et al*., 2020). Namibia has a strong reliance on groundwater, with 45% of the water budget being used for irrigation purposes in agriculture (Spear *et al*., 2018).

As temperatures are projected to increase with reduced precipitation and increased evaporation (Angula and Kaundjua, 2016), groundwater recharge will be reduced,

possibly by up to 70% (Spear *et al*., 2018). These factors raise the question of sustainability in desert towns (Angula and Kaundjua, 2016). Past climate reconstructions allow deductions to be made regarding climate patterns and cycles; this facilitates more accurate future climate projections (Archer *et al*., 2019).

Understanding palaeoclimatic variability is important as it allows present and future climate trends to be modelled (Jones *et al*., 2001). Woodborne *et al*. (2016) argue that there are insufficient climate records in southern Africa, that are adequately resolved temporally and spatially for this purpose. This has hindered the ability to fully understand synoptic shifts resulting from long-term climate forcing in southern Africa (Woodborne *et al*., 2016). The accuracy of model projections can be assessed by verifying how well they can construct a known trajectory (Hall *et al*., 2009). Models that perform well for contemporary climate projections may produce varying results in comparison to future changes in forcing (Braconnot *et al*., 2012). It then becomes imperative to assess, benchmark and hindcast climate models through a comparison between simulations of past climates and other palaeoenvironmental reconstructions (Braconnot *et al*., 2012). Compiling accurate palaeoclimate proxies is important for evaluating climate models and bridging the gap between paleoclimate records and historical climate data (Hall *et al*., 2009, Braconnot *et al*., 2012, Taylor *et al*., 2012). Thus, there is a need for longer-term palaeoenvironmental records that extend beyond the instrumental climate record. Accurately forecasting climate is crucial for mitigating the impacts of future climate change and implementing appropriate measures to reduce strain on the economy and agriculture (Jones *et al*., 2001).

Dendrochronology and dendroclimatology have potential in the validation of climate models in southern Africa (Fitchett *et al*., 2017; Pearl *et al*., 2020). Dendrochronology

is broadly defined as “the science of dating tree rings” (Kaennel and Schweingruber,1995: 65) while dendroclimatology utilizes “dated tree rings to reconstruct and study past and present climates” (Kaennel and Schweingruber,1995: 67). Dendroclimatological and other palaeoenvironmental research could strengthen the ability of climate models to accurately simulate scenarios (Fitchett *et al*., 2017; Pearl *et al*., 2020).

Climate research projects such as the Coupled Model Inter-Comparison Project (CMIP) have generated a multi-model dataset that is intended to improve knowledge of climate changes and climate variability and aims to facilitate an enhanced understanding of past and future climate changes in a multi-model context (Taylor *et al*., 2012). The CMIP process and products are an important and valuable source of high-quality climate data (Emori, *et al*., 2016). Additionally, the Palaeoclimate Modelling Inter-Comparison Project (PMIP), which is in its second phase, uses palaeodata to assess model performance, and test their sensitivity to changes in atmospheric composition (Braconnot *et al*., 2012). Data from this dissertation will add to the growing paleoenvironmental research base for Namibia and through projects such as PMIP, may be useful in improving climate models and facilitating an assessment of socio-environmental implications of climate change (Emori, *et al*., 2016).

Namibia’s extremely dry climate with unpredictable water inputs and high rates of evaporation mean that only highly adapted species are able to survive and flourish in the harsh environment (Lovegrove, 1993; Krug, 2017). Although some tree species have adapted to Namibia’s aridity, dendrochronological and dendroclimatological studies remain overlooked in the region (Shikangalah, 2020). In areas that lack clear

seasonality, such as Namibia, trees are prone to indistinct and non-annual rings (Worbes, 2002). This was previously a major hindrance in the field of dendroclimatology when identifying annual rings was imperative for creating a chronology (Villalba, 2000). However, with the advent of isotope analysis and radiocarbon dating, having identifiable annual rings is no longer necessary for inferring past climate allowing for dendroclimatological records to be generated in regions that lack clear seasonality such as subtropical southern Africa (McCarrolland Loader, 2004). Moreover, with improved methods for sample preparation and analysis, the generation of isotopic ratios from tree rings is becoming more efficient and more affordable (McCarrolland Loader, 2004; Hall *et al*., 2009).

Stable carbon isotopes assimilated into the cellulose of the trees can provide insight into the climatic conditions the tree experienced while growing (Figure 1, McCarrolland Loader, 2004). This occurs during the process of fractionation, in which ^{12}C is preferentially assimilated into leaf sugars with discrimination against ^{13}C due to the enzyme RUBISCO (Ribulose-1,5-bisphosphate carboxylase-oxygenase) (van der Sleen *et al*., 2017). The two stable isotopes are nearly identical except for the slight difference in mass, which allows for discrimination against one of them. This preference/ discrimination is what imparts the environmental signal into the tree ring cellulose (Loader *et al*., 2007). The isotopic ratio of ^{12}C to ^{13}C is represented as $\delta^{13}C$. This value is largely controlled by the C_i/C_a (intercellular Carbon / atmospheric Carbon) ratio (Loader *et al*., 2007). The CO_2 uptake is regulated by water availability due to stomatal conductance during photosynthesis (McCarroll and Loader, 2004; Loader *et al*., 2007).



Figure 1: Fractionation in trees (own figure).

The isotopic composition of CO_2 in the atmosphere has varied over time as a result of industrialisation (Belmecheri and Lavergne, 2020). This has caused the isotopic ratios of organic material to decline which affects the environmental signal (McCarroll *et al*., 2009). The isotopic ratios need to be corrected to a pre-industrial standard to remove the interference from the environmental signal (McCarroll *et al*., 2009).

This research project uses the stable-carbon isotope approach and radiocarbon dating on two *Acacia (Vachellia) erioloba* trees, to produce a high-resolution proxy precipitation record for the Erongo region in central Namibia. It is important to note that the genus *Acacia* underwent a reclassification and retypification, which was

suggested by a group of Australian botanists in 2003. The revision of *Acacia* was permitted to be replaced by the genus name '*Vachellia'* in 2011 at the 17th International Botanical Congress, which took place in Melbourne (Dyer, 2014). However, the tree species is still more commonly known as *Acacia erioloba* as described by E. Mey in 1836 and is thus referred to as such in this dissertation.

1.2 Rationale

There is a necessity for a more in-depth understanding of past climate change in the Namib Desert and Africa as a whole. Dendroclimatic proxies are one of the most useful and pervasive high-resolution stores of climate data (Gagen *et al*., 2010). In addition to traditional tree-ring research, using stable isotope ratios can provide robust climate signals in regions that may be unsuitable for the traditional dendrochronological approach. Moreover, stable isotope approaches allow trees with indistinguishable rings to be analysed and can be used to investigate multiple climate signals (Gagen *et al*., 2010). The use of the stable-carbon isotopes in dendroclimatology has been empirically verified internationally and on a regional and local scale in South Africa (February and Stock, 1999; Norström *et al*., 2005; Hall *et al*., 2008, 2009; Woodborne *et al*., 2015, 2016). Numerous studies have proven a correlation between $\delta^{13}C$ in tree rings and palaeoclimatic variability, including rainfall (Lipp *et al*., 1991; Saurer *et al*., 1995; February and Stock, 1998; Brookes *et al*., 1998; Danis *et al*., 2006; Reynolds-Henne *et al*., 2007; Liu *et al*., 2007; Hall *et al*., 2009; Fichtler *et al*., 2010; Kress *et al*., 2010; Woodborne *et al*., 2015, 2016). Using the stable-carbon isotope approach in tree rings, this research project adds to this strong research thrust by establishing past hydroclimatic variability in the central Namib Desert.

1.3 Aims and Objectives

The aim of this project is to extend knowledge of climate and rainfall variability by constructing a high-resolution hydro-climate record for the central Namib Desert, using stable carbon isotope ($\delta^{13}C$) analysis on two *Acacia erioloba* trees.

Objectives:

1. To determine the age of the *Acacia erioloba* samples by:
    a. Accelerator Mass Spectrometry (AMS) radiocarbon dating on selected samples.
    b. Creating an age model that assigns an age to each sample aliquot by interpolating the 1-sigma ranges of the radiocarbon dates.
2. To reconstruct the growth of the trees through $\delta^{13}C$ analysis on samples throughout the radii to create a stable isotope time series.
3. To test whether the time series represents a proxy for precipitation.
4. To compare the rainfall reconstruction to forcing mechanisms, by evaluating it against:
    a. El Niño Southern Oscillation (ENSO) using the Southern Oscillation Index (SOI) index,
    b. Southern Annular Mode (SAM),
    c. Indian Ocean Dipole (IOD),
    d. Sea Surface Temperature (SST)

1.4 Structure of dissertation

This dissertation will be structured as follows:

Chapter 2: Literature Review

This project is situated in the literature on palaeoclimate research within southern Africa and specifically central Namibia. Key themes that are explored in this chapter include dendroclimatology, the main advances and the key issues and debates in the field. As well as the scope of dendroclimatological studies within southern Africa. Other palaeoenvironmental research in southern Africa is discussed, highlighting the paucity of high-resolution palaeoclimate proxies. The chapter discusses the palaeoclimate research done in Namibia and highlights the need for further research in the region. Finally, the current research gaps in the literature are discussed.

Chapter 3: Study Site

The environmental setting of the research is presented, as well as an overview of the local climate driving forces and synoptic systems of Namibia. The forecast for future climate change is explained as well as the associated environmental and socio-economic impacts. The local geomorphology, flora and fauna of the region are also presented, highlighting the importance of preserving the endemic biodiversity in the region.

Chapter 4: Materials and Methods

The process of acquiring and subsampling the tree specimens, as well as the complex process of sample preparation is detailed in this chapter. This includes the Soxhlet extraction process, the alpha-cellulose reduction, the mass spectrometry isotope analysis and the method for correcting the isotopic record for temporal changes of $\delta^{13}C$ in the atmosphere. This is followed by outlining the process of AMS radiocarbon dating. The use and acquisition of contemporary meteorological records are explained.

Chapter 5: Results

The age model and chronology are presented in this chapter. This underpins the isotope time series. Key wet and dry events within the time period are highlighted.

Chapter 6: Discussion

This chapter presents the interpretation, evaluation, and analysis of the main findings in the research. The palaeoclimate interpretation from the isotope chronology is discussed, followed by examining the synoptic drivers which may have influenced the climate for the research period. Comparisons of the data with SAM, SOI, IOD, and SST are evaluated and discussed. A regional synthesis of central Namibia is presented, and finally, the limitations of the research are discussed.

Chapter 7: Conclusion

A synthesis of the research is presented in the context of the aims and objectives. The chapter explores opportunities for future research.

CHAPTER 2: LITERATURE REVIEW

2.1 Introduction

Southern Africa spans multiple climate belts (tropical, subtropical, and temperate), located at the convergence of the Indian, and Atlantic Oceans (Chase and Meadows, 2007; Fitchett *et al*., 2016). This unique locality results in regions of distinct rainfall seasonality, and subsequently environments that range from hyper-arid to high precipitation across the subcontinent (Nash *et al*., 2016). Due to this climatic diversity, southern Africa has a rich biodiversity, made up of nine different biomes (Finch and Meadows, 2019). Southern Africa is vulnerable to climate change and much of the region is projected to become hotter and drier by the year 2100, especially in the western parts with an expansion of the hot arid desert (bWh Köppen-Geiger climate classification) (Figure 2). For countries vulnerable to climate change, being able to project drought conditions accurately is essential for managing drought risk in the future (Abiodun *et al*., 2019). Understanding and quantifying climate variability for the past two millennia is important for distinguishing between natural climate variability and anthropogenic induced climate variability (Neukom and Gergis, 2012). However, in comparison to the Northern Hemisphere, information regarding past climatic change in the Southern Hemisphere is limited (Neukom and Gergis 2012; Fitchett *et al*., 2017; Grab and Zumthurn 2018). This lack of knowledge results in uncertainty concerning how the southern African sub-continent will respond to global climate change (Fitchett *et al*., 2017). This makes the use of high-resolution palaeoenvironmental proxies to reconstruct past climates more pertinent (Gasse *et al*., 2008; Fitchett *et al*., 2017).

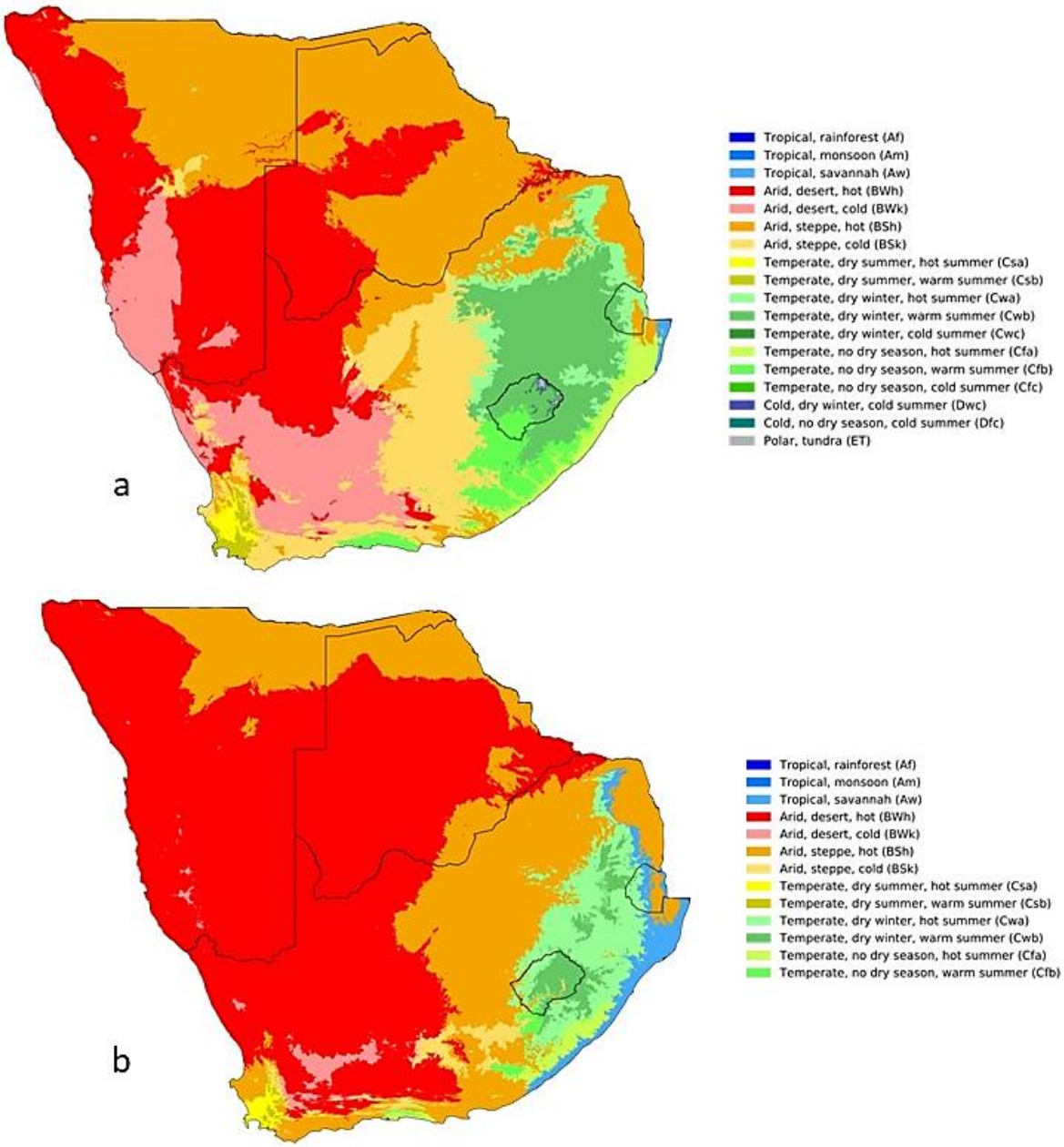


Figure 2: Köppen-Geiger Climate classification maps for Southern Africa (a) 1980-2016, and (b) 2071-2100 (Beck *et al*., 2018).

This chapter explores literature pertaining to dendrochronology, its history, and its development both globally and within southern Africa. The key issues present in the field of dendrochronology are discussed, as well as how limitations, such as inconsistent growth patterns, sampling difficulties, and complex wood anatomy, have

been overcome. Furthermore, the literature surrounding palaeoenvironmental change in southern Africa is explored, specifically focusing on palaeoclimate, historical climate (discerned from historical documents) and as well as meteorological data from recent decades. The use of isotopes as palaeoenvironmental proxies is examined critically. The chapter then provides a synthesis of evidence for past climate change in the hyper-arid Namib Desert identifying the gaps in the literature and opportunities for future research.

2.2 Background to palaeoclimatic resources in southern Africa

There are multiple palaeoclimatic resources that are useful to investigate past climates (Knight and Fitchett, 2019). Palaeoclimate proxies such as pollen records (Scott and Neumann, 2018) and diatoms (Ekblom *et al*., 2012), as well as archives such as speleothems (Braun *et al*., 2020), sediment cores (Humphries *et al*., 2019), and marine cores (Urrego *et al*., 2015; Hahn *et al*., 2018), provide data on long term climatic fluctuations and cyclic variations in climate variables (Knight and Fitchett, 2019). Although annual resolution is rarely achieved (McCarroll and Loader, 2004). Without high-resolution palaeoclimatic data it is difficult to investigate the climate in detail, such as discerning specific drought or flood events throughout time (Grab and Zumthurn, 2018). Many studies use recorded instrumental data, but this information only goes as far back in time as the availability of meteorological instruments within a country (Nash *et al*., 2016). For the most part in southern Africa, *reliable* meteorological observations start in the early 1900s, however, a recent study has slightly extended the record, providing the longest known single station instrumental weather record for the Southern Hemisphere spanning 1834-1899 (Picas *et al*., 2019). Moreover, instrumental records have limited scope for testing future climate responses

highlighting the need for longer high-resolution climate records (Woodborne *et al*., 2016). Historical documents and records can provide high-resolution data, but these datasets are most often short-term and can only provide information from the time when people began recording such information (Nash *et al*, 2016). Historical climate research in southern Africa has focused on the eastern and southern Cape (Vogel, 1989), central southern Africa (Lindesay and Vogel, 1990; Nash and Endfield, 2002), Lesotho (Grab and Nash, 2010; Nash and Grab, 2010), Namaqualand (Kelso and Vogel, 2007, 2015), south-eastern Africa, specifically KwaZulu-Natal and Madagascar (Nash *et al.*, 2015a,b), as well as Angola and Mozambique (Hannaford and Beck, 2021) but spatio-temporal coverage is variable. In between the range of long-term coarse resolution proxies (e.g., ice cores), and short-term meteorological records, there is an information gap, this is where dendroclimatology can be particularly useful, as it can provide long-term chronologies with up to perfect annual resolution (McCarroll and Loader, 2004). Dendroclimatology has been well-established in other parts of the world, especially in the Northern Hemisphere, and is an emerging field in southern Africa (February *et al*., 2003; Norström *et al*., 2005).

Trees provide a record of past environmental changes within their rings, and dendroclimatology uses this climatic information to gain insight into moisture variability, temperature variability, humidity, drought frequency, fires, and even insect damage (Pearl *et al*., 2020). The primary advantage of tree rings is their potential for extremely accurate dating, this means that a very high level of calibration between tree rings and climatic data can be achieved, which is unique amongst natural proxies (McCarroll and Loader, 2004; Jones *et al*., 2009). However, this level of accuracy is restricted to chronologies created using tree rings directly. Using secondary dating methods such as radiocarbon dating can diminish accuracy. It is also possible to

cross-date multiple trees in an area (historical and modern tree ring datasets) and construct extended tree ring chronologies spanning thousands of years (Loader *et al*., 2007). Dendroclimatic research has the potential to bridge the gap by providing high-resolution palaeoclimatic information for southern Africa.

2.3 Dendroclimatology

2.3.1 Global developments

Ferguson (1970: 183) stated that “dendrochronology may be defined as the study of the chronological sequence of annual growth in trees”. Dendroclimatology, a subdivision of dendrochronology, was defined as “dendrochronological studies that use climatic information in dated growth layers to study variability in the present and past climate” (Frits, 1971: 420). These are still valid descriptions of what dendrochronology and dendroclimatology entail and although these definitions describe the core tenets of the fields, they have since been expanded as dendrochronology has grown (Kaennel and Schweingruber, 1995). Research suggests that growth in trees is usually, but not always annual and that in some instances trees may not form a ring in a particular year resulting in missing rings (Hererra-Ramirez *et al*., 2017). In other cases, more than one ring can be found from the same year, referred to as false rings (Worbes, 2002; Rozendaal and Zuidema, 2011; Hererra-Ramirez *et al*., 2017) The definition of dendroclimatology by Frits (1971: 420) uses “dated growth layers”, instead of using the term “annual growth” (Ferguson, 1970: 183), the former highlights the use of carbon dating together with ring counts which may yield a more precise sequence if the date of the outermost ring is not known.

Dendrochronology was pioneered by A.E Douglass in the early 20th Century (Sheppard, 2010). The notion that trees could reflect climatic history was proposed much earlier (see Table 1; Speer, 2010). The potential to cross-date trees was mentioned by Alexander Twining in 1827, but because A.E. Douglass first presented the formal scholarly definition of dendrochronology, he was deemed the founding father of dendrochronology (Berger, 2011). Douglass also established the first research centre dedicated to dendrochronological work in 1937, *The University of Arizona Laboratory of Tree Ring Research (LTRR)* (Speer, 2010). This laboratory has also been crucial in establishing the International Tree-Ring Data Bank (ITRDB) (St. George, 2014). The ITRDB is currently the largest database of tree ring information available to the public (Zhao *et al*., 2019).

Table 1: Early dendrochronological research (Adapted from Speer, 2010: 30-31).

Scientist	**Location**	**Year(s) tree rings were studied**	**Contribution**
Theophrastus	Greece	322 B.C.	Noted that trees have annual growth.
Leonardo da Vinci	Italy	1452-1519	Noted the relationship between climate and tree growth.
		1482-1498	Wrote the *Trattato della Pittura* mentioning tree rings.
Michel de Montaigne	Italy	1581	The idea of counting tree rings to determine age was related to Montaigne by a carpenter.
Duhamel and George Louis Leclerc de Buffon	France	1737	Counted rings to determine the date of a conspicuous frost ring.
Carl Linnaeus	Sweden	1707-1778	Counted rings to determine the age of trees.
A.C. Twinning	Connecticut	1827	Used cross-dating and noted the common signal across a site.
Theodor Hartig	Germany	1837	Set up the ecological basis for dendrochronology in Germany.
Charles Babbage	England	1838	Noted the concepts of competition, complacency, replication, reaction wood in trees, the concept of parent trees, climate reconstruction, and specific tree ring patterns from storms and floods.
Jacob Kuechler	Texas	1859	Used modern principles of site selection by choosing trees on low ridges with good drainage and used tables to note ring characteristics demonstrating an early example of cross-dating.
Robert Hartig	Germany	1867	Used tree rings to date events of hail, frost, insect damage, and examined trees that were likely killed by pollution.
A.L. Child	Nebraska	1871	Compared tree growth in red maple to meteorological data for spring and summer.
A. Stoekhardt	Western Europe	1871	Examined forest damage from air pollution.
Jacobus C. Kapteyn	Denmark	1880-1881	Examined the relationship between tree growth in oaks and rainfall.
F. Shvedov	Ukraine	1892	Examined black locust trees for a dendroclimatic analysis which was used for prediction.
B.E Fernow	New England	1897	Wrote a paper determining the age of blazing on trees by counting rings.
A.E. Douglass	Arizona	1904	Developed cross-dating as a tool and trained future dendrochronologists.
Bruno Huber	Germany	1940	Spent time dating wood samples and developed new statistical techniques to quantify the strength of dating different specimens.

There has been an increase in dendrochronological studies over time, specifically relating to the sub-disciplines of dendroclimatology and dendroarchaeology (Figure 3; Pearl *et al*., 2020). There has also been an increase in the use of stable isotopes in dendroclimatic studies, which uses the carbon, oxygen, or hydrogen isotopes, that assimilated into tree rings, to infer past environments (McCarrolland Loader, 2004; Loader *et al*., 2007; McCarroll*et al*., 2009; Pearl *et al*., 2020; Shestakova and Martinez-Sancho, 2021).

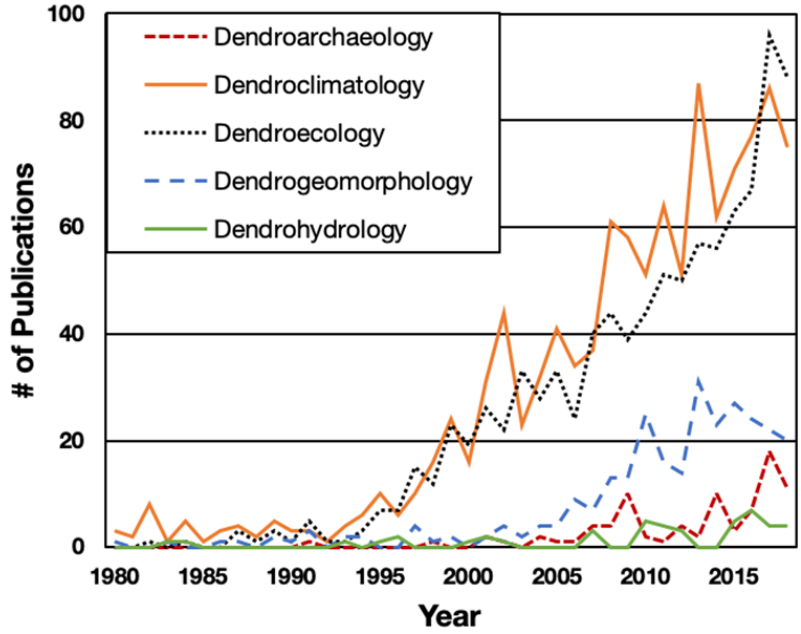


Figure 3: Graph indicating the number of publications over time (1980-2019) which use specific keywords related to dendrochronology (Pearl *et al*., 2020: 3).

Overwhelmingly, the temperate regions in the Northern Hemisphere have received more attention when it comes to dendroclimatic studies in comparison to the tropics and sub-tropics (Norström *et al*., 2005; Rozendaal and Zuidema, 2010; Pearl *et al*., 2020). The main reason is that the application of dendroscience in the tropics and sub-tropics is inherently more complex than in temperate regions (Norström *et al*., 2005). The less distinct seasonality in the tropics and subtropics of the Southern Hemisphere

means that trees are not as likely to produce well-defined annual rings, which is a prerequisite in most dendrochronological studies (Gebrekirstos *et al*., 2014). Even though seasonality and annual rings have been proven to be present in tropical and sub-tropical trees, and dendroclimatic research using tropical tree species is increasing, there is still a large research gap (Rozendaal and Zuidema, 2010; Trouet *et al*., 2010; Neukom and Gergis, 2012; Gebrekirstos *et al*., 2014; Herrera-Ramirez *et al*., 2017). North America and Eurasia have the most published tree ring chronologies while Africa has the least (Figure 4; Pearl *et al*., 2020).

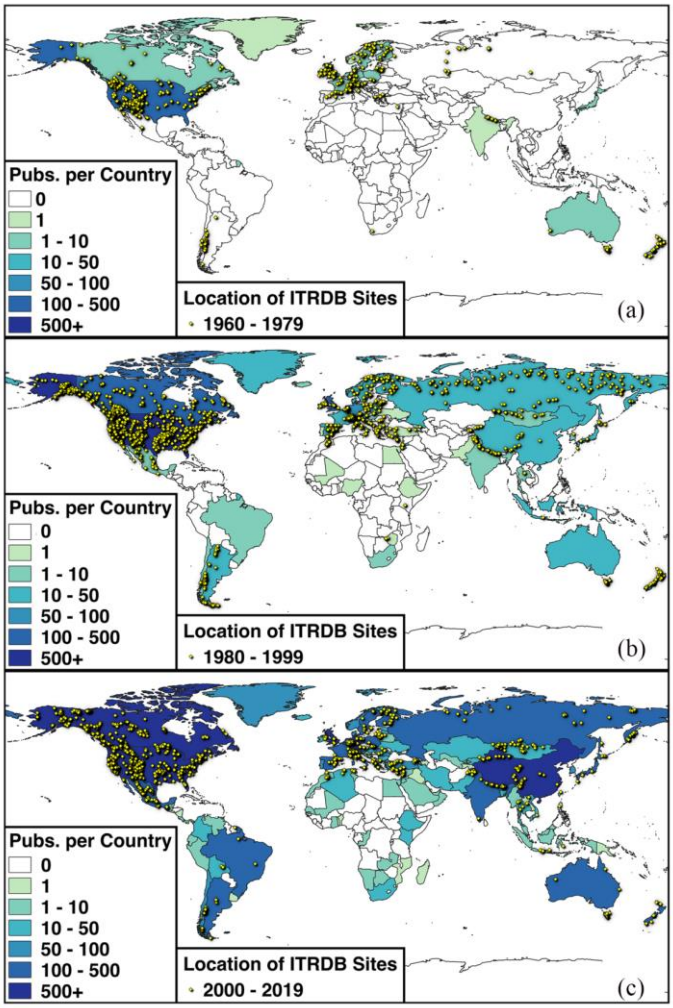


Figure 4: Locations and number of published tree ring chronologies over the period 60-year period 1960-2019. Points represent ITRDB (International Tree-Ring Data Bank) sites collected in each 20-year period. Shaded areas represent the number of publications per country in each 20-year period determined by the authors' affiliated institution (Pearl *et al*., 2020: 925).

The use of ring width and density has been successfully validated as a reliable environmental proxy globally (St. George, 2014). With absolute dating techniques such as ^{14}C radiocarbon, it is possible to cross-date multiple tree ring chronologies and extend tree ring archives by thousands of years (Loader *et al*., 2007). Absolute dating also allows for tree ring chronologies to be calibrated against modern meteorological data if there is overlap, resulting in very high accuracy and a way to extend climate datasets globally (Sheppard, 2010; Gebrekirstos *et al*., 2014; Pearl *et al*., 2020). In addition to ring width and relative density, there has been an increase in research extracting stable isotopic ratios of Carbon (^{12}C, ^{13}C), Oxygen (^{16}O,^{17}O and ^{18}O) and Hydrogen (^{1}H, ^{2}H) from tree rings providing improved accuracy in palaeoclimatic reconstructions (McCarroll and Loader, 2004; Loader *et al*., 2007). Tree ring widths remain the most widely used application in dendrochronology, especially in regions where trees have clear and distinct annual rings (St. George, 2014). Early dendroclimatic research relied solely on trees that were deemed *climatically sensitive* and had distinct annual rings which could be easily identified (Fritts, 1971). Manual cross-dating of the ring series was important to ensure that the dating was precise, and the climate signal was accurate. This also helped in identifying missing and or false rings that may have been present (Palakit *et al*., 2012). Cross-dating is still an essential practice in dendroclimatological research, and often the quality of the cross-dating dictates the accuracy of the environmental signal interpretations from the tree rings (Maxwell *et al*., 2011).

Harmon Craig (1954) was the first to publish research on the carbon isotope composition of tree rings. Craig (1954) noted that isotopic variations in sequoia trees were a result of changes in external conditions such as light, temperature and precipitation. The relationship between stomatal conductance and the photosynthetic

rate was described by Farquhar *et al*. (1982). This relationship explained the discrimination against ^{13}C during fractionation (Δ) and was expressed by the following equation, known as the "Farquhar equation":

$$\Delta \approx \boldsymbol{\alpha} + (\boldsymbol{\beta} - \boldsymbol{\alpha}) \frac{\boldsymbol{C_i}}{\boldsymbol{C_a}} ,$$

Where α and β are constants representing fractionation due to diffusion (α = 4.4 ‰) and carboxylation (β = 27 ‰). C_i and C_a are the intercellular and atmospheric CO_2 concentrations, respectively (Farquhar *et al*., 1982; Loader *et al*., 2007; McCarroll *et al*., 2009). Due to the complexities of stable isotope analysis on trees, this method did not become popular until the mid-1990s, but there has been an exponential rise in published research regarding stable isotope analysis on tree rings since then (Shestakova and Martinez-Sancho, 2021).

With improvements to methods regarding sample preparation and analysis, the generation of isotopic ratios from wood samples has become more efficient and affordable (McCarroll and Loader, 2004; Hall *et al*., 2009). The most frequently used stable isotope ratios in palaeoclimatic reconstructions are carbon and oxygen (Pearl *et al*., 2020). Both these stable isotopes can be used to reconstruct multiple climatic variables, including precipitation, temperature, relative humidity, and insolation (Hall *et al*., 2009). Since $\delta^{18}O$ is not the focus of this research project, the intricacies regarding oxygen isotope theory will not be discussed. Carbon isotope theory is explained briefly in the methodology section.

Temperature and precipitation are the most regularly reconstructed variables from tree rings in the literature (Lipp *et al*., 1991; Saurer *et al*., 1996; Brookes *et al*., 1998; February and Stock, 1998; Danis *et al*., 2006; Liu *et al*., 2007; Reynolds-Henne *et al*.,

2007; Hall *et al*., 2009; Fichtler *et al*., 2010; Kress *et al*., 2010; Woodborne *et al*., 2015, 2016). Determining which climatic variable will be best proxied by isotopic values of the tree rings is dependent on the site conditions (Saurer *et al*., 1995, 1998). McCarroll and Loader (2004) state that the value of the isotopic records in tree rings is not that they directly represent past air and water, but rather that they provide insight into the tree's physiological responses to environmental variability as it grew. In sites that are moisture stressed, the dominant control on $\delta^{13}C$ is stomatal conductance (i.e., transpiration rate), thus the $\delta^{13}C$ values will reflect rainfall: high values would indicate periods of less rainfall and *vice versa* (Saurer *et al*, 1995, Gagen *et al*., 2007; McCarroll and Loader 2004, Woodborne *et al*., 2015). However, in a site that is not moisture stressed, the control on the $\delta^{13}C$ may be photosynthetic rate, and therefore $\delta^{13}C$ values would better reflect sunlight and cloud cover (Young *et al.,* 2010). This can indirectly represent temperatures as sunlight and temperatures are usually closely coupled (Young *et al*., 2010). There are exceptions as shown in the successful construction of rainfall chronology for broadleaf tropical trees in wet conditions (Fichtler *et al*., 2010), but this still highlights the importance of site selection regarding this type of research.

Shestakova and Martinez-Sancho (2021) highlight four important trends within research on carbon isotope analysis on tree rings. The first trend is a noticeable shift toward using tree-ring $\delta^{13}C$ in the field of dendroecology, and more research is focusing on understanding tree physiological responses to global change, such as drought responses (Figure 5a). The second trend is that cellulose, as opposed to whole wood samples, is the most frequently analysed material in carbon isotope studies (Figure 5b; Shestakova and Martinez-Sancho, 2021). The third is that conifers (*Pinus, Picea, Abies, Larix ,Juniperus, Afrocarpus* and *Widdringtonia*) are the most

commonly investigated tree type, which is likely due to their heightened sensitivity to climate fluctuations, and capacity to be easily crossdated, which allow for long-term climate reconstructions across wide geographic regions (Figure 5c). Fourth, among precipitation and temperature-related variables (including irradiance and cloud cover), precipitation is more commonly investigated (Figure 5d). Additionally, it was noted that there has been an increase in research delving into water-use efficiency in trees and how this relates to increasing levels of CO_2 in the atmosphere (Adams *et al.,* 2020; Shestakova and Martinez-Sancho, 2021).

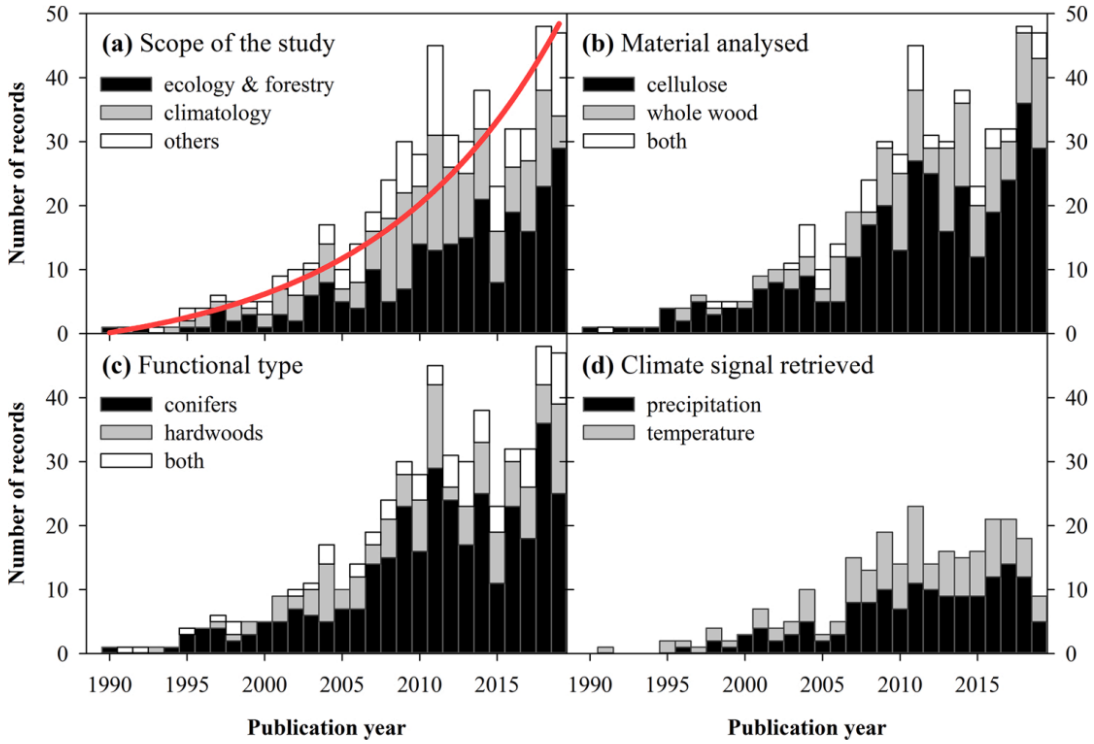


Figure 5: Trends in carbon isotope research derived from a search for ("tree rings" AND "carbon isotopes") in the title, abstract, or keywords of scientific literature using Scopus (Shestakova and Martinez-Sancho, 2021: 2).

Internationally, research relating to the use of tree ring isotope chronologies, for palaeoenvironmental reconstructions, has focused on the Northern Hemisphere with the majority of studies being based in Europe (Lipp *et al*., 1991; Saurer *et al*., 1995, 1996, 1997, Waterhouse *et al*., 2000; Anderson *et al*., 2002; Danis *et al*., 2006;

Skomarkova *et al*., 2006; Reynolds-Henne *et al*., 2007; Treydte *et al*., 2007; Kress *et al*., 2010), Northern and Central America (D'Arrigo and Jacoby, 1991; Brooks *et al*.,1998; Cleaveland *et al*., 2003) and Asia (Kitagawa and Matsumoto, 1995; Sheu *et al*., 1996; Zimmermann *et al*., 1997; Liu *et al*., 2005, 2007, 2008, 2010; Li *et al*., 2017). Northern Europe pine tree chronologies reach more than 7000 years, where over 250 samples from living Scots pines and over 1700 samples of subfossil pines were used to build the chronology (Eronen *et al*., 2002), and Oak chronologies from Ireland, Britain and Europe extend more than 12000 years (Leuschner *et al*., 2002; Spurk *et al*., 2002; Friedrich *et al*., 2004; McCarroll and Loader, 2004).

Tree ring research has diversified into many disciplines, with studies encompassing the biosphere, hydrosphere, lithosphere, and atmosphere (Pearl *et al*., 2020). Tree ring science has been used in multiple disciplines such as archaeological research, through aspects such as charcoal analysis to understand wood use within a site, ^{14}C dating of tree rings to date a site, or tree-ring analysis to understand climate variation relating to occupation layers within a site (Nash, 2002; Boswijk *et al*., 2021). Climate phenomena, such as extreme flooding (Ballesteros-Cánovas *et al*., 2015) and drought events (Gou *et al*., 2015; Chen *et al*., 2017), major cooling or warming events such as the Little Ice Age (LIA) (Luoto and Helama, 2010; Malcomb and Wiles, 2013; Norström *et al*., 2005; Svarva *et al*., 2018; Woodborne *et al*., 2015, 2016) or the Medieval Climate Anomaly (MCA) (Cook *et al*., 2002; Luoto and Helama, 2010), have been investigated using dendroclimatology. Geophysical processes such as the impact of volcanoes can be recorded in tree rings as the trees respond to physical changes in their environment (Zang *et al*., 2020). Tree ring science and climate chronologies are also useful in verifying climate models, where climate reconstructions can be compared to climatic tree ring chronologies to prove the accuracy of the climate

models (Briffa *et al*., 2004). Tree ring data have also been used in the construction and extension of radiocarbon calibration curves, which are used to map radiocarbon dates to calendar ages (Blackwell and Buck, 2008; Reimer, 2021)

Dendrochronology and dendroclimatology have tremendous potential in the validation of climate models (Pearl *et al*., 2020). Dendroclimatological and other palaeoenvironmental research could be the key in strengthening the ability of climate models to accurately predict scenarios and this, in turn, would assist in the identification of important areas in need of further palaeoenvironmental research to bridge data/knowledge gaps (Pearl *et al*., 2020).

2.3.2 Key issues and debates

Previous limitations or hindrances encountered in tree ring science have prompted new and innovative approaches and technological advances (Pearl *et al*., 2020). In southern Africa, there are some limitations noted in the literature (February *et al*., 2003). Tree rings can only provide climatic information for the lifespan of the tree, and thus far, there have only been a few studies where the trees have produced chronologies spanning 400 years or more (cf. Dunwiddie and LaMarch, 1980; Woodborne *et al*., 2015). Additionally, many hindrances are encountered when analyzing tree rings, such as wedging rings, discontinuous rings, locally absent/missing rings, false rings, and the fusing of stems (Trouet *et al*., 2001, 2006; Fichtler *et al*., 2004; Robertson *et al*., 2006; Patrut *et al*., 2007; Norström *et al*., 2008). Ring wedging occurs when there is a failure in cambial activity along certain parts of the radial growth, this results in ring boundaries merging at some sections (Worbes, 2010). Missing rings are a result of rapid growth in certain parts of the tree and

nonexistent growth in other parts of the tree, or when trees limit growth due to drought or other unfavourable climate stresses (Novak *et al*., 2016). False rings occur when multiple growth rings are produced in a single year, this is commonly a result of a period of drought followed by increased rainfall (Trouet, 2004; Copenheaver *et al*., 2006). Fused stems are commonly found in baobab trees, which makes dendroclimatic studies more complex, as individual stems need to be identified before analyses can be completed (Patrut *et al*., 2018).

Ring abnormalities are common in southern Africa and other tropical regions due to there being less distinct seasonality, with only minor temperature changes in an annual cycle (Worbes, 2002; Wils *et al*., 2010). The occurrence of droughts is irregular and not always linked to specific seasons (Gebrekirstos *et al*., 2014) and there is often less defined seasonal precipitation, which is a common cause of indistinct and or nonannual rings (Wils *et al.,* 2010).

Radiocarbon dating should be done on selected growth rings, and isotopic analysis should be performed to better understand the climatic signals preserved in the tree (McCarroll and Loader, 2004). Technological advancements have improved methods for distinguishing ring boundaries and identifying ring abnormalities, such as microscopic analysis of cells (Gebrekirstos *et al*., 2014). It is also imperative that, in all future research, corrections are made for increased anthropogenic CO_2 in the atmosphere, and changes in intrinsic water use efficiency of trees due to increased concentrations of CO_2, to ensure accurate interpretations (McCarroll and Loader, 2004; Woodborne *et al*., 2016). The annual $\delta^{13}C$ atmospheric values are available, thus, tree ring values can be corrected to a pre-industrial standard value (Belmecheri and Lavergne, 2020). The correction value was considered to be a constant in earlier

studies (-6.4‰), but new calibrations of ice core measurements suggest that $\delta^{13}CO_2$ (pre-industrial) has varied over time (Belmecheri and Lavergne, 2020).

The most common approach to correct declining $\delta^{13}C$ values has been to add a standard $\delta^{13}C$ value per unit increase in the CO_2 content of the atmosphere (McCarroll *et al*., 2009). Different values were used ranging from 0.007 to 0.02‰. This approach was subjective and thus had varying results (McCarroll *et al*., 2009). Adding a standard $\delta^{13}C$ value per unit increase to the C_a value assumes that an increase in atmospheric CO_2 has the same effect on isotopic fractionation in all trees. This is not true (McCarroll *et al*., 2009). Belmecheri and Lavergne (2020) compiled data to provide the pre-industrial values per year to do corrections for tree ring research. These values can be found online as supplementary data here: https://doi.org/10.1016/j.dendro.2020.125748.

More research is needed to develop longer high-resolution climate chronologies for southern Africa. High-resolution rainfall reconstructions are necessary to better understand and interpret the dynamic variability of climate forcing in southern Africa (Woodborne, *et al*., 2016), particularly the hyper-arid region of Namibia. This research project will add to this growing body of literature and provide new data and add to the literature pertaining to the Namib Desert, Namibia.

2.4 Dendroclimatological research in southern Africa

In southern Africa, traditional dendroclimatic studies using tree ring width have been limited in comparison to the Northern Hemisphere (February and Stock, 1999; February *et al*, 2006; Jones *et al*., 2009). This is partly because there is an apparent

absence of annual growth rings in tree species from the region (Lilly, 1977; February *et al*., 2006). Another aspect that has hampered dendrochronological studies in the region is the depletion of indigenous forests due to intensive logging and exploitation since the arrival of the Europeans in the 17th Century, which has seriously restricted the availability of mature trees that would be appropriate for dendrochronological analyses (Jones *et al.,* 2009). Furthermore, forest vegetation is naturally highly restricted in distribution in southern Africa (Eeley *et al*., 1999). The temporal scales of dendro-climatic reconstructions in the Southern Hemisphere are much shorter than those of the Northern Hemisphere, with the longest proxy record spanning 1000 years (*Adansonia digitata*; Woodborne *et al*., 2015). Despite this, a growing number of dendroclimatic chronologies have been developed in southern Africa (Table 2, Figure 8), which demonstrate the potential and value of dendrochronology and dendroclimatology within the region (Norström *et al.,* 2005, Trouet *et al.,* 2006; Therrell *et al.* 2007). For the most part, dendrochronological research in southern Africa has focused on the summer rainfall region (Figure 8; Norström *et al*., 2005; Robertson *et al*., 2006; Therrell *et al*., 2007; Hall *et al*., 2009; Woodborne *et al*., 2015), and there is very little dendrochronological research for the winter rainfall region (Dunwiddie and LaMarche, 1980; February and Stock, 1999; De Mil *et al*., 2021).

In Zambia, *Brachystegia spiciformis* was shown to be climatically sensitive, with a positive correlation between ring-width chronology and regional climate chronology (Trouet *et al.,* 2006). *Pterocarpus angolensis* was investigated by Therrell *et al.* (2007) at nine sites across southern Africa, spanning Botswana, Zambia, Mozambique, Zimbabwe, and South Africa, for which a positive relationship between the mean annual diameter of the rings and mean seasonal rainfall was concluded. Therrell *et al.* (2007) also indicated a positive correlation between tree diameter and heartwood

percentage, and that these findings may be useful in sustainably managing the species.

In Zimbabwe, *Pterocarpus angolensis* tree rings were used to create a 200-year rainfall chronology for tropical Africa (Therrell *et al.,* 2006). For Mozambique, southeastern Africa, a study on *Millettia stuhlmannii* demonstrated dendrochronological potential due to annual growth rings and a significant correlation between annual growth and seasonal rainfall (Remane and Therrell, 2015).

Within the summer rainfall region of South Africa, dendrochronological studies have been conducted in Limpopo on *Breonadia salicina* and *Adansonia digitata*, where both trees indicated dendrochronological potential, however, *Breonadia salicina* did not have continuous annual rings (Norström *et al.,* 2005; Robertson *et al.*, 2006; Woodborne *et al*., 2015). *Adansonia digitata* also presented challenges, as the fibrous wood makes it difficult to identify annual growth rings (Robertson *et al.,* 2006).

In KwaZulu-Natal, *Mimusops caffra* was investigated for dendrochronological potential. Hall *et al*. (2009) presented that using stable carbon isotope analysis, whole wood samples from *Mimusops caffra* provide an accurate record of climatic variability. In addition, at Sibudu Cave, KwaZulu-Natal, archaeological charcoal (*Afrocarpus* genus) as an indicator of environmental change using isotopic analysis was investigated with successful results (Hall *et al*., 2008). These palaeoenvironmental chronologies are important, but they are not enough to make synchronous inter-regional comparisons (Hall *et al*., 2009).

There is very little published research on dendrochronology or dendroclimatology in the winter rainfall region. In the Western Cape, Dunwiddie and LaMarche (1980) were

the first to publish an investigation of *Widdringtonia cedarbergensis* rings. This study (Dunwiddie and LaMarche, 1980) was one of the first to provide annually dated tree ring width indexes (TRWI) in the Southern Hemisphere. The samples for this chronology, which spanned 411 years (1564-1976), were cross dated using frost rings as they were easily identifiable (Dunwiddie and LaMarche, 1980). TRWI was interpreted as indicating moisture availability during spring and early summer and that frost rings may be linked to the Tambora volcanic eruption (1815) (Dunwiddie and LaMarche). February and Stock (1999) reanalysed the rings using $\delta^{13}C$ analysis and presented that the results indicated that there is no correlation between tree rings and annual precipitation data from a weather station nearby. February *et al.* (2007) undertook further research on *Widdringtonia cedarbergensis*, which focused on stable oxygen isotope analysis, and concluded that there is a significant correlation between $\delta^{18}O$ in the tree ring and rain $\delta^{18}O$ values. This indicates that the trees may rely on rain that is collected in sumps between the rocks on which they grow (February *et al.,* 2007). However, the studies done by February and Stock (1999) and February *et al*. (2007), did not include the correction to the $\delta^{13}C$ record for changing intrinsic water use efficiency, which is critical to account for the tree's response to increased concentrations of atmospheric CO_2 after the industrial revolution (McCarroll and Loader, 2004). De Mil *et al*. (2021) re-examined 20 of the tree cores collected in 1978 by Dunwiddie and LaMarche from the Die Bos site, and performed multi-parameter dendroclimatic analyses, as well as $\delta^{13}C$ and $\delta^{18}O$ measurements. Their study revealed that TRWI was positively influenced by November-December precipitation, but no statistically significant relationships were found for $\delta^{13}C$ and $\delta^{18}O$ isotope analyses (De Mil *et al*., 2021).

Table 2: Tree species used in dendroclimatic reconstructions in southern Africa

Tree Species	Location	Time span covered	Main findings	Reference
Acacia (Vachellia) erioloba	Namibia, southern Botswana	1758-2013 cal yr CE	Used stable carbon and oxygen isotope analyses to produce a rainfall proxy	Woodborne, 2004; Woodborne *et al*., 2018
Adansonia digitata	Limpopo, Botswana, Namibia	999-2009 cal yr CE	A significant relationship between isotope analysis and climate.	Woodborne *et al*., 2015, 2016
Brachystegia spiciformis	Zambia	1940-2002 cal CE	A positive correlation between ring-width chronology and regional climate	Trouet *et al*., 2006
Breonadia salicina	Limpopo	1375-1995 cal yr CE	Used stable carbon isotope analyses and wood anatomy to produce a rainfall proxy	Norström *et al*., 2005
Burkea africana	Namibia	1890 cal yr CE-2000 cal yr CE	Positively correlated to rainfall	Fichtler, *et al*., 2004
Millettia stuhlmannii	Mozambique	1997 cal yr CE-2009 cal yr CE	Significant correlation between annual growth and seasonal rainfall	Remane and Therrell, 2015
Mimusops caffra	KwaZulu-Natal	1987 cal yr CE-2003 cal yr CE	Whole wood samples from *M. caffra* provide an accurate record of climatic variability	Hall *et al*., 2009
Pittosporum viridiflorum	Mpumalanga	1895 cal yr CE-2013 cal yr CE	Reflects climatic patterns going back to the late 19th Century	Schoeman *et al*., 2019
Afrocarpus genus	KwaZulu-Natal	multiple	An indicator of environmental change through isotopic analysis	Hall *et al*., 2008
Afrocarpus falcatus	Midlands	1142-1916 cal yr CE	Results produced a precipitation chronology.	Vogel *et al*., 2001
Prunus africana	Mpumalanga	1895-2013 cal yr CE	Reflects climatic patterns going back to the late 19th Century	Schoeman *et al*., 2019
Pterocarpus angolensis	Botswana, Zambia, Mozambique, Zimbabwe and South Africa, Northern Namibia	n/a	A positive relationship between the mean annual diameter of the trees and mean seasonal rainfall	Fitchtler *et al*., 2004; Therrell *et al*., 2007
Widdringtonia cedarbergensis	Western Cape province	1564-1976 cal yr CE	The TRWI could indicate moisture availability during spring and early summer	Dunwiddie and LaMarche 1980

2.5 Palaeoenvironmental research in southern Africa

Analysis of climate proxies to infer environmental change was introduced to southern Africa relatively late in comparison to other parts of the world (Meadows, 2015). However, palaeoenvironmental research within the subcontinent has increased considerably (Fitchett *et al*., 2017). Proxies that can infer long-term climate change (thousands of years) include speleothems (McDermott, 2004; Sundqvist *et al*., 2013), sediment cores (Ekblom and Stabell, 2008; Holmgren *et al*., 2012), palynology (Scott and Neumann, 2018), faunal remains (Sealy *et al*., 2020) hyrax middens (Chase *et*

al., 2012) and marine cores (Hahn *et al*., 2017; Urrego *et al*., 2015). Historical climatology can provide great insight into climate change from the 17th -19th Centuries (Nash *et al*., 2016). The climate over recent decades can be understood using meteorological data collected from weather stations where available, unfortunately, the distribution of modern instrumental records is sparse (Nicholson *et al*., 2013, 2014). The most widely used palaeoenvironmental proxy in southern Africa is pollen, followed by sediment analysis and isotopes (Figure 6). It is evident that there is a paucity of palaeoclimatic research in Namibia in comparison to other parts of the region when examining the spatial extent of palaeoclimatic reconstructions for southern Africa (Figure 7, Fitchett *et al*., 2017).

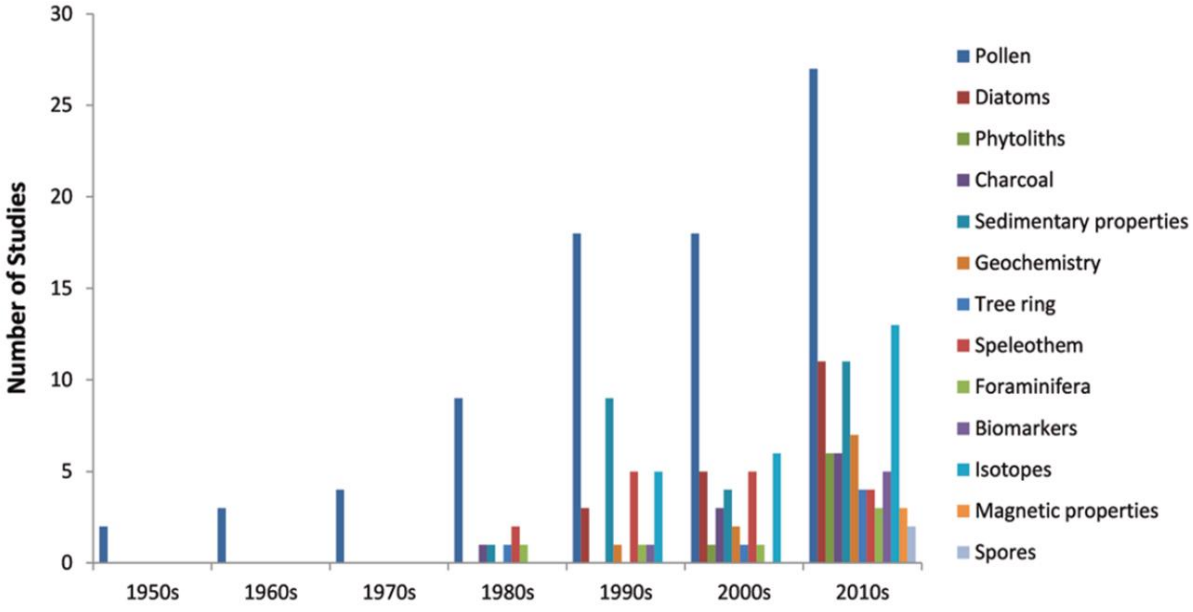


Figure 6:The number of, and different kinds of proxies used in published Quaternary palaeoenvironmental studies for southern Africa from 1950-2017 (Knight and Fitchett, 2019: 39).

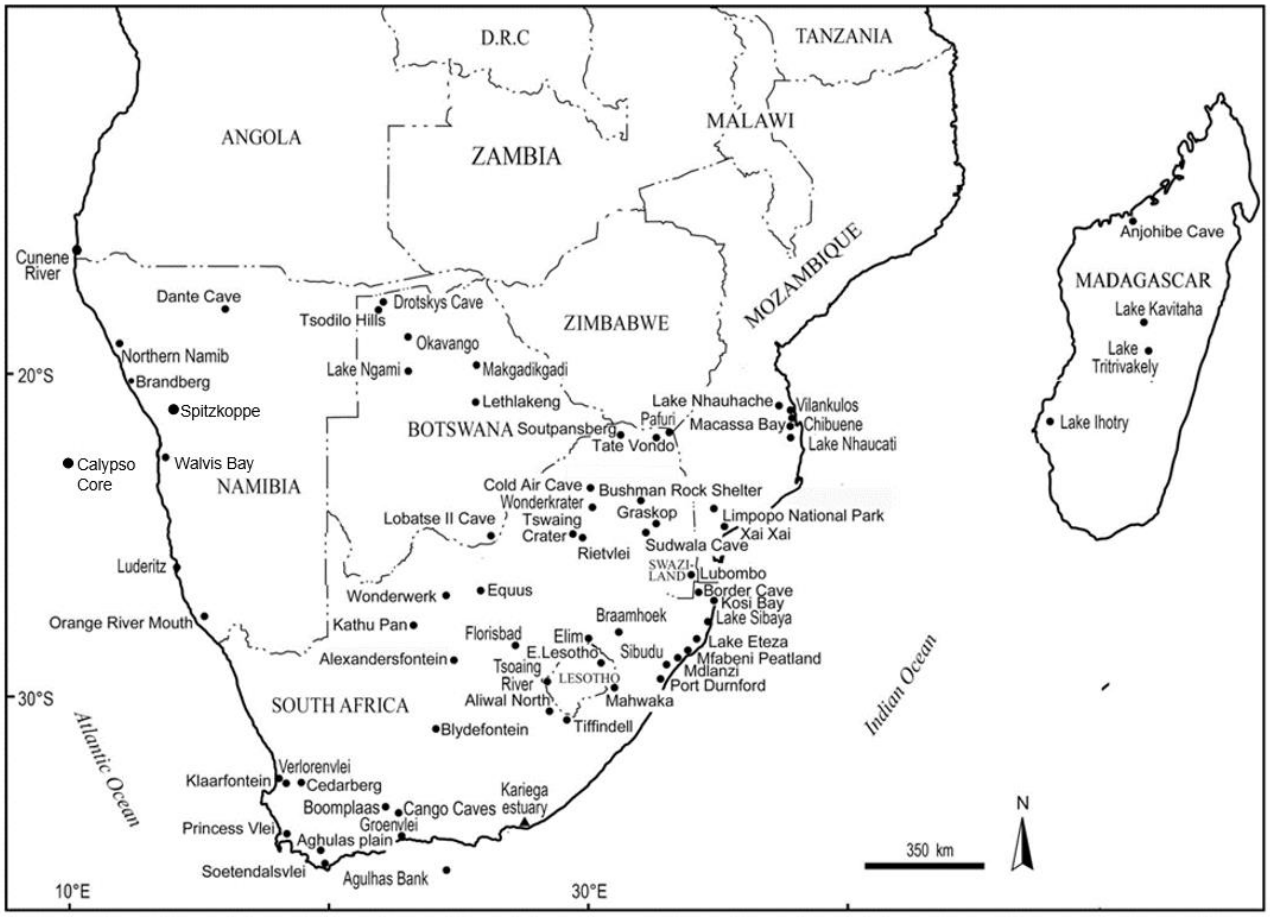


Figure 7:Spatial extent of published palaeoenvironmental studies in southern Africa (adapted from Fitchett *et al*., 2017: 281).

In southern Africa, there is a fast-growing body of research on historical climatology where instrumental records are either not available or not reliable. The research included inter-regional comparisons allowing for the identification of widespread drought/wet periods which is important in understanding the overall climate variability for the historical period (Lindesay and Vogel, 1990; Nash and Endfield, 2002; Kelso and Vogel, 2007; Kelso and Vogel 2015; Nash *et al.*, 2015b; Grab and Zumthurn, 2018). The temporal focus of the research varies according to the historical records being used, but mostly the research pertains to the 19th and 20th Centuries, with a few studies extending back to the late 18th Century. There is no published information relating to earlier years, indicating a gap in the current literature. For most of the

literature from southern Africa, there seems to be a focus on rainfall and drought variability and the construction of temporal and spatial wetness-dryness indices. This may be due to precipitation information being more easily extracted from historical documentary sources (Nash *et al*., 2016).

Links have also been made between tree ring records and climate chronologies (Vogel, 1989; Worbes, 1999; Touchan *et al*., 2003; Brienen and Zuidema, 2005; O' Donnell *et al*., 2015). Comparisons of historical-documentary derived data, to dendro-climatological data provide a means to further verify the accuracy of documentary derived chronologies or to further extend their datasets (Vogel, 1989; Bradley and Jonest, 1993; Leijonhufvud *et al*., 2010).

Two climatic events which are often investigated during the past millennium include the MCA from 950-1250 cal yr CE (Luning *et al*., 2018) and the LIA which occurred from 1300-1850 cal yr CE (Nicholson *et al*., 2013). There is heterogeneity across southern Africa during these periods, and the ability to fully understand this is hampered by the lack of long term, high-resolution palaeoclimate records (Ekblom and Stabell, 2008). There are some common trends that allow for broad conclusions for southern Africa (Nicholson *et al*., 2013). Overall, during the MCA there were generally warmer temperatures, with increased rainfall in the summer rainfall zone (SRZ), but decreased rainfall in the winter rainfall zone (WRZ) (Hahn *et al*., 2017; Luning *et al*., 2018). This may have been caused by a southward shift of the intertropical convergence zone (ITCZ) and an intensification of rain-bearing tropical easterlies, with a southward shift of rain-bearing westerlies away from the continent (Luning *et al*., 2018; Hahn *et al*., 2021). There is also evidence of a strengthening of the South Atlantic and South Indian anti-cyclones during the MCA (Hahn *et al*., 2017, 2021).

During the LIA there is consensus on widespread cooling, however, some areas of the WRZ experienced wetter conditions (Hahn *et al*., 2021; Völkel *et al*., 2021) and the SRZ experienced drought conditions (Ekblom and Stabell, 2008) with a northward shift in the Southern Hemisphere westerlies (Hahn *et al*., 2017). On the whole, the climate was highly variable during the past millennium in southern Africa (Nicholson *et al*., 2013; Nash *et al*., 2016; Hopper *et al*., 2018).

2.6 Palaeoclimate research in the Namib Desert

Evidence for past climate change in the hyper-arid Namib Desert is extremely limited (Chase *et al*., 2019). Some valuable information has been gathered through the analysis of pollen from rock hyrax middens (Gil-Romera *et al*., 2006, 2007; Chase *et al*., 2012, 2019), lake sediments (Brook *et al*., 2007), speleothems (Sletten *et al*., 2013), as well as documentary data (Grab and Zumthurn, 2018). The use of dendrochronology and dendroclimatology has been underutilised (Shikangalah, 2020) and there is a distinct lack of high-resolution palaeoclimate data for the region (Zhu *et al*., 2016). While proxies such as rock hyrax middens provide coarse long-term climatic records, they cannot provide the high-resolution which can be achieved through dendrochronology (Grab and Zumthurn, 2018).

Dendroclimatological studies in Namibia are limited, and most focus on the north-central region which is more temperate (Shikangalah, 2020; Shikangalah *et al*., 2020; Mapani *et al*., 2021). The few published dendrochronological studies for Namibia (Table 3) illustrate the potential for dendroclimatology in the Namib region.

Table 3:Dendrochronological studies from Namibia (adapted from Shikangalah, 2020: 0195-0196).

Analysed Trees	Regions of Study Area	Method	Rings	Conclusion	Reference
Pterocarpus angolensis	Zambezi and Otjozondjupa	Tree ring widths with two radii were measured with a microscopic device	Yes	Rainfall amount is not necessarily the limiting factor, as a weak correlation in both regions was found, regardless of the amount of rainfall received in the region.	Angombe and Shikangalah, 2021
Dichrostachys cinerea and *Senegalia (Acacia) mellifera*	Oshikoto, Otjozondjupa, Omaheke	Growth rings on stem discs and their variability along rainfall gradient	Yes	Distinctive rings observed and responsive to precipitation, patterns clearer in *D. cinerea* than *S. mellifera*. Can be used as proxies for climate signals.	Shikangalah *et al*., 2020
Pterocarpus angolensis	Kavango West, Otjozondjupa	Growth rings on stem discs and cores	Yes	Distinctive rings observed and might be useful for climate signals at local scale.	De Cauwer *et al*., 2017
Pterocarpus angolensis, Terminalia sericea, Baikiaea plurijuga, Burkea africana, Schinzio phyton rautanenii	Oshikoto, Kavango West, Kavango East, Zambezi region	Growth rings on cores and stem discs	Yes	Distinctive rings observed	Van Holsbeeck *et al*., 2016
Terminalia sericea	Zambezi region	Growth rings on stem discs and inter-annual analysis of variability	Yes	Distinctive rings observed, inter-annual variability clear	Fichtler *et al*., 2010
Adansonia digitata	Otjozondjupa	Age determination by radiocarbon dating	N/A	Tree older than 1200 years	Patrut *et al*., 2007
Pterocarpus angolensis, Burkea africana	Oshikoto and Zambezi region	Growth rings on stem disc	Yes	Strong responses to relative humidity and temperature at Ondangwa. At Katima only *angolensis* is more responsive to climate variables.	Fichtler *et al*., 2004
Acacia erioloba	Koichab	$\delta^{13}C$ analysis on growth rings, and radiocarbon dating	Yes	Cyclicity between high and low water stress identified in the tree correlates with rainfall.	Woodborne, 2004
Pterocarpus angolensis, Terminalia sericea, Baikiaea plurijuga, Burkea africana, Colophos permum mopane, Combretum collinum, Lonchocarpus nelsii	Oshikoto, Zambezi region	Growth rings on stem disc and radiocarbon dating	Yes	Distinctive rings observed, *Terminelia sericea* hashigh increment in Katima but low at Oshikoto	Worbes, 1999

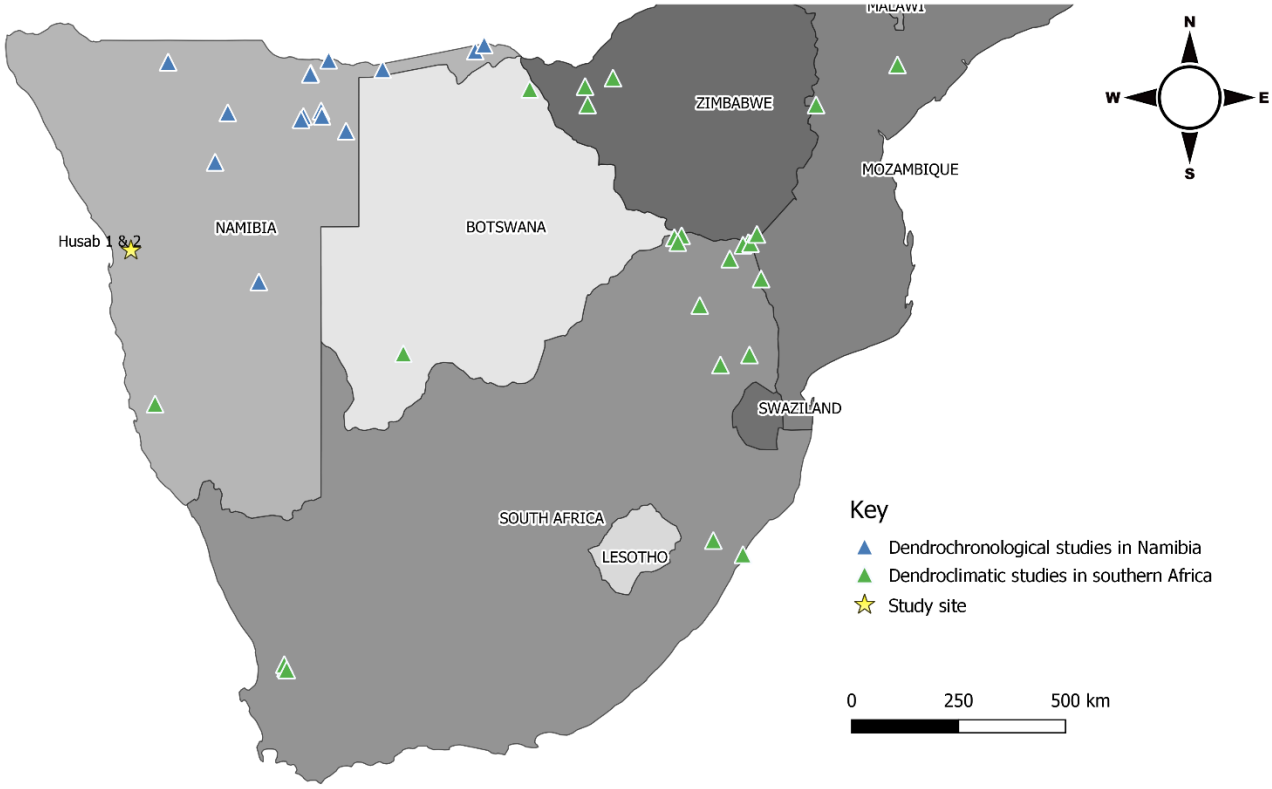


Figure 8: Map showing locations of dendroclimatic and dendrochronological studies in southern Africa and Namibia (Own figure).

2.7 Summary of climate variability over the past millennium in Namibia

The climate in Namibia has been highly variable over the past 1000 years (Nash *et al*., 2016). During the MCA there was a perceived trend towards increased rainfall (Luning *et al*., 2018). Along with high climatic variability, there are indications of increased humidity between 900 cal yr CE and 1250 cal yr CE, with a drier period at 1200 cal yr CE (Nash *et al*., 2016). Pollen records from hyrax middens located along the Kuiseb River valley indicate warmer conditions during the MCA, peaking at 1100 cal yr CE and 1250 cal yr CE (Scott, 1996; Nash *et al*., 2016). The Spitzkoppe hyrax middens from the Namib Desert indicate increased aridity in the early LIA. Following this, there is a transition toward increased moisture availability between 1600 cal yr

CE and 1850 cal yr CE (Chase *et al*., 2009; Nash *et al*., 2016). Evidence from palaeoflood deposit sites along the Kuiseb River indicates a greater frequency of floods during 1865-1715 cal yr CE (Grodek *et al*., 2013). This instance of increased flood frequency in the LIA coincides with the Maunder Minimum which occurred from 1645-1715 cal yr CE (Grodek *et al*., 2013). There were also multiple documented historical floods during the 19th and early 20th Centuries for the Swakop River in Namibia (Greenbaum *et al*., 2014). Evidence from an analysis of historical documents indicates that pronounced interannual rainfall variability occurred from 1845-1900 cal yr CE (Grab and Zumthurn, 2018). Studies based on the alluvial stratigraphy of Namibian rivers indicate the occurrence of large floods during the LIA (Greenbaum *et al*., 2014). However, it is possible for floods to occur against a background of increased aridity (Heine and Völkel, 2011).

While these palaeoclimatic studies are useful, more research is needed to improve understanding of the climatic variability of the past millennium, and the links to the main circulation systems and climatic drivers for the region (Nash *et al*., 2016). The high-resolution historical records are limited to the 19th and 20th Centuries for Namibia, but there is potential to validate and further extended these historical records with the use of dendroclimatological studies. This research project provides much-needed insight into the hydroclimate of Namibia and adds valuable information to the current research thrust regarding past climate variability in the Namib Desert.

2.8 Conclusions

This chapter provides an overview of dendrochronology and dendroclimatology as well as global developments in the field. It highlights that palaeoclimatic research is

increasing within southern Africa, but that there is still far more palaeoclimatic research in the Northern Hemisphere. Southern Africa and particularly the water-stressed regions such as Namibia are vulnerable to climate change, and thus there is a need for more palaeoclimatic research. Dendroclimatology has the potential to provide the high-resolution, long-term data that is needed to better understand the regional responses to climatic change. This has led to an increase in dendroclimatic studies in the tropics and subtropics, despite the complexities of tree-ring growth that occur with less distinct seasonality. This chapter emphasises the lack of palaeoclimate research in Namibia and shows why dendroclimatic research is needed to close the gaps in the literature pertaining to climatic research for the past 1000 years.

CHAPTER 3: STUDY SITE

3.1 Environmental Setting

Namibia is located on the west coast of southern Africa and has a varied climate ranging from semi-arid in the central interior, to hyper-arid along the coast (Grab and Zumthurn, 2018). The climate of the region is influenced by distinct circulation patterns, the South Atlantic High Pressure (SAHP) drives upwelling of the cold Benguela Current which plays a major role in the hyper-aridity experienced in the region (Tyson and Preston-Whyte, 2000). The anti-cyclonic system results in subsiding air, which causes clear, dry conditions to prevail, limiting the reach of convectional rainfall into the interior of the country (Tyson and Preston-Whyte, 2000; Kaseke *et al*., 2016).

The research presented in this dissertation uses sample discs acquired from two *Acacia erioloba* trees (Husab-1 and 2) that were felled during road building. The trees were located at 22°34'24.20"S, 15°0'21.42"E along a tributary of the Khan River in the Erongo Region of central Namibia (Figure 9). This species is known to grow for hundreds of years and is therefore useful as a climate proxy (Kinahan, 2016).

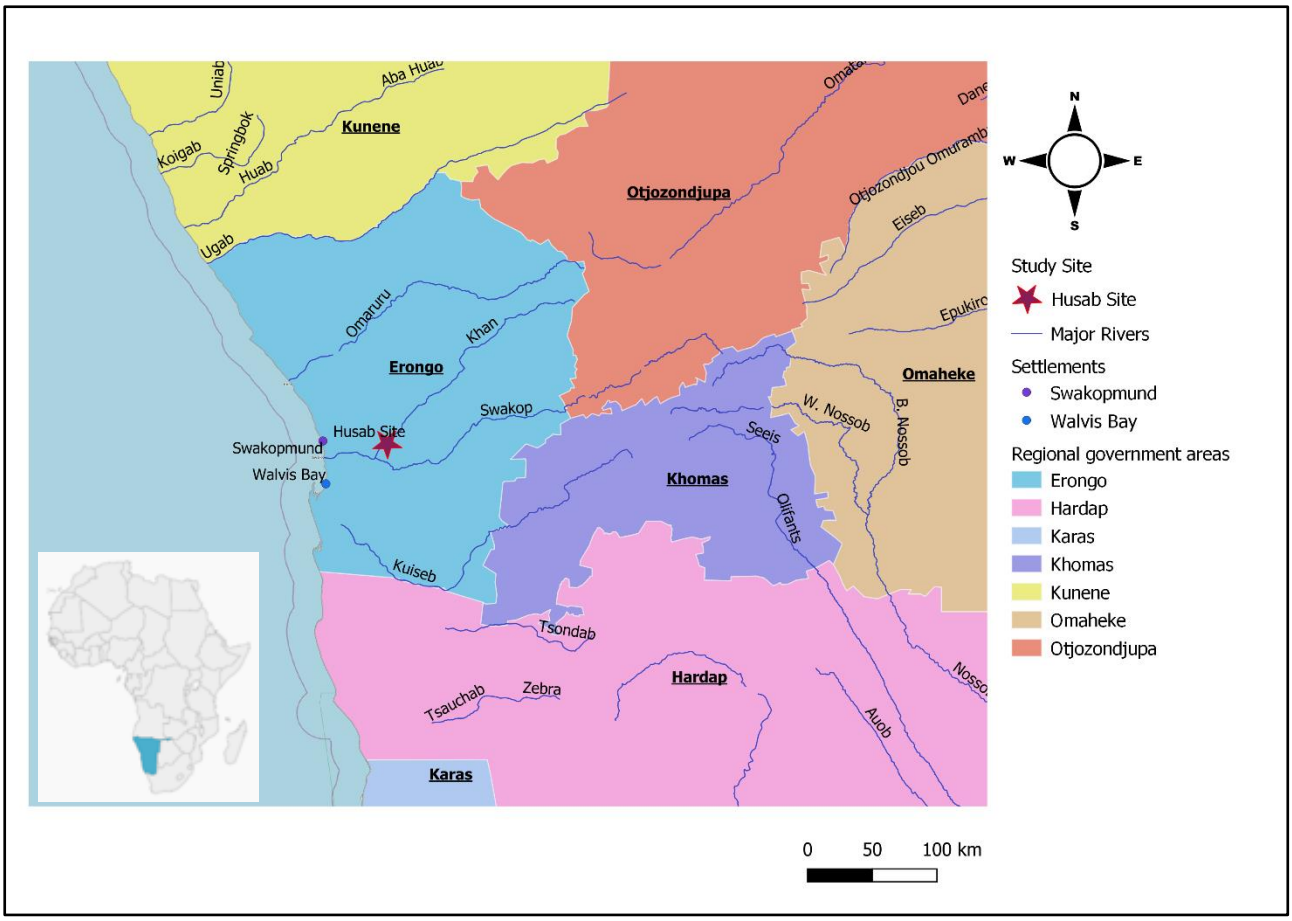


Figure 9: The African continent, indicating the location of Namibia and the location of study site:22°34'24.20"S, 15°0'21.42"E (Data source: Atlas of Namibia Project, 2002).

3.2 Climate

The central Namib Desert is located near the southwestern boundary of the summer rainfall zone in Namibia (Lancaster *et al*., 1984). Rainfall and convective showers are suppressed due to cool stable air associated with the Benguela Current and the South Atlantic high-pressure anti-cyclone (Eckardt *et al*., 2013), and so rainfall is highly variable, highly localized, and of low intensity, and is mostly in the form of sporadic convective showers (Kinahan, 2016; Mupambwa *et al*., 2019). On average, Namibia receives approximately 270mm of annual rainfall, with up to 5% of the country receiving more than 500mm per annum (Mupambwa *et al*., 2019). In the southern and western parts of Namibia, most rainfall occurs in February and March, while in the

north there are two peak rainy seasons in January and March (Mendelsohn *et al*., 2002). There is a strong moisture gradient, with the most rainfall occurring in the northernmost parts of Namibia with more than 600mm of rainfall per annum, and the least occurring along the coast, with less than 50mm per annum (Figure 10). Rainfall reaches around 15mm per annum on the coast and increases to around 80-100mm per annum approaching the great escarpment (Kaseke *et al*., 2018, Mupambwa *et al*., 2019).

In the Namib Desert, consecutive years of no rainfall is a common feature (Mupambwa *et al*., 2019) and between 92% and 97% of Namibia is considered to be semi-arid to hyper-arid (Shanyengana *et al*., 2002; Crawford and Terton, 2016). Windhoek in central Namibia receives around 300-350mm per year (Grab and Zumthurn, 2018). In the study area where the samples were collected the average annual rainfall is less than 50mm (Figure 10).

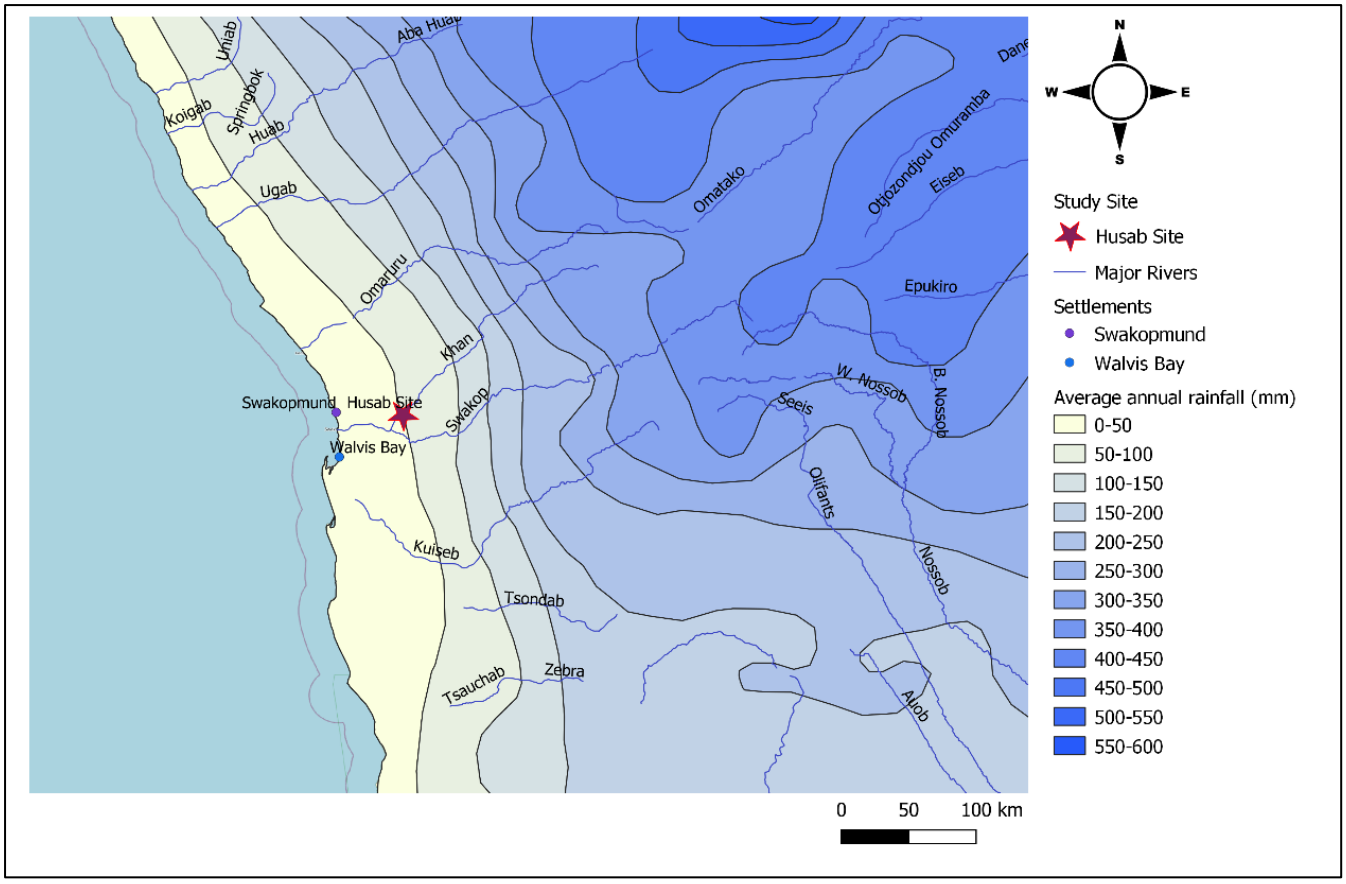


Figure 10: Average annual rainfall in Central Namibia (Data source: Atlas of Namibia Project, 2002).

There are various precipitation systems that impact rainfall in Namibia (Figure 11). The most prominent systems are the Congo Air Boundary (CAB), Tropical Temperate Troughs (TTTs) and the Angola Low (AL) (Eckardt *et al*., 2013). During austral summers, there is an influx of moisture through the CAB which marks the boundary between the low-level westerlies originating from the Atlantic Ocean and the easterly trade winds originating from the Indian Ocean (Howard and Washington, 2019). This convergence results in atmospheric instability, cloud formation and precipitation that occasionally reaches as far as the Kalahari and Namibia during the summer months (Eckardt *et al*., 2013). This moisture dissipates as it moves southwards from Northern Namibia (Eckardt *et al*., 2013).

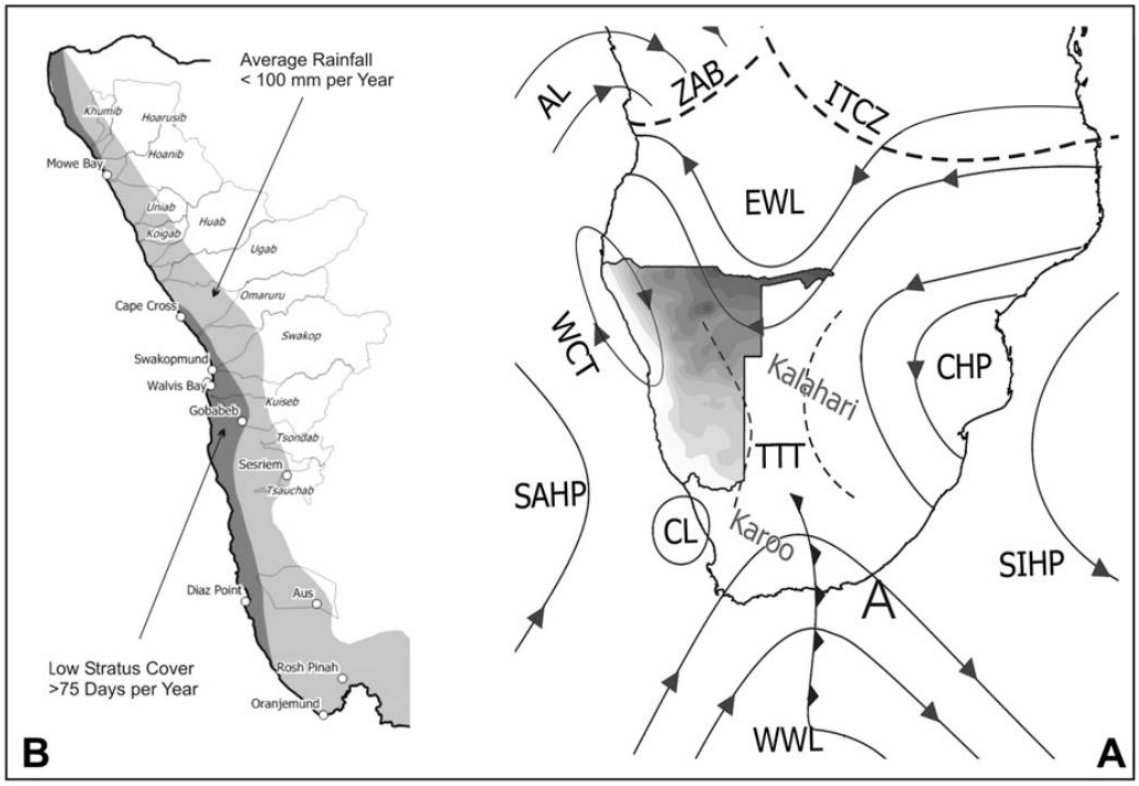


Figure 11: (A) Southern African synoptics which promote rainfall in Namibia: Angola Low (AL), Coastal Low (CL), Cold Front (CF), Intertropical Convergence Zone (ITCZ), Tropical Temperate Trough (TTT), West Coast Trough (WCT), Westerly Wave Low (WWL), Zaire/Congo Air Boundary (ZAB) and the major pressure systems: Continental High Pressure (CHP), South Atlantic High pressure (SAHP), and the South Indian Ocean High Pressure (SIPH). (B) The Namibian Coastline (Eckardt *et al*., 2013: 2).

The occurrence of TTTs may also promote rainfall in Namibia (Eckardt *et al*., 2013). TTTs are one of the most prominent rainfall bearing systems for summer rainfall in southern Africa (Usman and Reason, 2004). TTTs form a band of precipitation by linking tropical easterly waves to westerly waves in the south through a trough (Eckardt *et al*., 2013; Macron *et al*., 2014; Grab and Zumthurn, 2018). The Angola low can be another source of moisture, it begins as a shallow heat low, which receives an influx of moisture from the Atlantic Ocean and develops into a deeper tropical low (Reason *et al*., 2006; Munday and Washington, 2017). The low-pressure cell generally develops in October and strengthens towards January/February. This can also act as a moisture

source for TTTs (Reason *et al*., 2006). TTTs are more likely to develop over Namibia during La Niña years in comparison to El Niño years (Grab and Zumthurn, 2018).

Fog is another crucial source of moisture for this desert environment (Soderberg, 2010). Non-rainfall moisture sources such as fog are among the most overlooked hydrological aspects in most ecosystems (Kaseke *et al*., 2017, 2018). Fog can be critical in maintaining ecosystem functioning and are especially important for hyper-arid ecosystems such as the Namib Desert (Henschel and Seely, 2008, Wang *et al.*, 2017, 2019). Fog deposits around 34mm per year of water along the coast, increasing to 184mm annually at 35-60km inland, and decreasing at 60km inland with 60-15mm annually (Mupambwa *et al*., 2019).

Fog in the Namib Desert occurs through the advection of moist oceanic air over the cold Benguela Current (Kaseke *et al*., 2018). As the warm air from over the Atlantic moves northward over the current, the temperature is reduced to dewpoint, and this results in fog (Tyson and Preston-Whyte, 2004). Fog can reach up to 60km from the coastline, but the fog belt is known to stretch over 100km inland (Shanyengana *et al*., 2002; Soderberg, 2010). Fog is also less erratic than rainfall, thus the flora and fauna in the region rely on it heavily as a source of water (Soderberg, 2010). The study site of this research project receives around 25 to 50 days of fog per year (Figure 12).

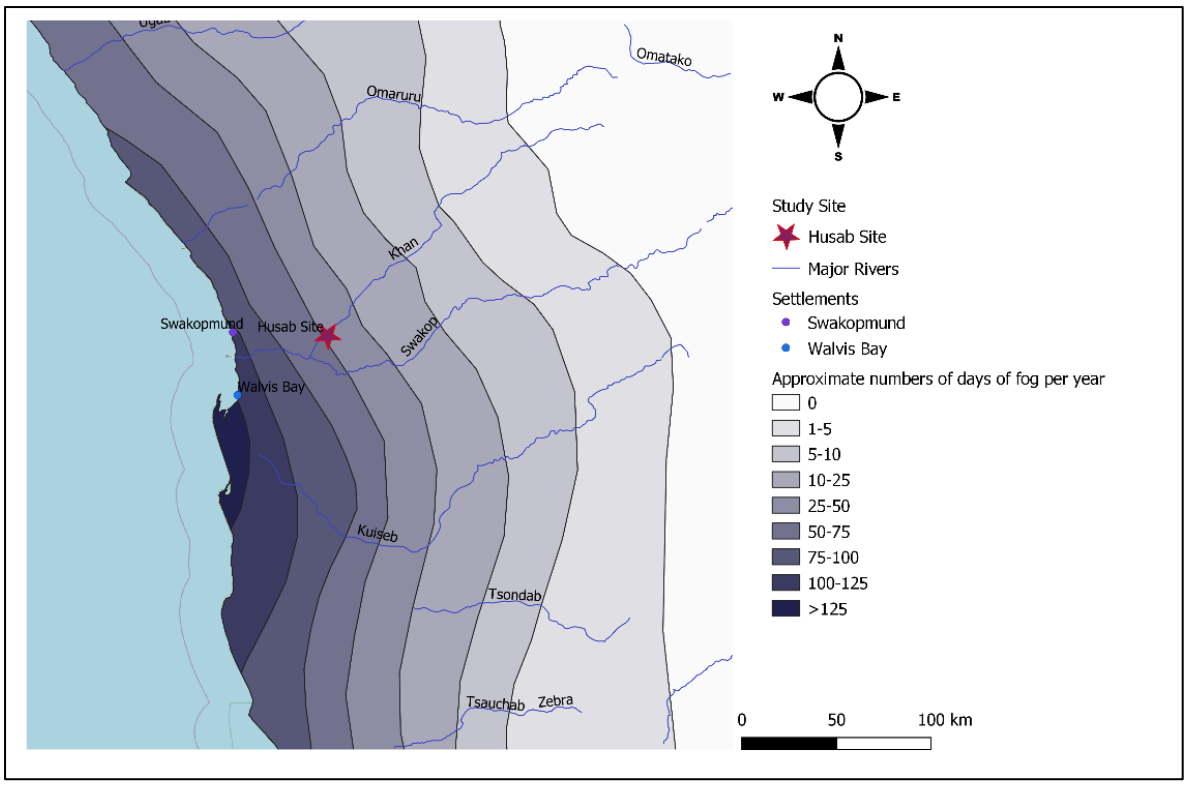


Figure 12: Approximate number of fog days in Central Namibia (Data source: Atlas of Namibia Project, 2002).

On average, the hottest month in Namibia and the Namib Desert is October with daily temperatures of around 34°C (Okitsu, 2005). The coldest month is July, except along the coast where the coldest month is August when minimum temperatures are between 2-10°C (Okitsu, 2005). Average annual temperatures range from higher than 22°C in the northwestern region of Namibia, 19-21°C over central Namibia and 18-16°C and below toward the coastline (Figure 13). In comparison with many other deserts characterized by extremely high temperatures, the Namib has moderately low temperatures due to the cooling effect of the Benguela Current, making this a unique coastal desert (Mupambwa, 2019).

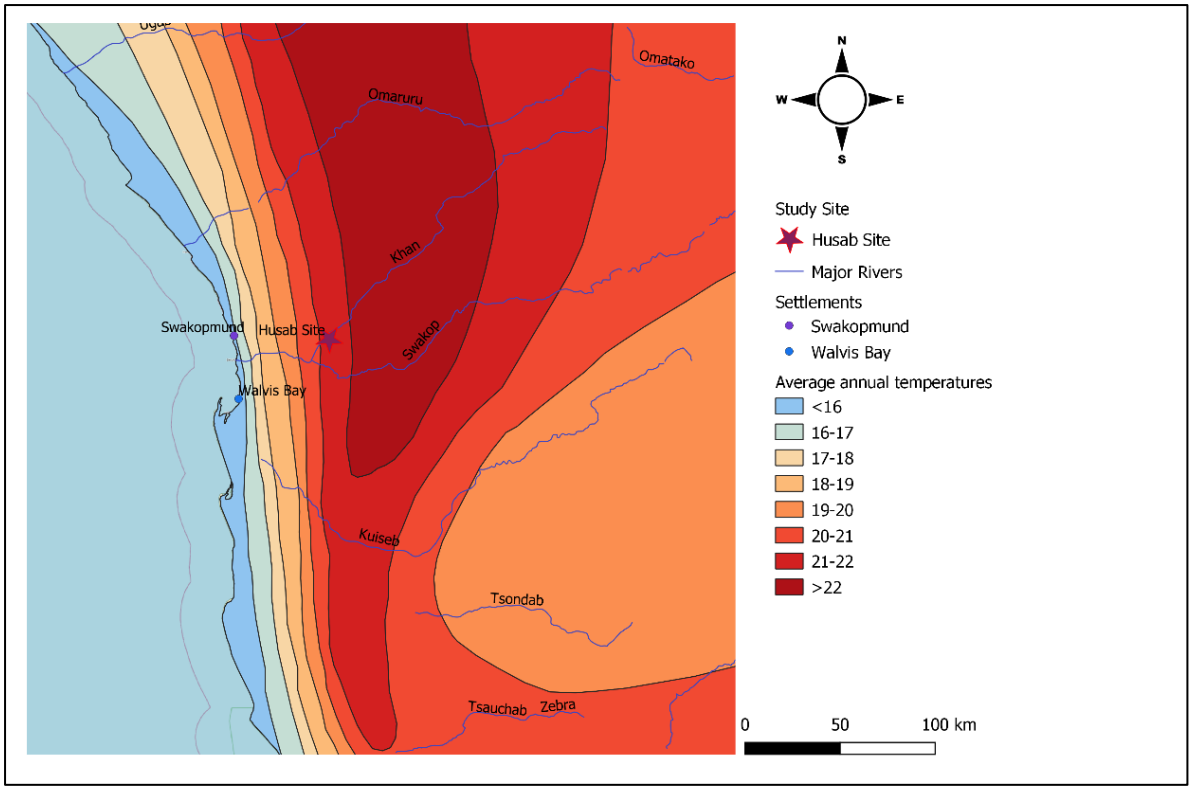


Figure 13: Average annual temperatures in Central Namibia (Data source; Atlas of Namibia Project, 2002).

Future climate projections for Namibia indicate an increase in temperatures (Angula and Kaundjua, 2016). During the summer months, minimum expected increases in the temperature range from 1-2°C, with maximum expected increases ranging from 2-3.5°C (Dirkx *et al*., 2008). In winter, minimum expected temperature increases are 1-2°C and maximum expected increases are as high as 2.5-4°C (Dirkx *et al*., 2008). A more variable pattern of precipitation is likely to occur, together with increased evaporation rates is expected to result in increased aridity in the region (Angula and Kaundjua, 2016; Lendelvo *et al*., 2018).

3.3 Geomorphology

The Namib Desert is reported to be the oldest in the world (Seely and Pallett, 2008). It is characterised by a landscape of gently sloping gravel plains dotted with inselbergs,

and deep ephemeral river valleys (Geyh and Heine, 2014). Approximately 46% of Namibia's surface is exposed bedrock, and the remainder comprises of the younger surface deposits of the Namib and Kalahari Deserts (Schlüter, 2006). Namibia's underlying geology includes the northern Congo craton and the southern Kalahari craton. In-between these, in central Namibia, lies the Damara belt (Oliver and Kinnaird, 1996).

Three fundamental geological events led to the environment in the central Namib Desert (Goudie and Eckardt, 1999). The first was the Damara orogenic phase, started by the rifting of the Congo and Kalahari cratons. The second was the continental break up of west Gondwanaland, and the third was the development of aridity during the Tertiary and Quaternary (Goudie and Eckardt, 1999). The latter is thought to be largely influenced by the opening of the Southern Ocean seaways and the origination of the cold Benguela Current (Goudie and Eckardt, 1999).

The Damara orogenic phase resulted in the Precambrian/ Palaeozoic Damara sequence. These Damara rocks include granites, schists, migmatites, amphibolite, quartzites and gneisses (Goudie and Eckardt, 1999; Schlüter, 2006; Longridge *et al*., 2011). The Damara belt can be separated into northern, central and southern zones (Anthonissen, 2009). The location of the study site in central Namibia is positioned in the central zone of the Damara belt where the most ancient rocks are represented by the Abbabis Metamorphic Complex (AMC), which are around 2100 Ma (Goudie and Eckardt, 1999). The basal Damara rests unconformably on the AMC, with carbonites and pelites overlying it. Several generations of granite intrusions exist, including uranium-bearing Alaskite (uriniferous leucogranite) which is commonly mined in the area (Goudie and Eckardt, 1999; Longridge *et al*., 2011; Corvino and Pretorius, 2013).

The surface geology at the study site comprises of the AMC (Figure 14). The AMC is largely heterogeneous and consists mainly of orthogneisses (Oliver and Kinnaird, 1996).

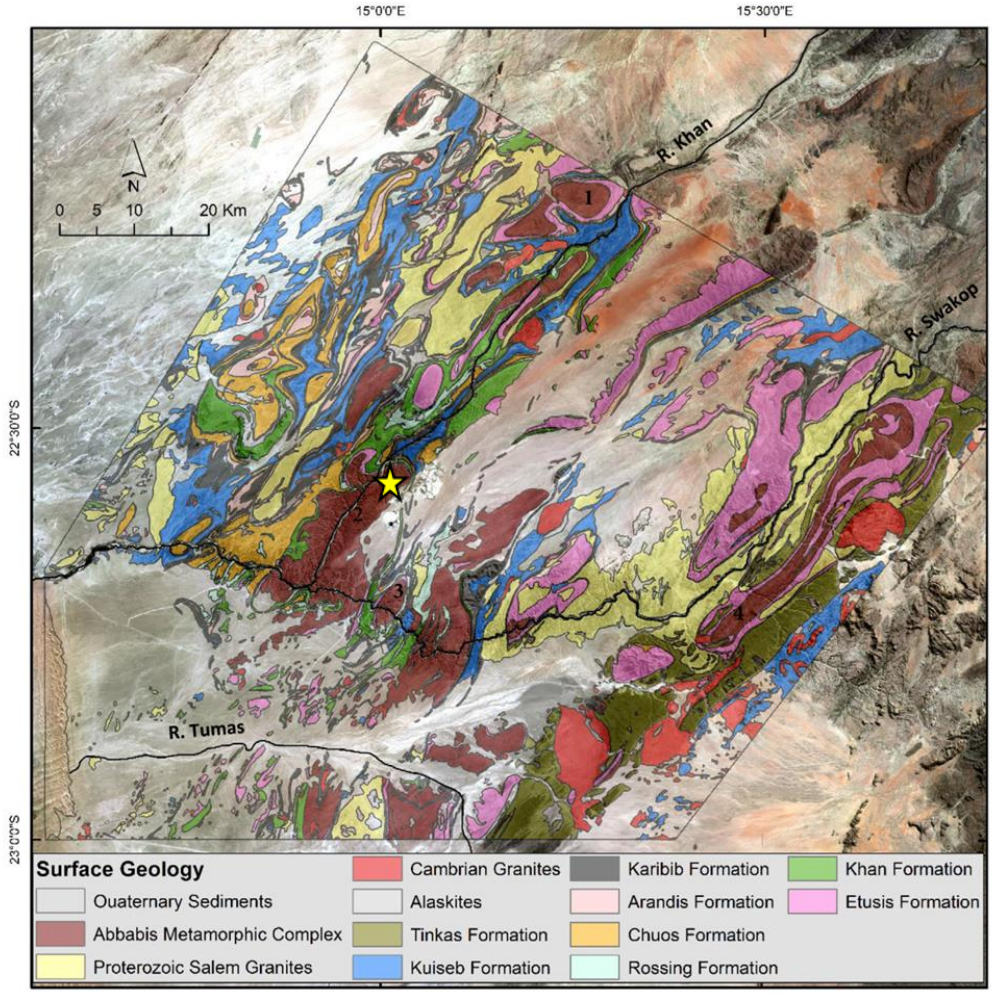


Figure 14: Surface geological map with study site marked as a yellow star (Chudasama *et al*., 2019: 16).

3.4 Flora and Fauna

Namibia comprises of the Caprivi Region, the Central Plateau, the Kalahari, the Great Escarpment, and the Namib Desert (Figure 15, Info-Namibia, 2021).

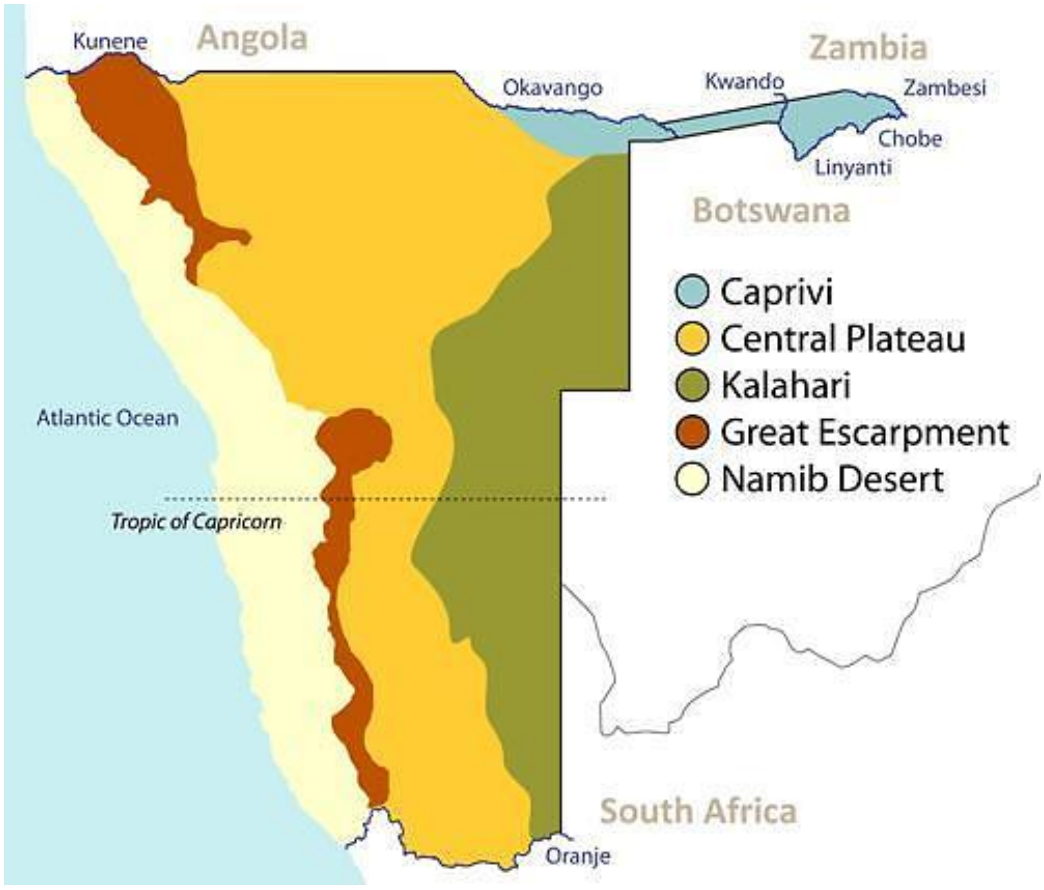


Figure 15: Natural regions of Namibia (Info-Namibia, 2021).

Despite the hyper-arid conditions of the Namib Desert, a wide variety of flora and fauna thrive in the area, many of which are endemic (Midgely *et al*., 2005; Cowan *et al*., 2020). The central Namib Desert is home to numerous species of arachnids, myriapods, crustaceans, insects, amphibians, lizards, birds, mammals and at least 127 different plant species (Pallett *et al*., 2008). Much of the biodiversity in the Namib Desert is sustained by fog, and it is considered to be a fog-dependent habitat (Mitchell *et al*., 2020). Many of the animals and plants that live in the area are specially adapted to harness the moisture brought by the fog, and some animals are adapted to survive without water for long periods (Mitchell *et al*., 2020).

The climatic drivers and geological factors within the Namib, result in distinct plant and animal communities (Wassenaar *et al*., 2013). Irish (1994) identified five different

biomes for Namibia, namely the Savanna, Nama-Karoo, Edaphic Nama Karoo (Etosha basin), Desert and Succulent Karoo biomes. The Erongo region in central Namibia where the study site is located contains the desert, savanna, and Nama karoo biomes (Figure 16).

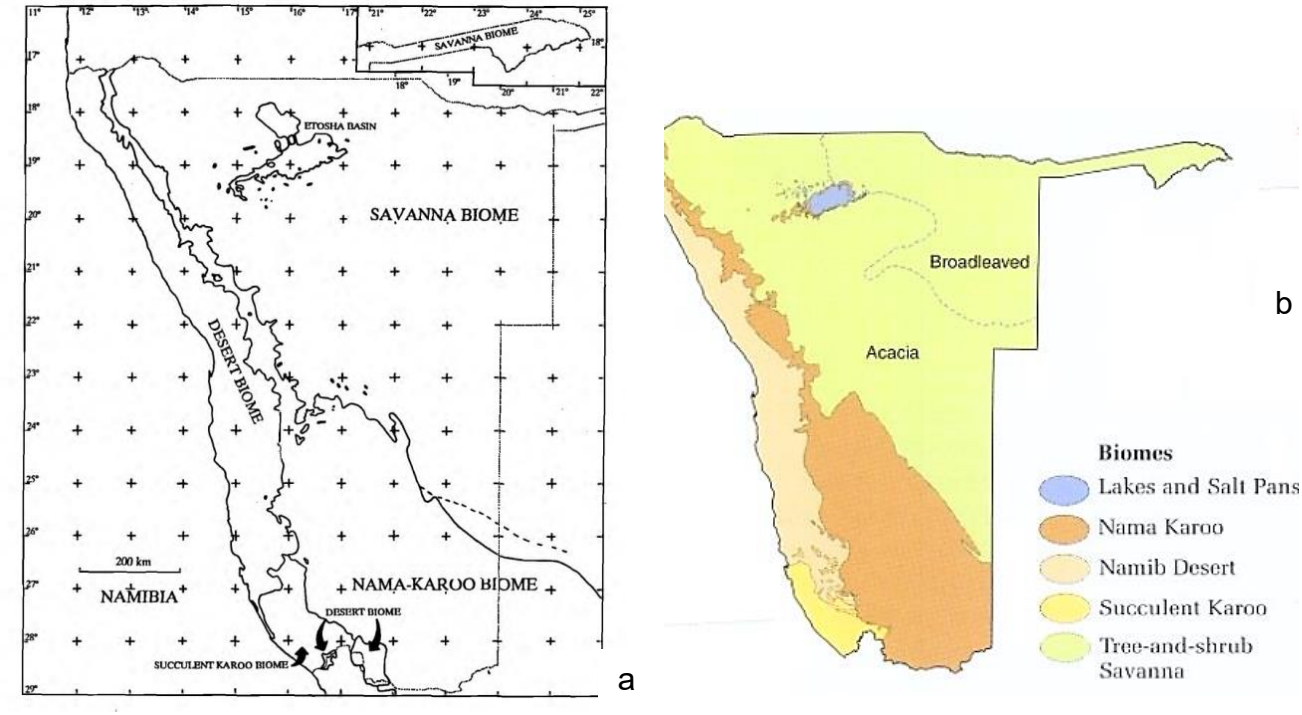


Figure 16: Biomes of Namibia (a) adapted from Irish (1994: 553) and (b) adapted from Mendelsohn *et al*. (2002: 98).

Mendelsohn *et al*. (2002) updated the biomes which now include the Nama Karoo, Namib Desert, Succulent Karoo and the tree-and-shrub Savanna (Figure 16). Under this approach, 29 different vegetation types were identified, with recorded vegetation type along with the associated soils, structure and landscape for each (Table 4; Mendelsohn *et al*., 2002). The study site falls within the Central Desert vegetation type (Mendelsohn *et al*., 2002).

Table 4: Vegetation types in Namibia (adapted from Mendelsohn *et al*., 2002: 99).

Vegetation type		Dominant soils	Dominant structure	Dominant landscape
1	Central Desert	Petric Gypsisols and Petric Calcisols	Sparse shrubs and grasses	Mainlu Central-western Plains
2	Northern Desert	Various	Sparse grasslands	Various
3	Southern Desert	Dune sands	Grassland and dwarf shrublands	Namib Sand Sea
4	Succulent Steppe	Sand, gravel and calcrete	Succulent shrubs	Namib Plains
5	Pans	Mainly Sodic Solonchaks	Pans and grasslands	Salt Pans
6	Western-central Escarpmemt and Inselbergs	Various	Varied shrubland and grasslands	Central-westen Plains
7	Desert – Dwarf Shrub Transition	Mainly Eutric Regosols	Low shrubs and grasslands	Various
8	Dwarf Shrub Transition	Eutric Leptosols	Low shrubs	Nama-Karoo Basin
9	Dwarf Shrub – Southern Kalahari Transition	Ferralic Arenosols and rock outcrops	Grassland and shrublands	Nama-Karoo Basin
10	Etosha Grass and Dwarf Shrubland	Mainly Calcaric Regosols	Grassland and low shrubs	Kalahari Sandveld
11	Karas Dwarf Shrubland	Eutric Leptosols and Petric Calcisols	Grassland and low shrubs	Various
12	North-western Escarpment and Inselbergs	Various	Varied shrubland and grasslands	Kunene Hills
13	Central Kalahari	Ferralic Arenosols	Open *acacia* woodlands	Kalahari Sandveld and Khomas Hochland Plateau
14	Cuvelai Drainage	Eutric Cambisols	Floodplain grasslands or woodlands	Culevai System
15	Highland Shrubland	Lithic Leptosols and Eutric Regosols	Shrubs and low trees	Khomas Hochland Plateau
16	Karstveld	Mainly Mollic Leptosols	Mixed woodlands	Various
17	Mopane Shrubland	Mainly Ferralic Arenosols	Mopane shrub and woodlands	Kalahari Sandveld
18	Southern Kalahari	Ferralic Arenosols	Open *acacia* woodlands	Kalahari Sandveld
19	Thornbush Shrubland	Various	*Acacia* shrublands	Various
20	Western Kalahari	Ferralic Arenosols	Broadleaved woodlands	Kalahari Sandveld
21	Western Highlands	Various	Grasslands and scattered trees	Various
22	Caprivi Floodplains	Eutric Fluvisols	Floodplain grasslands	Caprivi Floodplains
23	Caprivi Mopane Woodland	Eutric Fluvisols and Ferralic Arenosols	Grasslands or woodlands	Kalahari Sandveld and Caprivi Floodplains
24	Eastern Drainage	Ferralic Arenosols	Broadleaved woodlands	Kalahari Sandveld
25	North-eastern Kalahari Woodland	Ferralic Arenosols	Broadleaved woodlands	Kalahari Sandveld
26	Northern Kalahari	Ferralic Arenosols	Broadleaved woodlands	Kalahari Sandveld
27	Okavango Valley	Eutric Fluvisols	Floodplain grasslands or woodlands	Okavango Valley
28	Omtako Drainage	Eutric Fluvisols	Floodplain grasslands or woodlands	Kalahari Sandveld
29	Riverine Woodlands and Islands	Eutric Fluvisols	Tall woodlands	Various

The endemism in Namibia is notable, especially amongst the plant species. Nearly 700 plant taxa that have been recorded in Namibia are endemic (Midgley *et al.* 2005). The Rössing biodiversity assessment compiled a list of endemic plant species

surrounding the Rössing Uranium Mine (Pallet *et al*., 2008). The Rössing Uranium Mine is roughly 10km from the study site and so it would be a good indication of some of the endemic plant species found near the study site location. Table 5 lists endemic plants in the Rössing Uranium Mine project area. Each species has an endemism rating according to the range in which it is found. A more exhaustive list of the assessed taxa found in this area can be found in Appendix C of the Rössing Biodiversity Assessment (Pallet *et al*., 2008).

Table 5: Endemic plant species found within the project area of the Rössing uranium mine recorded 2003-2006. Endemism rating: '3' means that it is only found in central Namib, '2' if the plant is found in the central Namib and one other region, and '1' if the plant is also found in several other regions in Namibia (Pallet *et al*., 2008, Appendix F).

Plant species	**Endemism**
Aizoanthemum galenioides	3
Lithops ruschiorum	3
Cleome carnosa	3
*Adenia pechuelii (*on red list*)*	1
Aizoanthemum membrumconnectens	2
Arthraerua leubnitziae	2
Calostephane marlothiana	2
Euphorbia giessii	2
Hermbstaedtia spathulifolia	2
Marcelliopsis splendens	2
Sarcocaulon marlothii	2
Zygophyllum stapffii	2
Aloe asperifolia	1
Anticharis imbricate	1
Anticharis inflata	1
Commiphora saxicola	1
Commiphora virgata	1
Engleria africana	1
Euphorbia damarana	1
Hermannia amabilis	1
Jamesbrittenia barbata	1
Jamesbrittenia hereroensis	1
Monechma desertorum	1
Nolletia ericoides	1
Ornithogalum stapffii	1
Petalidium canescens	1
Polygala guerichiana	1
Psilocaulon salicornioides	1
Senecio alliariifolius	1
Sesamum marlothii	1
Sesbania pachycarpa subsp. *dinterana*	1
Solanum rigescentoides	1
Stipagrostis damarensis	1
Stipagrostis giessii	1
Stipagrostis hochstetteriana var. *hochstetteriana*	1
Tephrosia monophylla	1
Zygophyllum cylindrifolium	1

The study site is located along a tributary of the Khan River Two protected keystone species of riparian tree (*Acacia erioloba* and *Faidherbia albida*) are mostly found along the ephemeral riverbeds in Central Namibia (AWR, 2012). *Acacia erioloba* (common name: Camelthorn) can occur where no other woody vegetation survives (Kinahan, 2016; Kaseke *et al*., 2018). There are very few young trees, with mature trees being more prevalent indicating slow recruitment. Kinahan (2016) showed that *Acacia erioloba* trees can reach up to 900 years of age, making them ideal as a relatively long-term, high-resolution climate proxy.

Apart from the diverse plant species, the central Namib is also home to many invertebrates, reptiles, birds, and mammals (AWR, 2012). The most common hooved mammals include springbok, kudu, zebra, hartebeest, giraffe and oryx (Mendelsohn *et al*., 2002). Carnivores that can be found in the area include lions, leopards, cheetah, wild dogs, spotted and brown hyenas. However, the largest portion of mammals found is rodents and bats. Up to 258 reptile species can be found in Namibia, with 125 of these being Lizards (Mendelsohn *et al*., 2002). Six different species of tortoise can be found, which is the second-highest number of species found in one area, in the world. A total of 658 species of bird are present, 70% of which live and breed within Namibia (Mendelsohn *et al*., 2002). Scorpions, spiders, and insects are also widespread with hundreds of species occurring (Pallet *et al*., 2008). There is also a relatively high level of diversity and endemism within the animal species in the Central Namib (Pallet *et al*., 2008) that is suggestive of many species evolving in the area and highlights the importance of arid to hyper-arid ecosystems in sustaining incredibly unique and specially adapted species which cannot be found elsewhere (Mendelsohn *et al*., 2002).

Climate change will impact this unique desert ecosystem and may cause major biodiversity loss, especially for endemic species and those that are unable to migrate (Midgley *et al*., 2005; Thuiller *et al*., 2006). Increased aridity may lead to an expansion of the desert, and reduction of grassland and savanna vegetation (Reid *et al*., 2008). Arid ecosystems such as those found in Namibia are extremely sensitive to fluctuations in precipitation and water availability, due to the function of soil moisture in maintaining ecosystem services and floristic diversity (Reid *et al*., 2008). Vegetation changes will also inadvertently impact livestock production, as available grazing lands (Savannah and Woodland and Karoo biomes) could be reduced (Barnes *et al*., 2012). Rainfed crops will also be adversely impacted with increased rainfall variability, placing strain on subsistence farming practices (Reid *et al*., 2008).

3.5 Conclusion

The Namib Desert region is arid, and on average the study site only receives 50mm of annual rainfall. The little rainfall that does occur is predominantly influenced by the CAB, TTT and AL (Eckardt *et al*., 203). Despite this hyper aridity, the region is home to an extensive variety of flora and fauna which thrive. The flora and fauna in the area are able to survive due to the fog that occurs (Kaseke *et al*., 2017). This fog is more dependable than rainfall and is often the only source of water for some species. The geology and sediments of the central Namib Desert also play a role in the vegetation that grows there and subsequently the animals that feed on and shelter in it. Increased rainfall variability and rising temperatures will have negative impacts on biodiversity, and subsistence farming agricultural practices, making the region highly vulnerable to climate change (Reid *et al*., 2008).

CHAPTER 4: MATERIALS AND METHODS

4.1 Introduction

This research project builds on past dendroclimatological research, globally and within southern Africa (Norström *et al.,* 2005; Robertson *et al.*, 2006; Woodborne *et al*., 2015, 2016). Particularly, the methods presented in McCarroll *et al*. (2009) and Woodborne *et al.* (2015, 2016) were used as guidelines from which to carry out this research.

The research is based on carbon isotope theory, which proxies a climatic signal in tree rings. In plants, during transpiration, the stomata on their leaves open allowing, via diffusion, water vapour to escape and CO_2 to be absorbed (Figure 17; McCarroll and Loader, 2004). During the process of carboxylation, there is preferential absorption of $^{12}CO_2$ over $^{13}CO_2$ by the photosynthetic enzyme RUBISCO, and thus ^{12}C is preferentially assimilated into leaf sugars (Hall *et al.,* 2009). The discrimination process is what imparts an environmental signal (McCarroll and Loader, 2004; Hall *et al*., 2009). The ratio of ^{12}C to ^{13}C that is assimilated into leaf sugars provides insight into the environmental conditions experienced by the tree (McCarroll and Loader, 2004). During dry conditions, transpiration rates are reduced to conserve water within the plant through decreased stomatal conductance, and simultaneously, CO_2 intake is decreased (Buckley, 2019). The concentration of CO_2 within the leaf then decreases as the plant initially preferentially assimilates ^{12}C into leaf sugars (McCarroll and Loader, 2004). When the ^{12}C concentration within the leaf is reduced, RUBISCO necessarily assimilates more ^{13}C into leaf sugars ultimately yielding higher $\delta^{13}C$ values (McCarroll and Loader, 2004; Hall *et al*., 2009). The availability of water, therefore, controls the isotopic uptake of carbon, and in areas of low rainfall, and high

temperatures, a higher ratio of assimilated ^{12}C to ^{13}C (more negative $\delta^{13}C$ values) is associated with wetter periods whereas a lower ratio of ^{12}C to ^{13}C (less negative $\delta^{13}C$ values) is associated with dry periods during wood growth (McCarroll and Loader, 2004; Hall *et al.,* 2009; Woodborne *et al.,* 2015). The trees used in this research project were sampled from a location where their major water source would have been rainfall, and because they grew in a desert environment with temperatures being consistently warm, the factor limiting their growth would be water availability. Therefore, the climatic signal in the $\delta^{13}C$ record would more strongly reflect changes in precipitation rather than temperature (Saurer *et al*., 2008).

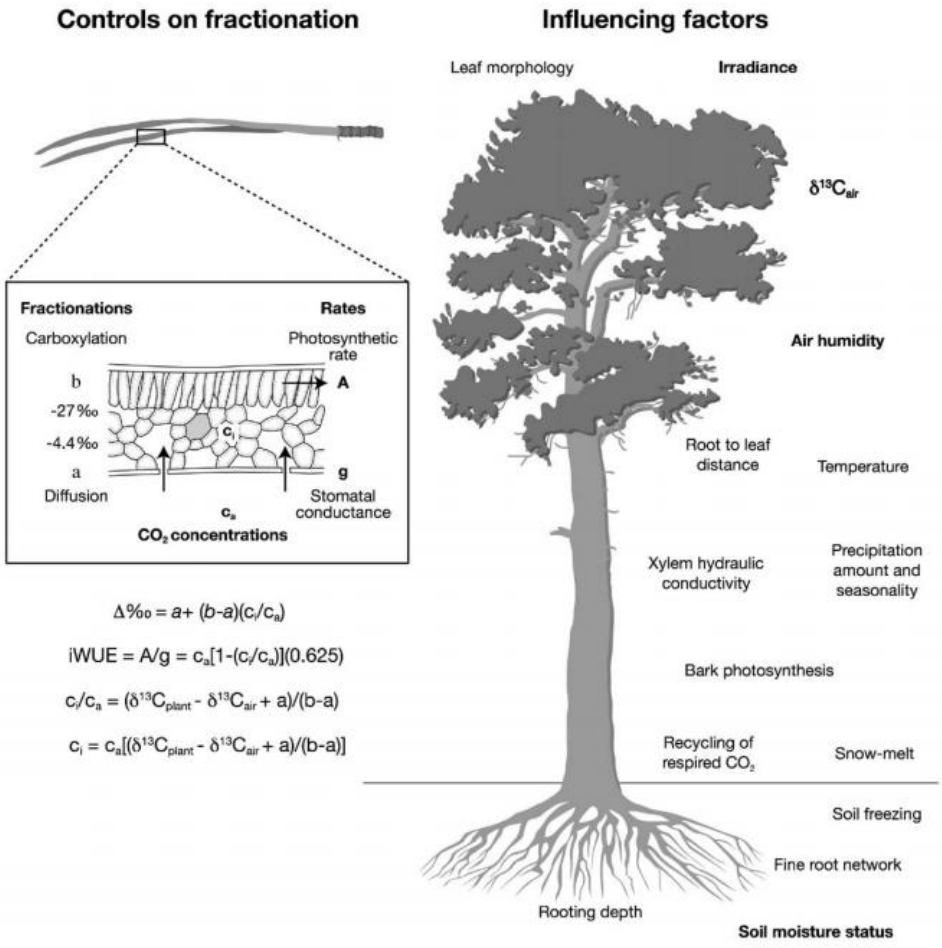


Figure 17: The main controls on carbon isotope fractionation (McCarroll and Loader, 2004: 774).

4.2 Acquisition of tree specimens

This research project uses sample discs acquired from two *Acacia (Vachellia) erioloba* trees (Husab-1 and 2) that were felled during road building near the Husab uranium mine. The trees were discovered at 22°34'24.20"S, 15°0'21.42"E along a tributary of the Khan River in the Erongo Region of central Namibia by Prof. Stephan Woodborne in 2015 under permits issued in Namibia and South Africa (import permits). The trees were specifically chosen as they were situated outside of the main river channel. At the time of sampling, both trees were dead. The discs were obtained using a chainsaw on-site, prior to the commencement of this study. This species is known to grow for hundreds of years and is therefore useful as a climate proxy (Kinahan, 2016). For each tree, a radial section of the trunk disc was prepared and divided in half, one half was used for $\delta^{13}C$ isotopic analysis, and the other half was preserved as a witness section.

4.3 Sampling and subsampling

Due to growth rings being microscopic in *A. erioloba* and prone to occlusion, sampling was not done based on the ring structure. Sub-sampling for $\delta^{13}C$ analysis was performed at the most practical resolution (±0.5mm per isotope sample) along each radial section. The two radial sections that were analysed for this project were named ‘Husab-1’ and ‘Husab-2’ and are 169mm and 445mm in length, respectively (Figure 18). The lighter ends represent the sapwood of the outer part of the tree (the youngest part of the tree), the other end is the centre (pith) of the tree (Figure 18).

The radial tree sections from Husab-1 and Husab-2 were subsampled using a hand-held chisel (Figure 19). To the extent that it was possible, the subsampling followed the wood grain and rings that could be identified, to maintain chronological precision

(Figure 19). Each subsample was placed into a sample bag and labelled accordingly.

A total of 324 and 857 sub-samples were collected for Husab-1 and 2, respectively.



Figure 18: Radial sections Husab-1 and 2 (own photo).



Figure 19a (left) and b (right): indicating the sub-sampling process (own photo).



Figure 20: A close-up of the radial section of Husab-2 (own photo).

4.4 Sample preparation

4.4.1 Soxhlet extraction process

The first step in reducing the sample to cellulose from whole wood is to place them into a specialised test tube that has a small basal hole that allows solvent flow, but no physical sample loss. These specialised test tubes are required for the Soxhlet extraction process which removes resins from the whole wood samples. Each test tube was placed in a specially made carousel that fits into the Soxhlet extractor (Figure 21 and 22).

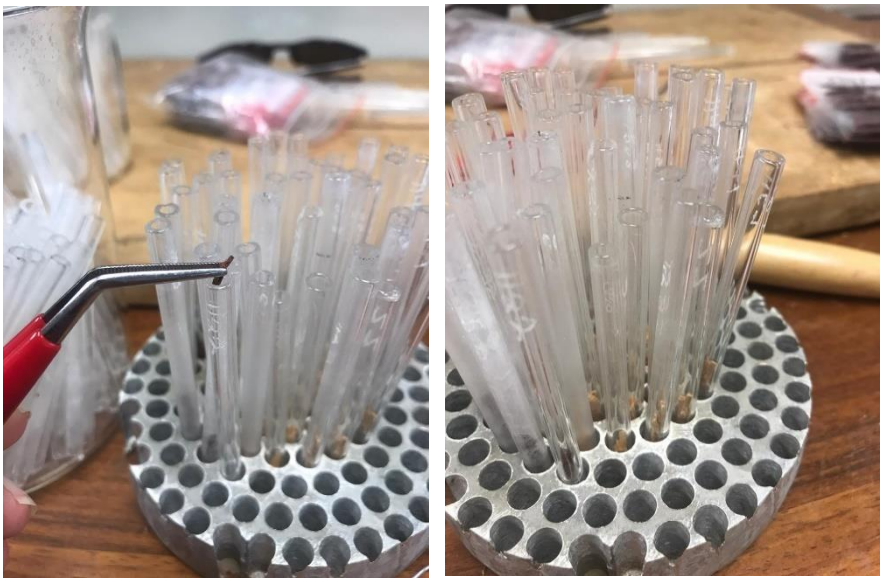


Figure 21: Showing specialised test tubes and carousel used in the Soxhlet extraction process (own photo).

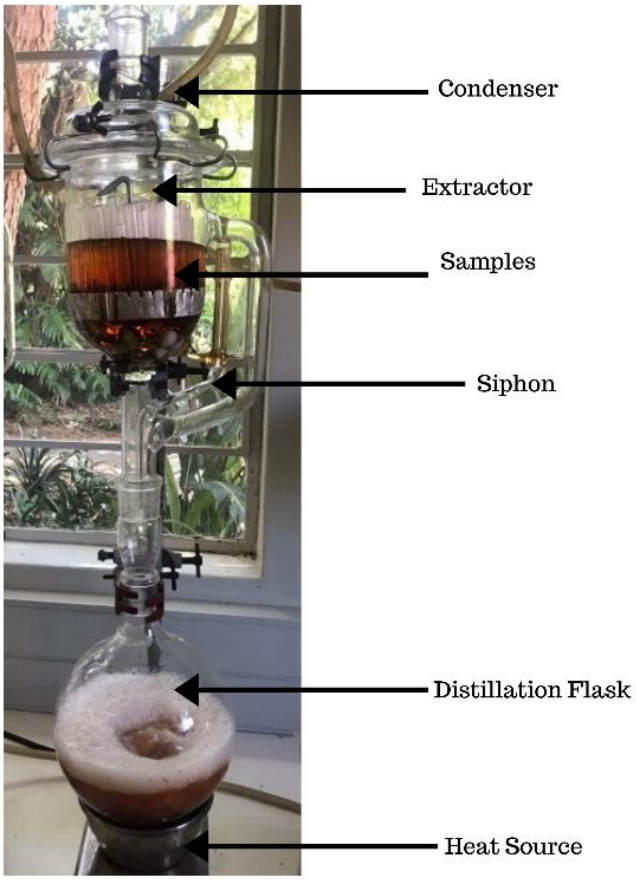


Figure 22: Diagram of the Soxhlet extractor setup microbalance housed at the University of Pretoria Stable isotope laboratory, Mammal research institute (own photo).

During the first Soxhlet extraction an ethanol and toluene mixture was placed in the distillation flask (Figure 22), and in the second extraction, only ethanol was used. This ensures that any resins oils and waxes are removed, which may affect the climate signal in the isotope analysis (Loader *et al*., 1997; 2007). The solvent in the distillation flask turned from clear to a reddish-brown colour as the lipids and resins were extracted from the wood samples.

The samples were processed in the Soxhlet for six hours for each of the solvent systems. Occasionally as the extractor filled up, and the samples were immersed in the solvent which results in the loss of a portion of the sample material. This is one of

the drawbacks of this process, but it is mitigated by the fact that the bulk processing technique allows 124 samples to be processed simultaneously.

The solvent in the extractor becomes clear as the resins are progressively removed and concentrated in the distillation flask. Samples were cooled before removal from the Soxhlet. After each round in the Soxhlet extractor, the samples were dried in a 70°C oven overnight (at least 12 hours).

4.4.2 α-cellulose reduction process:

Samples that had been through both rounds in the Soxhlet and fully dried, were further processed to reduce the whole wood samples into cellulose. A solution of acetic acid and sodium chloride was made by adding 700ml of water, 24ml of acetic acid and 25g of sodium chloride to a beaker and mixed thoroughly.

The dry samples (still in test tubes) were placed in a beaker in a water bath at 70°C (Figure 23). The water was regularly topped up as it evaporated. The acid/chloride solution was added to the beaker and test tubes, taking care to ensure each test tube was about halfway filled with the solution.



Figure 23: Photo of the samples in water bath during the α-cellulose reduction process (own photo).

The length of the α-cellulose reduction process depended on the samples in each test tube as well as the density of the wood. Denser wood and a larger sample size took longer for this process. After each day the solution was decanted, and a new batch of the solution was added to ensure maximum efficacy of the α-cellulose reduction process. Once samples turned white, they were removed (but kept in the test tubes) and placed in distilled water to be kept moist, whilst the other samples continued with the process in the acid bath (Figure 24). The samples took approximately 2 weeks each for the process to be completed. After the samples had sufficiently bleached during α-cellulose reduction, they were vacuum filtered and rinsed twice with distilled water.

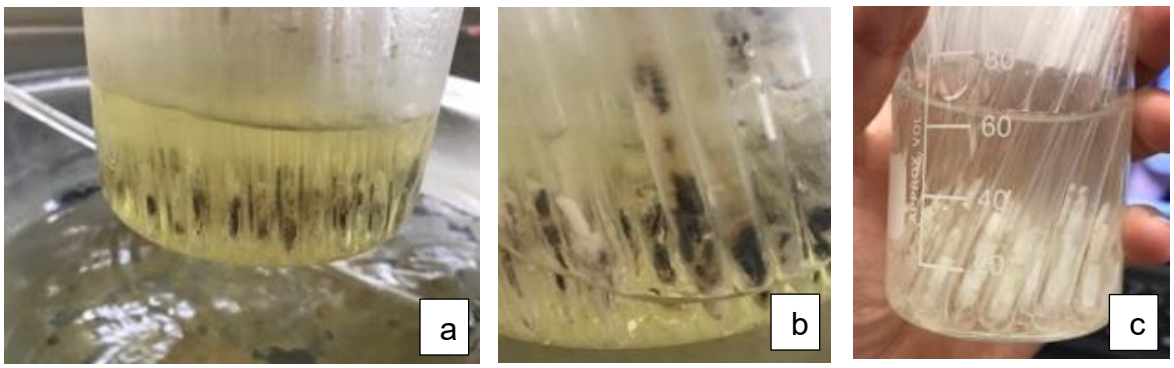


Figure 24: (a) and (b) illustrating samples in the process of α-cellulose reduction and (c) when the process was complete (own photos).

The final step in the alpha-cellulose isolation process was to make a 10% sodium hydroxide (NaOH) solution using 10g NaOH and 1000ml of distilled water. The samples were placed back into the water bath at 70°C covered in the NaOH. After 45 minutes, the samples were vacuum filtered and rinsed once with distilled water.

Next, a 17% NaOH solution was made using 17g NaOH and 1000ml of distilled water mixed in a beaker. The samples were placed back in the water bath and covered in

the sodium hydroxide solution. After 45 minutes, they were vacuum filtered and rinsed once with distilled water. Following this, the samples were washed once with 17% NaOH solution, then with a 1% HCl solution. The samples were vacuum filtered after each wash. After this, the samples were washed four times with distilled water. The samples were then placed in the oven to dry overnight at a temperature of 70°C. Once dry, the samples were carefully placed in labelled sample bags ready for weighing.

4.4.3 Weighing samples

Aliquots of 0.05mg from each sample were weighed, using a Mettler Toledo microbalance (Figure 25), and carefully placed into tin capsules that were precleaned with toluene and dried at 50°C for 24hrs. Each capsule was carefully moulded into a ball (Figure 26) and placed into a tray with an inventory that captured the sample name, weight, and placement in the tray.

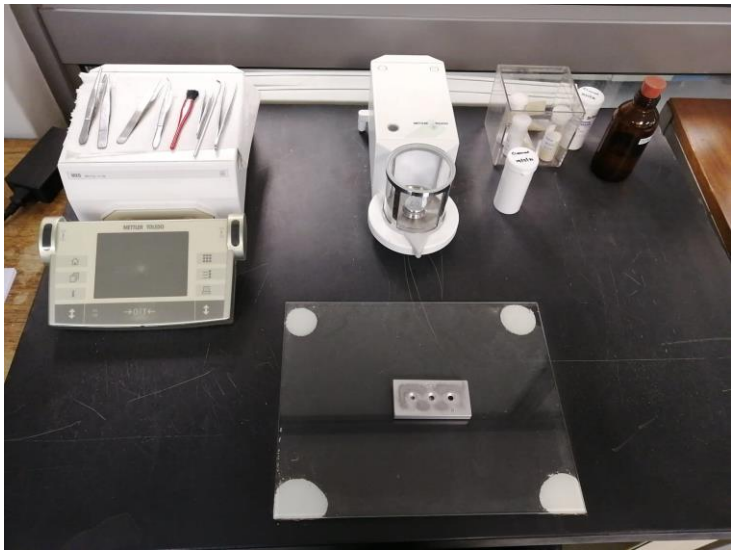


Figure 25: The Mettler Toledo microbalance housed at the University of Pretoria Stable isotope laboratory, Mammal research institute (Robertson, 2021).

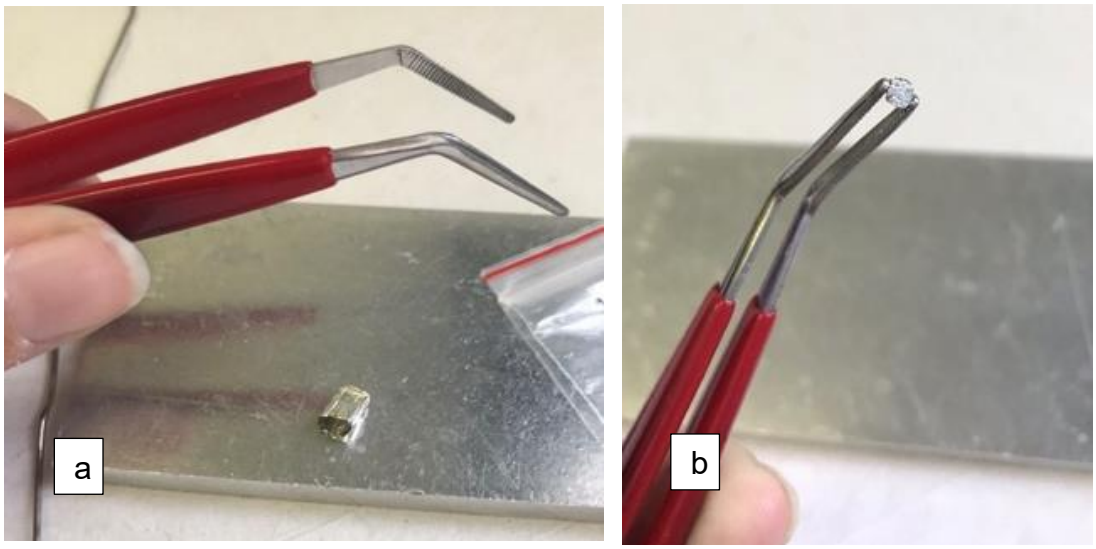


Figure 26: (a) indicating the tin capsule used for weighing, and (b) after it is moulded into a ball (own photos).

4.5 Stable carbon isotope analysis

The samples were analysed using a Delta-V stable light isotope mass spectrometer coupled with a CHNSO 1100 series elemental analyser by a Conflo III interface (supplied by Thermo Fisher, Bremen, Germany) housed at the University of Pretoria Stable Isotope Laboratory (Figure 27 a-b). All samples were measured with the in-house running C_3 standard (*Shorea superba*), of which the isotopic ratio is known, and blanks after every 12 samples with unknown isotopic ratio. Results are expressed as per mille (‰) deviations from the Vienna-Pee Dee Belemnite (VPDB) standard.

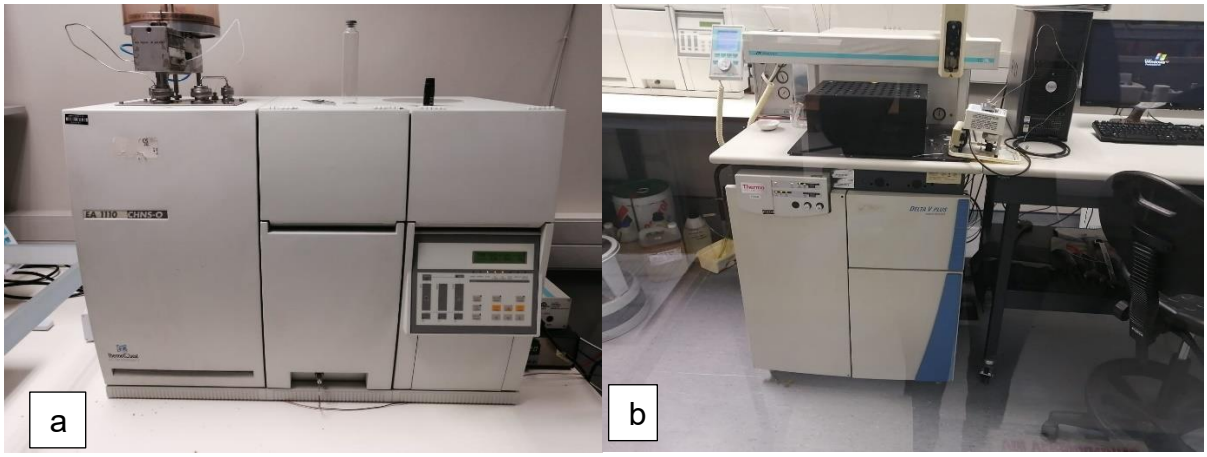


Figure 27: (a) The CHNSO 1100 series elemental analyser and (b) Delta-V stable light isotope mass spectrometer (Robertson, 2021).

4.6 AMS radiocarbon dating

AMS radiocarbon (^{14}C) dating was performed on selected samples to create a chronology for the two trees. Samples were submitted to iThemba LABS, Johannesburg, for analysis. A total of six samples were submitted for Husab-1 (1, 3, 85, 167, 251, and 252), and 11 samples were submitted for Husab-2 (1, 214, 215, 334, 430 and 431, 644, 645, 859 and 860). If there was insufficient sample material for analysis, two consecutive aliquots were added together. For Husab 1, samples 1 and 3 were merged, and for Husab 2 samples 430 and 431 were merged.

A linear age model was used to establish the time of death and the overall age of the trees (after Woodborne *et al*., 2016). The radiocarbon dates were calibrated using the Southern Hemisphere 'SHCal20' dataset, found at: http://calib.org/calib/ (Hogg *et al*., 2020). AMS radiocarbon ^{14}C ages with percent modern carbon (pMC) values above 100% were assumed to be post-bomb carbon values and were calibrated according to the post-bomb calibration dataset 'SHZ1_2' found at: http://calib.org/CALIBomb/ (Hua and Barbetti, 2004).

4.7 Corrections

The isotopic time series created for each tree was corrected for temporal changes of $\delta^{13}C$ in the atmosphere over time and for changes in intrinsic water use efficiency that have occurred because of the increase in atmospheric CO_2 concentrations (Farquhar *et al*., 1982; McCarroll and Loader, 2004; McCarroll *et al*., 2009; Belmecheri and Lavergne, 2020). The corrections were performed following the correction procedure used by Woodborne *et al*. (2015, 2016). These corrections have been known to improve correlations with local meteorological data (Loader *et al*., 2007; McCarroll and Loader, 2008; Belmecheri and Lavergne, 2020). The dataset provided by Belmecheri and Lavergne (2020) was used to ascertain the concentration of carbon dioxide in the atmosphere, and the isotopic ratio of ^{12}C to ^{13}C for each year.

4.8 Contemporary meteorological data

Contemporary meteorological data for the study site were obtained from Google Earth Engine (GEE), specifically the "CHIRPS Pentad: Climate Hazards Group InfraRed Precipitation with Station Data (version 2.0 final)" data set for precipitation from 1981-2021https://developers.google.com/earth-engine/datasets/catalog/UCSB-CHG_CHIRPS_PENTAD#description). Climate Hazards Group InfraRed Precipitation with Station data (CHIRPS) is listed as a 30+ year quasi-global rainfall dataset that uses 0.05° resolution satellite imagery with in-situ station data to create gridded rainfall time series for trend analysis and seasonal drought monitoring (Funk *et al*., 2015). The "MOD11A2.006 Terra Land Surface Temperature and Emissivity 8-Day Global 1km" data set was used to collect land surface temperature from 2000-2021 (https://doi.org/10.5067/MODIS/MOD11A2.006). The products are at 5km (rainfall) and 1km (land surface temperature) resolution in relation to the coordinates of the

study site. Additional ground-based and precipitation data were obtained from the Rössing uranium mine (-22.478, 15.048) for 1984-2021.

4.9 Statistical analyses

The Shapiro-Wilk normality test was performed for data sets from Husab-1 and Husab-2. The data was then correlated with environmental indices including ENSO using the SOI, IOD, SAM and SST using Spearman's rank correlation coefficient to determine if there were significant relationships.

The El Niño Southern Oscillation is known to impact climate in southern Africa, it is important to understand how it impacts rainfall in the Central Namib for the period before meteorological observations become available, as there is a paucity of information regarding this. The SOI dataset was obtained from the NOAA Physical sciences laboratory at https://psl.noaa.gov/gcos_wgsp/Timeseries/SOI/.

The SAM has significant links to dry periods experienced in the Southern Hemisphere (Malherbe *et al*., 2015). It is important to understand how the SAM may influence precipitation in the central Namib Desert. SAM dataset was obtained from Abram *et al*. (2014).

The IOD is known to be a driving mechanism for climate variability in parts of Africa (Merchant, *et al*., 2006). However, its influence on precipitation variability in the central Namib Desert is not well understood. IOD dataset (DMI HadISST1.1) was obtained from the NOAA Physical sciences laboratory at: https://psl.noaa/gov/data/timeseries/DMI.

SST is also well known to impact precipitation variability within southern Africa (Nichoson, 2000). Using these analyses, we can better understand how SST act as a driving force for precipitation variation in the central Namib Desert. The SST anomalies dataset was obtained from Zinke *et al*. (2014).

CHAPTER 5: RESULTS

5.1 Introduction

This project aims to extend knowledge of climate and rainfall variability for the central Namib Desert by constructing a high-resolution hydro-climate record using stable carbon isotope ($\delta^{13}C$) analysis on *Acacia erioloba.* In this chapter, the AMS radiocarbon dates, age model and the $\delta^{13}C$ time series are presented. Gridded data and meteorological station data from Pointbill station near Rössing uranium mine are presented to provide the modern context and possible calibration data for the $\delta^{13}C$ data. Non-parametric correlation analyses (Spearman's rank correlation coefficient) are presented, interrogating common forcing between the isotope time series and climatic drivers including SST and the SOI, IOD, and SAM. These indices were chosen for comparison as they are implicated in driving rainfall variability over the subcontinent (Jury, 1996; Jury and Engert, 1999; Merchant, *et al*., 2006; Malherbe *et al*., 2015).

5.2 Radiocarbon dates

5.2.1 Husab-1

A total of six AMS radiocarbon dates were obtained for Husab-1. The samples for dating were selected to span the growth of the tree, and include sample numbers 1 and 2, 85, 167, 168, 251 and 252 (out of a total of 334 samples for this tree) (Table 6). The errors on the ^{14}C dates ranged from 38 years (Hus1_168) to 98 years (Hus1_167). Some of these errors are higher than usual, which was caused by problems with the AMS system at iThemba LABS. Replicate samples were run to address this problem, which is the reason for duplicating samples so close to one another, but all results are presented here (Table 6 and 7). The measured AMS dates ranged from 253 ±81 ^{14}C

yr BP for sample Hus1_251 to the youngest date with a pMC of 145.7 ± 1.474 for sample Hus1_1 indicative of a post-bomb date (Table 6). The 1-sigma calibrated dates range from ~1973 cal yr CE for Hus1_1_2, to ~1546 cal yr CE for Hus1_251 (Table 7).

Table 6: AMS radiocarbon dates for Husab-1 and associated calibrated calendar dates (* asterisk symbol indicates pMC value)..

Sample Name	Lab number	^{14}C Age (BP) / **pMC value***	Error	Sample number	1-sigma	2-sigma
Hus1_1_2	IT-C-3519	**145.7***	**1.474***	2	1972-1973	1963-1964 1972-1974
Hus1_85	IT-C-3573	254	78	85	1512-1546 1721-1811 1837-1947 1868-1877 1928-1939 1943-1950	1503-1596 1902-1950
Hus1_167	IT-C-3578	214	98	167	1650-1712 1717-1814 1834-1890 1924-1950	1508-1587 1621-1950
Hus1_168	IT-C-3775	169	38	168	1681-1732 1803-1815 1833-1891 1923-1950	1672-1744 1753-1765 1772-1781 1796-1950
Hus1_251_252	IT-C-3572	218	69	252	1651-1708 1720-1812 1867-1878 1926-1950	1515-1541 1627-1950
Hus1_251	IT-C-3513	253	81	251	1512-1546 1624-1700 1721-1811 1868-1877 1927-1950	1503-1595 1615-1897 1901-1950

5.2.2 Husab-2

A total of 11 AMS radiocarbon dates were obtained for Husab-2 from sample numbers 1, 214, 215, 334, 430 and 431, 644, 645, 859 and 860. The errors on the ^{14}C dates ranged from 29 years (Hus2_859_860) to 141 ^{14}C yr BP (Hus2_430_431). These dates ranged from the oldest date of 480 ± 109 ^{14}C yr BP years and the youngest pMC value of 100,894 ± 0.534 (Table 7). The Sigma 1 calibrated dates for Husab-2 range from ~1960 cal yr CE for Hus2_1 to ~1628 cal yr CE for Hus2_860 (Table 7).

Table 7: AMS radiocarbon dates for Husab-2 and associated calibrated calendar dates (* asterisk symbol indicates pMC value).

Sample Name	Lab number	^{14}C Age (BP) / **pMC value***	Error	Sample number	1-sigma	2-sigma
Hus2_1	IT-C-3520	120	81	1	1648-1710 1719-1812 1836-1860 1925-1950	1510-1550 1560-1578 1623-1950
Hus2_1	IT-C-3777	**100.894***	**0.534***	1	1950-1950 1955-1957	1950-1950 1955-1957 2017-2019
Hus2_214	IT-C-3772	200	40	214	1668-1699 1722-1726 1792-1811 1837-1846 1869-1877 1928-1938 1943-1950	1659-1825 1828-1893 1921-1950
Hus2_215	IT-C-3530	377	80	215	1463-1469 1482-1628	1418-1674 1738-1757 1762-1775 1778-1798
Hus2_334	IT-C-3571	134	47	334	1698-1722 1810-1838 1845-1869 1876-1929 1937-1945	1674-1738 1757-1762 1775-1778 1798-1798
Hus2_430_431	IT-C-3569	413	141	431	1414-1663	1317-1357 1384-1714 1716-1815 1833-1891 1923-1950
Hus2_644	IT-C-3771	219	46	644	1654-1697 1724-1810 1840-1842 1871-1874 1947-1950	1644-1824 1829-1893 1921-1950
Hus2_645	IT-C-3532	480	109	645	1400-1512 1546-1565 1671-1624	1296-1369 1375-1668 1786-1792
Hus2_859	IT-C-3570	408	83	859	1452-1515 1541-1627	1406-1670 1783-1795
Hus2_859_860	IT-C-3776	283	29	860	1628-1671 1767-1771	1510-1549 1560-1577
Hus2_860	IT-C-3531	400	81	860	1782-1796 1455-1515 1540-1627	1623-1675 1412-1671 1767-1770 1782-1795

5.3 Age model

The calibration of the AMS radiocarbon results yields multiple possible date ranges (Tables 6, 7). This is caused by having multiple intersections along the calibration curve. Results such as this are very common during the period after the beginning of the industrial revolution, and nuclear testing and is referred to as the Suess effect

(Pazdur *et al*., 2007; Andreu-Hayles *et al*., 2015; Eide *et al*., 2017). Precise dating of single tree rings pre-nuclear testing (1650-1950) is especially difficult due to the large fluctuations in atmospheric ^{14}C, this results in poor precision of dates (Hua, 2009).

The termination dates for Husab-1 and 2 post-date the above-ground nuclear weapons testing which began in the 1950s. During this time, excess amounts of ^{14}C were injected into the atmosphere. Even after the nuclear test ban treaty in the 1960s, the percentage of ^{14}C in the atmosphere was extremely high (Hua and Barbetti, 2004). Detection of pMC values greater than 100 in tree rings is a temporally specific marker for this period (Andreu-Hayles *et al*., 2015; Santos *et al.*, 2015). To narrow down the possible calibrated date ranges for each sample, a linear age model is used which is similar to the approaches used by (Woodborne *et al*., 2016, 2018). The post bomb carbon values, for Hus1_1 and Husab 2_1 (Table 6 and 7), are used to constrain the younger end of the age models because the bomb carbon results are very specific in terms of age where the date of death of the tree is not known. However, due to the uncertainty and poor precision on the radiocarbon dates an alternative approach is required to further constrain the age model. The approach that is used presumes that both trees experienced the same climate (they grew a few 100m apart) and so the age model is afforded *a priori* knowledge from the patterning in the $\delta^{13}C$ time series. This is done within the constraints of the calibrated radiocarbon dates to improve the accuracy of the age model.

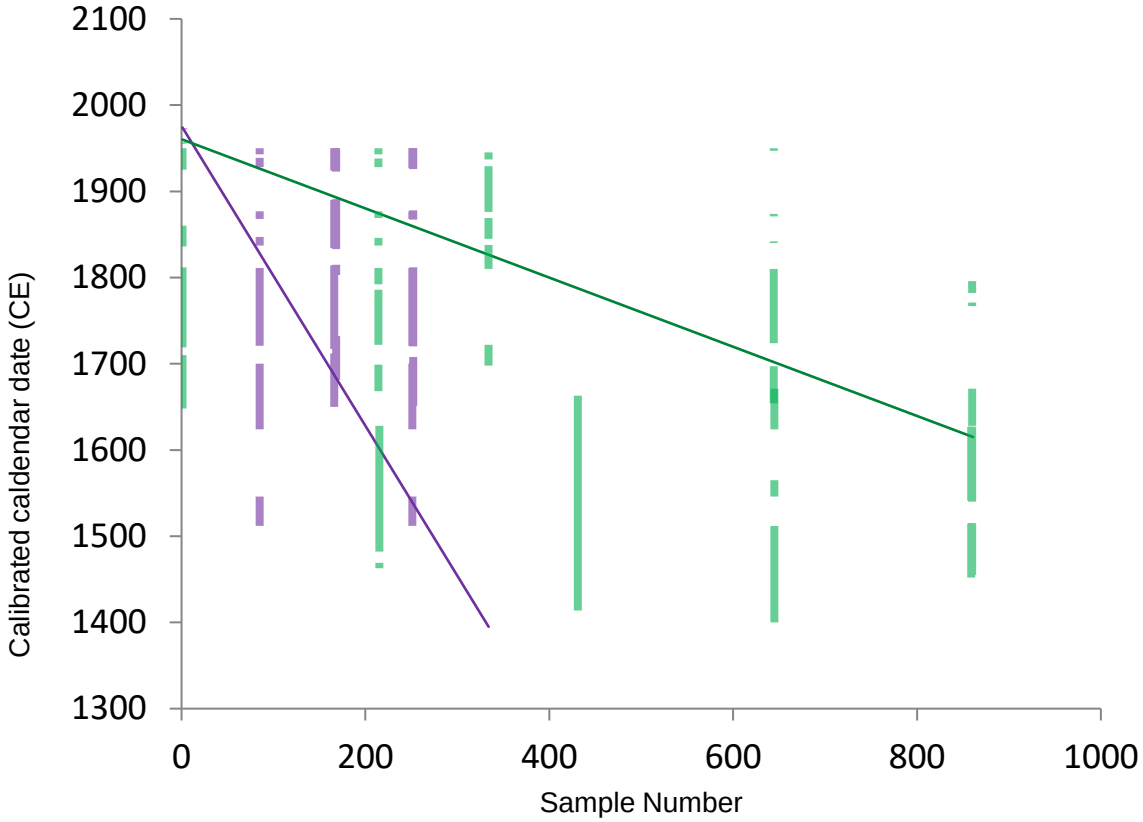


Figure 28: Calibrated intercept ranges (1-sigma) (Tables 6 and 7) are represented as the purple and green vertical bands. The thin horizontal lines of the same colours represent the age model, which is a linear relationship between sample number and calendar age commencing with '0' representing the bark of the tree. Husab-1 is represented in purple, and Husab-2 is represented in green.

The age model intercepts nearly all radiocarbon ages in the 1-sigma range and all in the 2-sigma range, respectively (Figure 28). This linear age model was applied to produce the interpolated values for the $\delta^{13}C$ samples. The precision of each model is not very good because of the Suess Effect, and due to the poor precision of the radiocarbon analyses. Woodborne *et al*. (2016) noted that in climate matched records between different trees from the same location the radiocarbon dates from either tree help to constrain the age model of the others and they suggested a precision of approximately +-5 years. In this case, it is not possible to obtain such good precision and a value of +-25 may be more appropriate. This means that analyses of the high-

frequency component of the records may be problematic, as are direct comparisons between trees in periods of rapid climate oscillations.

The age model suggests that the Husab-1 sample lived for ~579 years, with the earliest preserved growth (the centre of the tree had decayed away) in ~1395 cal yr CE and termination of the record in ~1974 cal yr CE. Husab-2 has an interpolated duration of age of ~345 years, with the first recorded year of growth in ~1615 cal yr CE and termination of the record in ~1960 cal yr CE(Figure 28). As there is no evidence for disturbances to the preservation of the outermost area of the tree sample, the termination dates can be interpreted to represent the year of death of each tree, which in both cases was prior to the date of sampling (2015). The sampling density of 0.5mm represents near-annual records for Husab-1 (0.5mm=1.08 samples/year) and near-biannual records for Husab-2 (0.5mm=2.15 samples/year).

5.4 Age constrained stable carbon isotope analysis

The $\delta^{13}C$ values for the samples from each of the trees, measured using the mass spectrometer, were corrected for intrinsic water use efficiency, and the increase in anthropogenic CO_2 in the atmosphere using the approach of Woodborne *et al*., (2015, 2016) and the dataset of Belmecherie and Lavergne, 2020). This is important in ensuring that the $\delta^{13}C$ values represent the only environmental signal and are not confounded by other factors that impact carbon isotope fractionation during photosynthesis.

Based on carbon isotope theory (detailed in chapter 4), more negative $\delta^{13}C$ values are interpreted to represented relatively wetter periods, while less negative values are

interpreted as indicative of relatively drier periods. Husab-1 and Husab-2 records overlap over the period ~1615-1960 cal yr CE (Figure 29). The period ~1395-1615 cal yr CE is represented only by Husab-1, and the period ~1960-1974 cal yr CE is represented only by samples from Husab-2 (Figure 29). Separate figures for Husab-1 and Husab-2 plotted against sample number can be found in Appendix 1 and 2.

The coherence of the two records for the period of overlap can be quantitatively assessed through correlation analysis. First, the normality of the distribution was assessed using the Shapiro-Wilk test, yielding W values of 0.97 ($p < 0.0001$) and 0.99 ($p < 0.1936$) for the $\delta^{13}C$ records for Husab-1 and Husab-2, respectively. This indicates that the $\delta^{13}C$ records for Husab-1 did not pass the normality test while those of Husab-2 are normally distributed. Due to at least one data set being non-Gaussian, non-parametric statistical methods are used, and correlation was explored through Spearman's Correlation Coefficient. This test reveals that there is no statistically significant correlation between Husab-1 and 2 for the period of overlap of the samples ($r=-0.04$; $p=0.2069$). It is important to note that the statistic is profoundly impacted by the precision of the age model, as errors of just a few years will superimpose wet and dry cycles yielding a negative correlation. From a more qualitative perspective, there is reasonably coherence in many of the periods of particularly high and low $\delta^{13}C$ values from the two records.

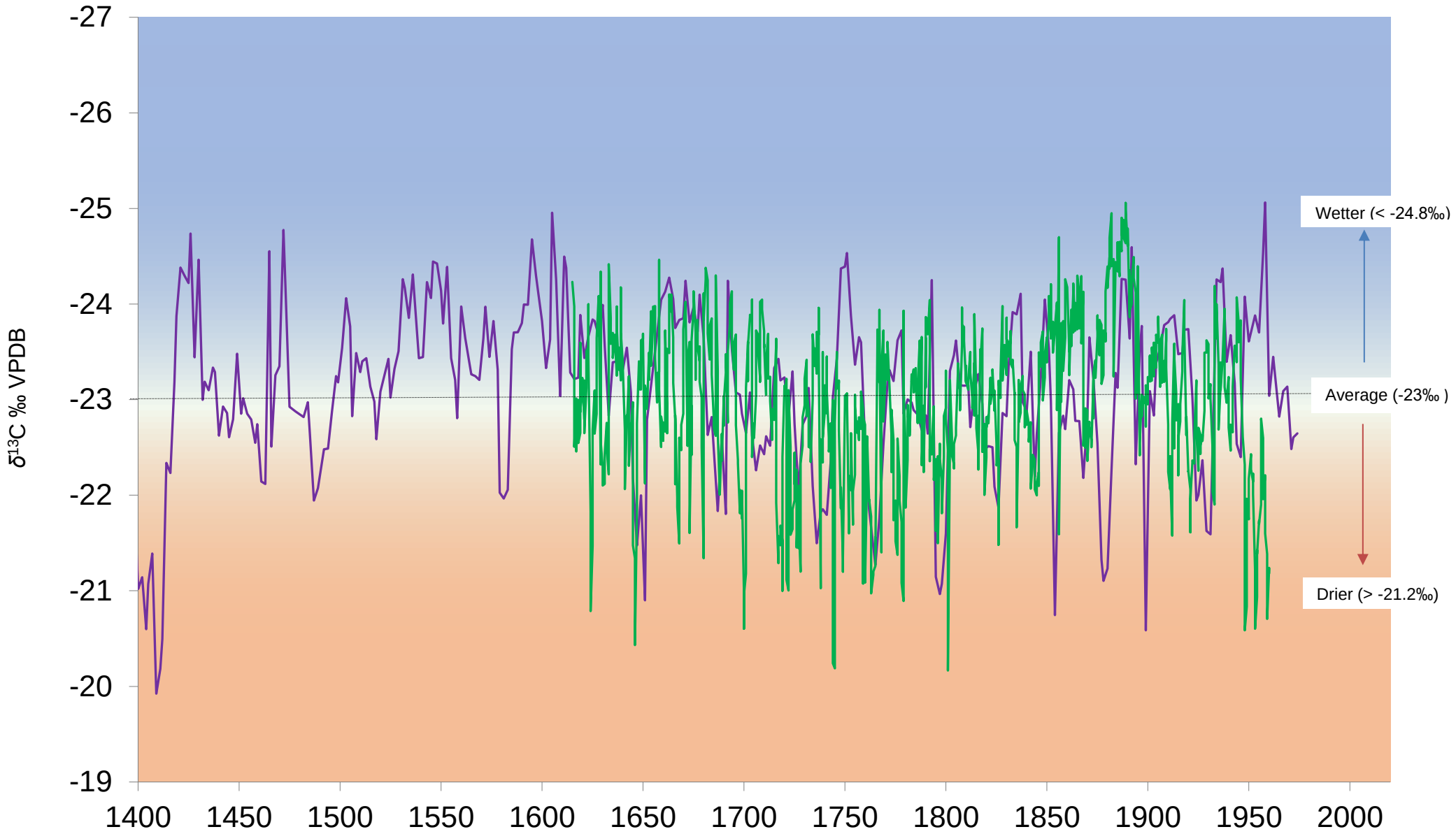


Figure 29: $\delta^{13}C$ (‰ VPDB) isotopic time series for Husab-1(purple) and Husab-2 (green) representing a proxy rainfall scale with wetter periods at the top and drier periods at the bottom of the graph.

The average $\delta^{13}C$ value across both trees is approximately -23‰ (-23.09 for Husab-1, -22.98‰ for Husab-2) (Figure 29). Values which are within ±2σ of the mean (1.8‰) can be considered representative of the average hydroclimate conditions through the record. Values outside of the 2σ range (i.e., <-24.8‰, or >-21.2‰) are therefore interpreted as representing comparatively wet or dry conditions respectively for the region (Table 8; Figure 30). The $\delta^{13}C$ records from both Husab-1 and Husab-2 have a high-frequency component with inter-annual variability, as well as approximately 25-year cycles of variability. Low amplitude cycles characterised by fluctuations in $\delta^{13}C$ between -20‰ and -25‰ have a periodicity of approximately 150-200 years.

Table 8 indicates a disparity between the relatively wet and dry years reflected in the $\delta^{13}C$ records from Husab-1 and 2 in the high-frequency component that reflects the problems in the precision of the respective age models. The periods of relatively average water availability coincide, and there is agreement for the relatively wet and dry periods but at different intensities. Most of the peaks and troughs for each tree follow the same trend but some of the values are within the 2σ range and are excluded from Table 8. There are some instances of disagreement, particularly there is a wet period between ~1856 and ~1893 reflected in the record for Husab-2 that is not present for Husab-1. ~1854 is a particularly dry year reflected in the $\delta^{13}C$ record for Husab-1. There is agreement in the record for Husab-2 but the $\delta^{13}C$ value falls within the 2σ range and is not represented in Table 8. It is important to note that these wet and dry years are approximate, and not exact due to the large error ranges in the radiocarbon dates.

Table 8: List of approximate relatively wet and dry years according to rainfall proxy for Husab-1 and 2 (extremely dry years are noted with an Asterix*).

Type of year	Husab-1	Husab-2
Wet (< -24.8‰)	~1472 cal yr CE ~1605 cal yr CE ~1958 cal yr CE	 ~1856 cal yr CE ~1881-1882 cal yr CE ~1886-1889 cal yr CE ~1890 cal yr CE ~1893 cal yr CE
Dry (> -21.2‰)	~1400 cal yr CE ~1402 cal yr CE ~1404-1405 cal yr CE ~1409 cal yr CE* ~1411*-1412 cal yr CE ~1651 cal yr CE ~1765 cal yr CE ~1795 cal yr CE ~1797-1798 cal yr CE ~1854 cal yr CE ~1878 cal yr CE ~1880 cal yr CE ~1899 cal yr CE	 ~1624 cal yr CE ~1646 cal yr CE* ~1668 cal yr CE ~1673 cal yr CE ~1680 cal yr CE ~1700-1701 cal yr CE ~1717 cal yr CE ~1719 cal yr CE ~1721-1722 cal yr CE ~1728 cal yr CE ~1738 cal yr CE ~1744-1745 cal yr CE* ~1759-1760 cal yr CE ~1763 cal yr CE ~1779 cal yr CE ~1801 cal yr CE ~1948-1949 cal yr CE ~1953-1954 cal yr CE ~1959-1960 cal yr CE

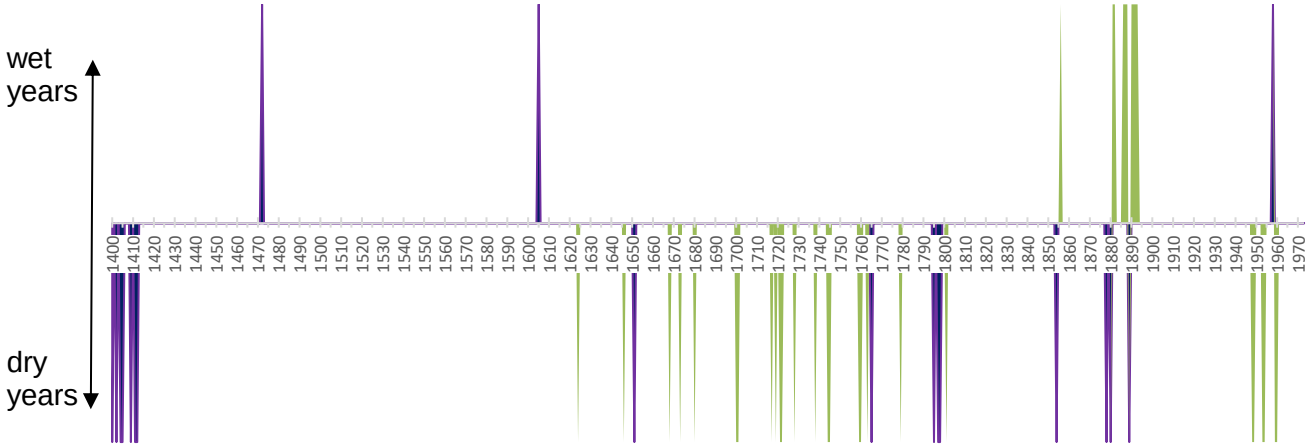


Figure 30: Relatively wet and dry years for Husab-1 (purple) and Husab-2 (green) between ~1400 and ~1970 cal yr CE. Wet years are above, and dry years are represented below the axis line.

Extreme events are categorised by values that fall within the 5th and 95th percentile of the data. Extremely dry years are present in the isotopic time series during ~1409 cal yr CE, ~1411 cal yr CE, ~1646 cal yr CE and ~1745 cal yr CE, and no extreme wet years are present (Table 8).

5.5 Meteorological data

Ideally, the dendroclimatic data would be compared to meteorological station data and/or gridded climate data for the same period to triangulate the interpretation of the $\delta^{13}C$ records, confirm the age model, and provide a quantitative measure of the absolute rainfall amounts and departures represented by the $\delta^{13}C$ values. The CHIRPS Pentad gridded dataset spans the period 1981-2021, and the ground-based and precipitation (Pointbill station) data obtained from the Rössing uranium mine span the period 1984-2021. No longer-term rainfall data have been found for this region.

This means there is no temporal overlap between the AMS-dated $\delta^{13}C$ records and the instrumental rainfall data. However, the meteorological data (Figure 31) can provide context as to the regional hydroclimate conditions and the synoptic drivers that may influence rainfall.

The instrumental and gridded data are highly significantly correlated ($r=0.7$; $p < 0.0001$). The mean annual precipitation for the gridded data is 75mm, while the Pointbill station data has mean annual precipitation of 28mm. The study area falls within the summer rainfall zone and the majority of the rainfall occurs from November to April. Overall, there is a decreasing rainfall trend from 1980-2020 for Pointbill station and CHIRPS data. This mean value can be expected to be slightly lower than what the average $\delta^{13}C$ (-23‰) for Husab-1 and 2 represents if the trend continued from where the $\delta^{13}C$ data set ends in 1973.

Both datasets indicate relatively wet years during 1985, 1997, 2000, 2006, 2008-2009 and 2011 which closely correspond to the La Niña events in the years 1984-85, 1995-1996, 2000-2001, 2008-2009 and 2010-2011. Both datasets indicate relatively dry years during 1992, 1996, 2005, 2007, 2016-2017 and 2019 which closely correspond to the El Niño events in the years 1991-1992, 1994-1995, 1997-1998, 2004-2005, 2006-2007, 2015-2016, 2018-2019. A relatively wet year occurs approximately every 5.2 years between 1980-2011, this is followed by a very dry period from 2012-2019 likely caused by strong El Niño years which occurred during that period.

Spearman rank correlation analyses (95% confidence interval, one-tailed) yielded a low but significant correlation between the CHIRPS Pentad gridded data set and SST data (Table 9). Correlation analyses between the Pointbill station data yielded a low

but significant correlation between SST data and SAM (Table 9). For the CHIRPS dataset, the only statistically significant relationship is with SST, but for the instrumental climate data, there is a significant correlation for SAM and SST. Furthermore, while there is good alignment between wet and dry years and SOI, the relationship is not statistically significant. The significant correlations between the rainfall data and SST and with SAM may indicate a link between these climate forcing mechanisms and precipitation at the study site.

Table 9: Summary of Spearman's Rank Correlation analyses for rainfall data for the study site and forcing datasets (see chapter 4, section 4.9 for datasets used).

CHIRPS Pentad gridded rainfall dataset (mm) VS.	Spearman r	P	Significant?
SOI	0.04	0.4262	No
IOD	0.01	0.4812	No
SAM	0.19	0.1526	No
SST	-0.34	0.015	**Yes**
Pointbill Station rainfall data (mm) VS.			
SOI	-0.10	0.3299	No
IOD	0.14	0.2079	No
SAM	0.40	0.0191	**Yes**
SST	-0.34	0.0191	**Yes**

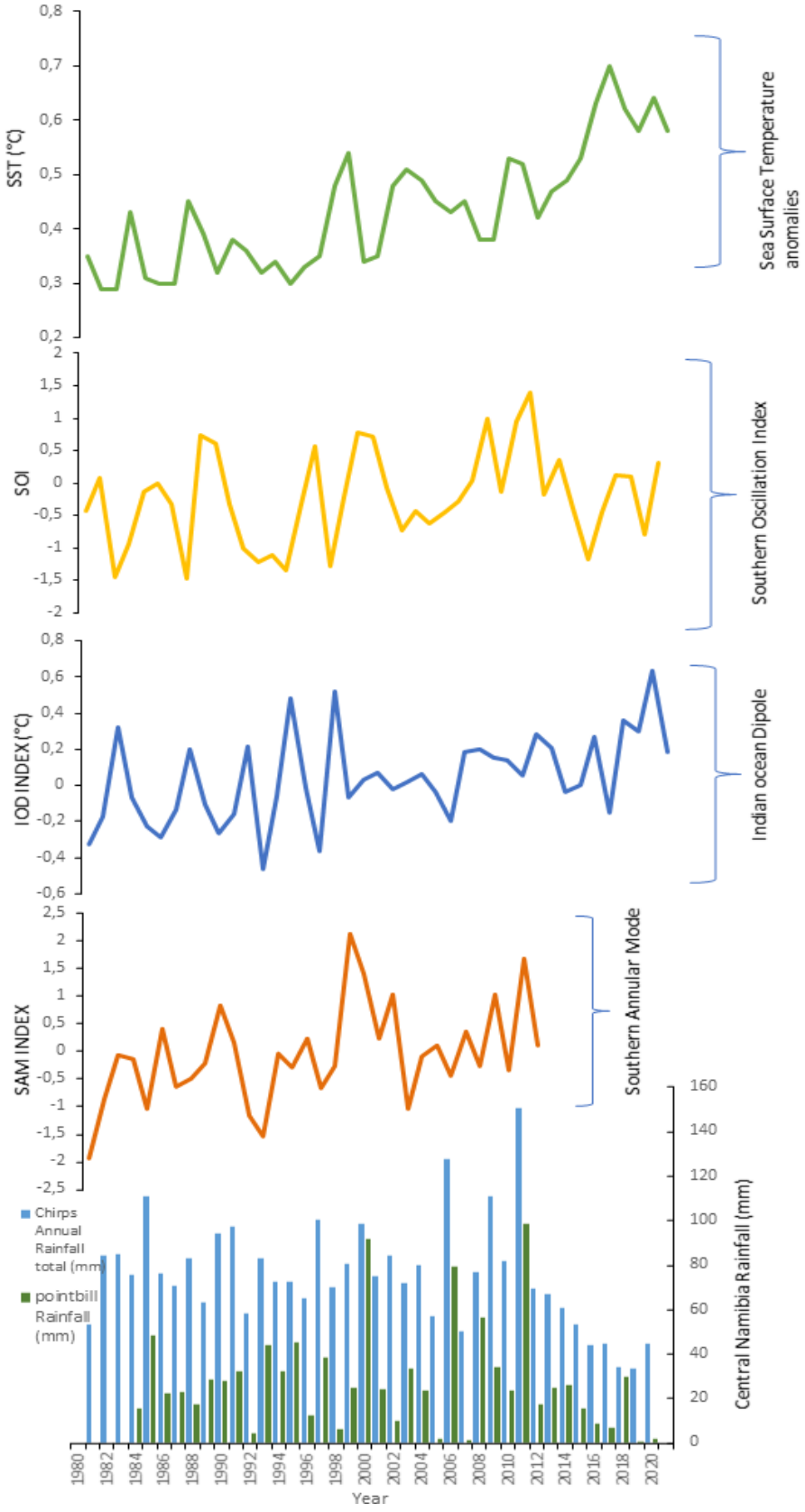


Figure 31: Composite Figure including rainfall data from the CHIRPS PENTAD gridded dataset (blue bars) and the Pointbill Station dataset (green bars) at the bottom with SAM (Orange), IOD (Blue), SOI (Yellow), and SST (Green) graphs for the period 1980-2020.

5.6 Comparisons between the tree record and climate forcing

5.6.1 Southern Oscillation Index

Using Spearman's rank correlation coefficient, there is no statistically significant correlation (r= 0.12, p= 0.2749) between the $\delta^{13}C$ isotope values and the SOI. Qualitatively, comparison between the two shows a reasonable level of covariance, particularly between 1964-1973, 1894-1902 cal yr CE (Figure 32). There is considerable divergence between 1911-1925 cal yr CE (Figure 32).

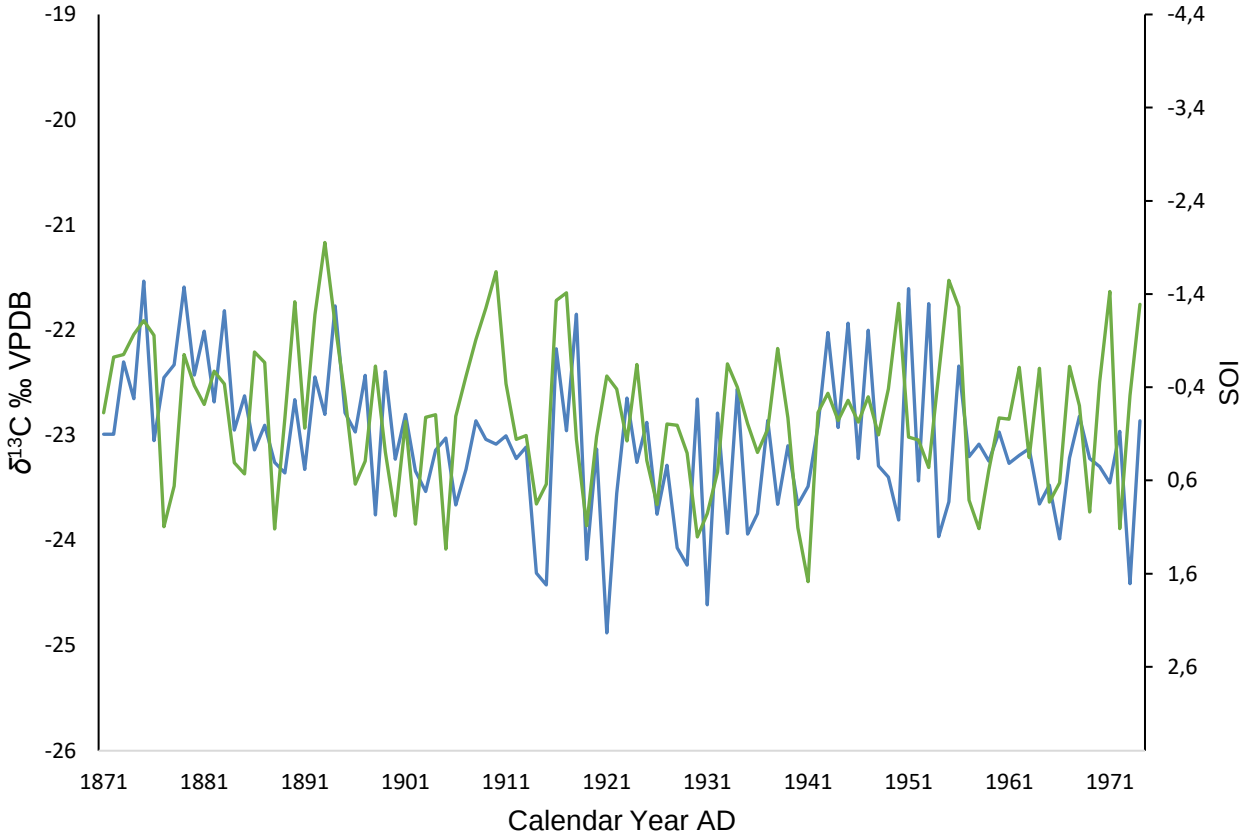


Figure 32: Comparison between $\delta^{13}C$ isotope values and the SOI (1871-1974) with $\delta^{13}C$ in blue and SOI in green.

5.6.2 Indian Ocean Dipole

Using Spearman's rank correlation coefficient, the correlation between the $\delta^{13}C$ isotope values and the IOD was not statistically significant (r= 0.12, p=0.1417). The comparison between the two shows a slight level of covariance, with peaks aligning during 1876, 1879, 1901 and strong alignment from 1943-1947 (Figure 33). There is disagreement from 1913-1918, 1934-1942 and 1966-1970 (Figure 33).

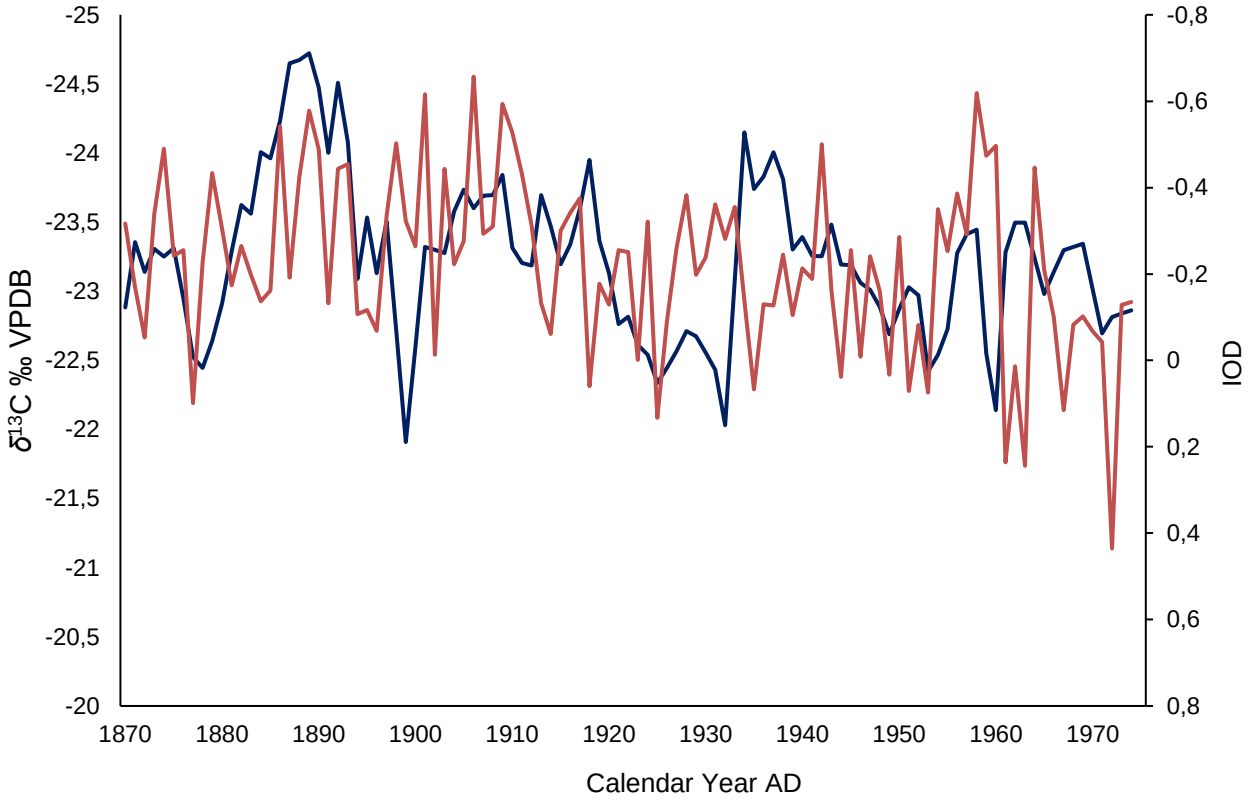


Figure 33: Comparison between $\delta^{13}C$ and the IOD (1870-1974) with $\delta^{13}C$ in blue and IOD in red.

5.6.3 Southern Annular Mode

Similar to the results for the instrumental meteorological data, there is a statistically significant correlation (r= 0.12, p= 0.0034) between the $\delta^{13}C$ isotope values and the SAM index. The comparison between the two shows a strong level of covariance, particularly between ~1660-1774 cal yr CE (Figure 34). However, there are $\delta^{13}C$ peaks in 1595 and 1888 that do not align with the SAM index (Figure 34).

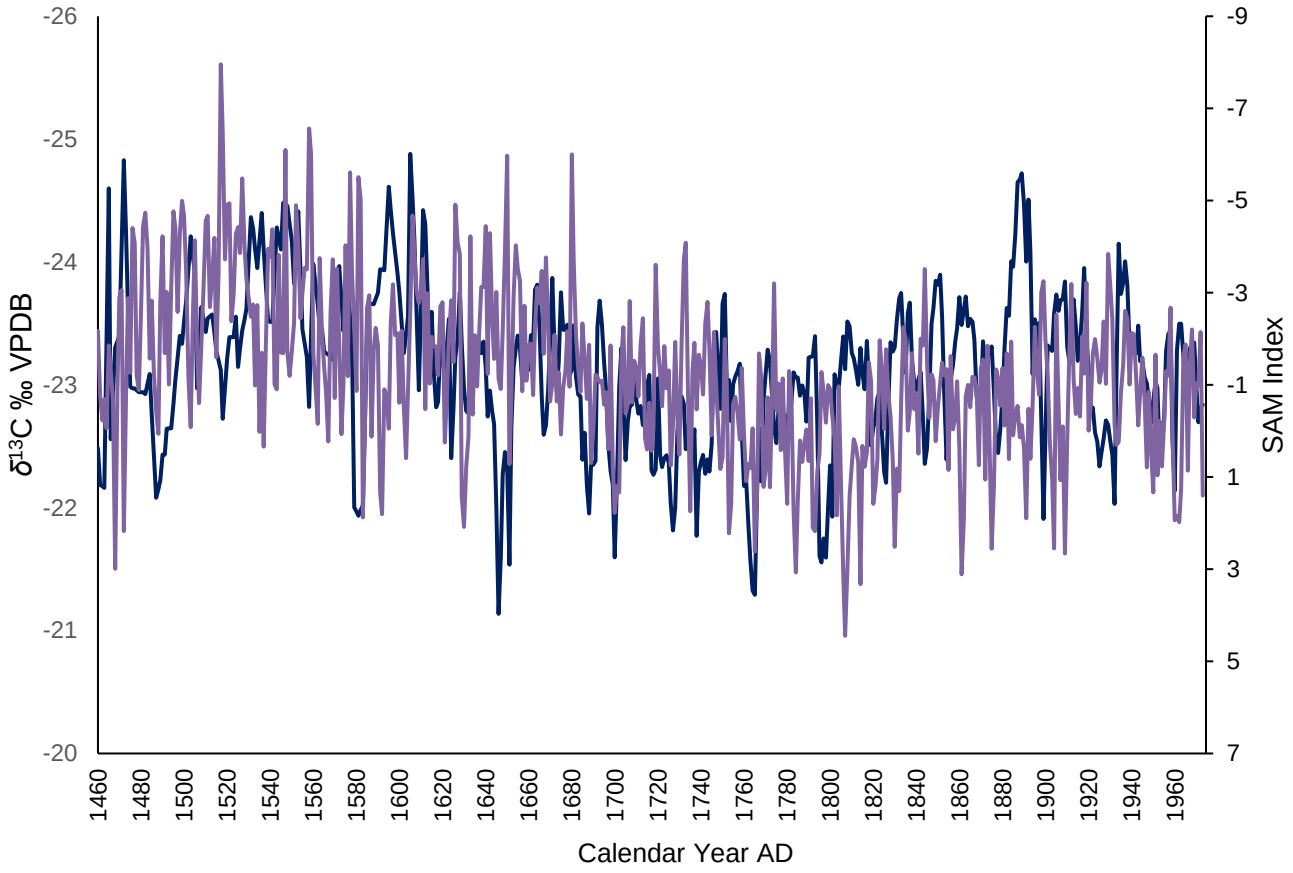


Figure 34: Comparison between $\delta^{13}C$ and the SAM index (1460-1974) with $\delta^{13}C$ in blue and SAM in purple.

5.6.4 Sea Surface Temperatures

Similar to both the gridded and instrumental meteorological data, there is a statistically significant correlation (r= -0.15, p= 0.0052) between the $\delta^{13}C$ isotope values and the SST anomaly index. The comparison between the two shows a reasonable level of covariance in the low-frequency component. Because there is a negative correlation, the SST axis is inverted to highlight the co-variance. Notably, there is disagreement between $\delta^{13}C$ and the SST anomaly index from 1795-1880, 1847-1855, and 1904-1918 (Figure 35).

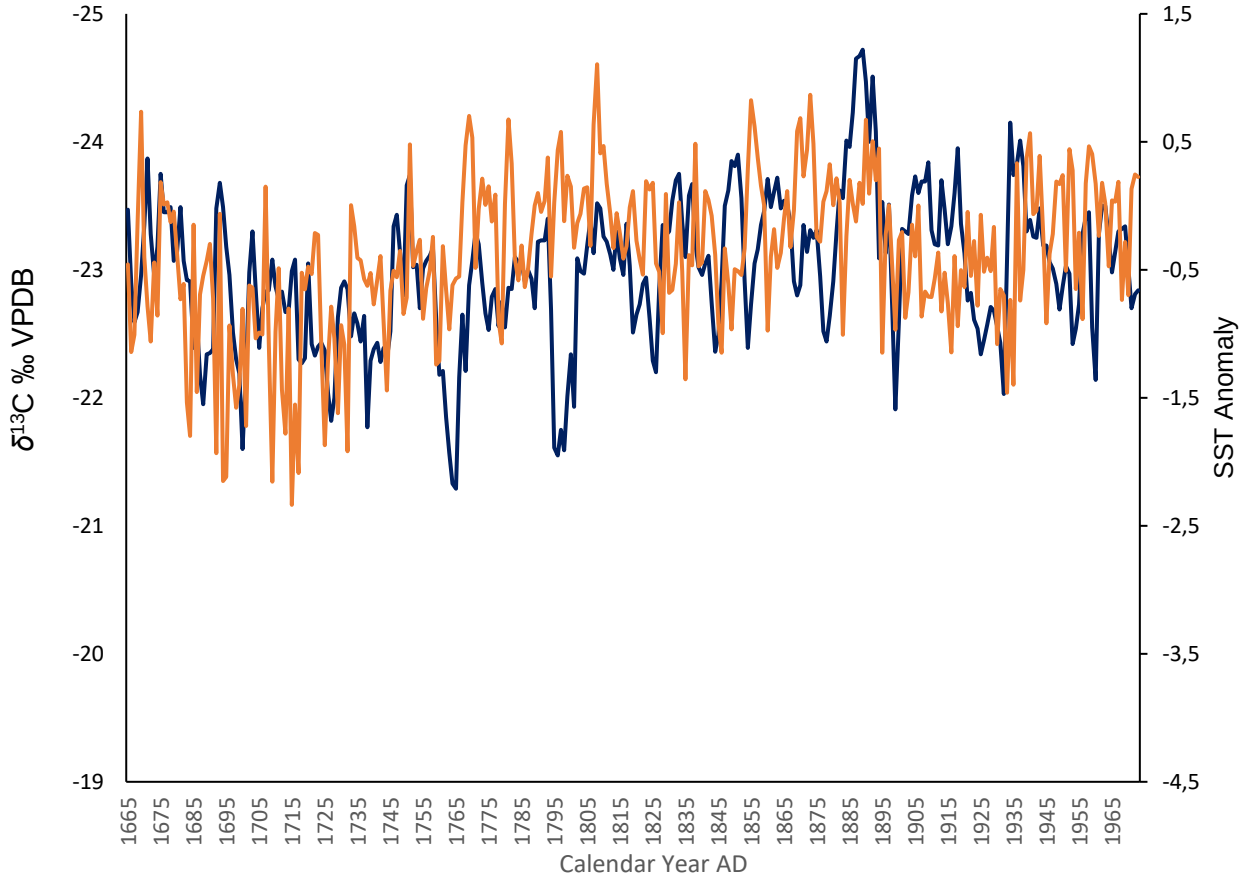


Figure 35: Comparison between $\delta^{13}C$ and SST anomalies (1665-1974) with $\delta^{13}C$ in blue and SST in orange.

5.7 Conclusion

This chapter presents calibrated AMS dates, and the age models indicate that Husab-1 spans ~1395-1974, and Husab-2 spans ~1615-1960. The isotope analysis indicates a mean $\delta^{13}C$ of -23‰ for both trees, with a variance from -25‰ indicating relatively wet conditions to -19‰ indicating relatively dry conditions (Figure 29). Analysis of meteorological data indicates that the contemporary mean annual total rainfall is 28mm for ground-based data from Pointbill station and 75mm for CHIRPS gridded data, ranging from 1-98mm (Pointbill) and 33-150mm (CHIRPS). Both ground-based rainfall and gridded rainfall are positively correlated with SST, as are the $\delta^{13}C$. Ground-based rainfall data and $\delta^{13}C$ are correlated with SAM. Neither the rainfall records nor the $\delta^{13}C$ is significantly correlated with ENSO or IOD, however extreme $\delta^{13}C$ values and extreme rainfall events do in some cases align with El Niño and La Niña years.

CHAPTER 6: DISCUSSION

6.1 Introduction

Using stable carbon isotope analysis ($\delta^{13}C$) on two *Acacia erioloba* trees from a tributary of the Khan River, this research project aims to construct a high-resolution hydro-climate record for the central Namib Desert. To achieve this aim, three main objectives were considered: 1. Determine the age of the trees, 2. Reconstruct the growth of the trees 3. To test whether the time series represents a proxy for precipitation and 4. Compare the hydro-climate record to driving forcing mechanisms that may influence the climate at the study site. This chapter discusses the isotope time series constructed from Husab-1 and Husab-2, and how it fits into the available literature pertaining to the climate in the central Namib desert for the past 600 years. A regional synthesis is presented for central Namibia and broader southern Africa and comparisons between the data with ENSO, SAM, SOI, and SST are evaluated and discussed. Finally, the limitations of the research are discussed.

The stable isotope series for Husab-1 and 2 spans the period ~1395-1974. The records for the two trees overlap from ~1615-1960. The contemporary rainfall data collected for the study site spans 1980-2021, within which there is a 6-year period where no rainfall data is available (1974-1980). The period of interest for this project falls within the late Holocene and specifically, the LIA which occurred between approximately 1300-1800 CE, although the exact timing is debated (Tyson *et al*., 2000; Sundqvist *et al*., 2013; Zinke *et al*., 2014; Fitchett *et al*., 2017; Du Plessis *et al*., 2020). There is a growing body of

palaeoenvironmental knowledge pertaining to this period for southern Africa (Heine and Völkel, 2011; Nicholson *et al*., 2013; Sletten *et al*., 2013; Woodborne *et al*., 2015, 2016, 2018; Voarintsoa *et al*., 2018), but high-resolution data are lacking, especially for hyper-arid regions such as Namibia.

6.2 Climate during the last millennium in Namibia

The climate record for Namibia is hampered by a paucity of long-term meteorological data, and few archives and proxies that are well preserved for high temporal resolution palaeoclimate reconstruction. However, archaeological (Kinahan, 2016), sedimentological analyses (Heine and Völkel, 2011), speleothems (Sletten *et al*., 2013), hyrax middens (Chase *et al*., 2009), documentary sources (Grab and Zumthurn, 2018) and more recently dendroclimatology (Mapani *et al*., 2021) have been used to investigate the past climates of the region, across varying time scales and spatio-temporal resolution.

Although past climatic data for the central Namib Desert are limited for the last 1000 years, there are a few key studies. Palaeoclimate evidence, from nitrogen isotope analysed in the Spitzkoppe rock-hyrax middens in west-central Namibia, suggests that the region was drier in the late Holocene between 3500- and 300- cal yr BP, but that wetter conditions prevailed during the last 300 years (Chase *et al*., 2009). The period from around 1450-1650 cal yr CE is reported as the coldest and driest period corresponding with the LIA, following this evidence suggests that at around 1700 cal yr CE there was an increase in humidity (Chase *et al*., 2009).

The Dante Cave speleothem record (DP1) is one of the longest palaeoclimate records available for Namibia, covering the last 4600 years (Sletten *et al*., 2013). Dante Cave is located in northern Namibia in the Otjozondjupa Region. While rainfall in northern Namibia is much higher than in the central Namib Desert, changes in total rainfall amounts are indicative of regional synoptic systems. Between 1250 and 1600 the Dante Cave record indicates that climatic conditions were relatively dry, following this there is an abrupt change to wetter conditions (Sletten *et al*., 2013). These trends are in agreement with the Spitzkoppe midden record (Chase *et al*., 2009). A wet hiatus is noted for the DP1 record during 1660-1690 (Sletten *et al*., 2013; Voarintsoa *et al*., 2017). This wet period is inferred because it corresponds with a 'Type E' surface that results from dissolution corrosion which occurs during exceptionally wet conditions (Railsback *et al*., 2013; Voarintsoa *et al*., 2017). The wet hiatus occurs during the coldest part of the LIA and falls within the Maunder minimum which is a period of exceptionally low solar activity (1645-1715 cal yr CE). A second Type E surface is noted for the period 1790-1830 along with a decrease in $\delta^{18}O$ and $\delta^{13}C$ values that coincide with the Dalton solar minimum (Voarintsoa *et al*., 2017). This evidence suggests that wet periods in north-eastern Namibia are linked to periods of low solar activity and cooler temperatures (Voarintsoa *et al*., 2017).

Analyses of slack water deposits found in the Swakop, and Khan River in Namibia suggest evidence of multiple floods occurring during the LIA with the majority dating to approximately 1600-1700 cal yr CE (Figure 36; Heine and Völkel, 2011). Slack water deposits are fluvial deposits that accumulate during a flash flood, particularly in a desert (Heine and Völkel, 2009, 2011). It is important to note that geomorphological records such as slack water deposits cannot be used in inferring mean long-term climate, as they are

representative of discrete, often extreme, weather events. However, a heightened incidence of extreme weather events in a particular period would likely be representative of a shift in mean climatic conditions or a cyclical phase within the climatic variability of a region (Heine and Völkel 2011). Floods in central Namib were also documented by the occurrence of sheet flood sediments and flood transported tree trunks (Heine and Völkel, 2011). The timing of the flash floods, suggested by the slack water deposits, coincides with the Maunder solar minimum and provides further evidence for wetter conditions during this time. Notably, the slack water deposits from central Namib indicate floods of much lower magnitude as opposed to the catchments in the northern parts of Namibia (Heine and Völkel, 2011). The central Namib Desert was thus not affected by extreme rainfall events, in the same manner as the northern Namib Desert (Heine and Völkel, 2011). The lower flood amounts in central Namibia could be a result of seepage and transmission losses of the palaeofloods as they travel through the desert (Greenbaum *et al*., 2014). It is important to note that despite the frequent occurrence of floods during the LIA in the central Namib Desert, the general climatic trend may be one of increased aridity overall (Heine, 2005; Heine and Völkel, 2011).

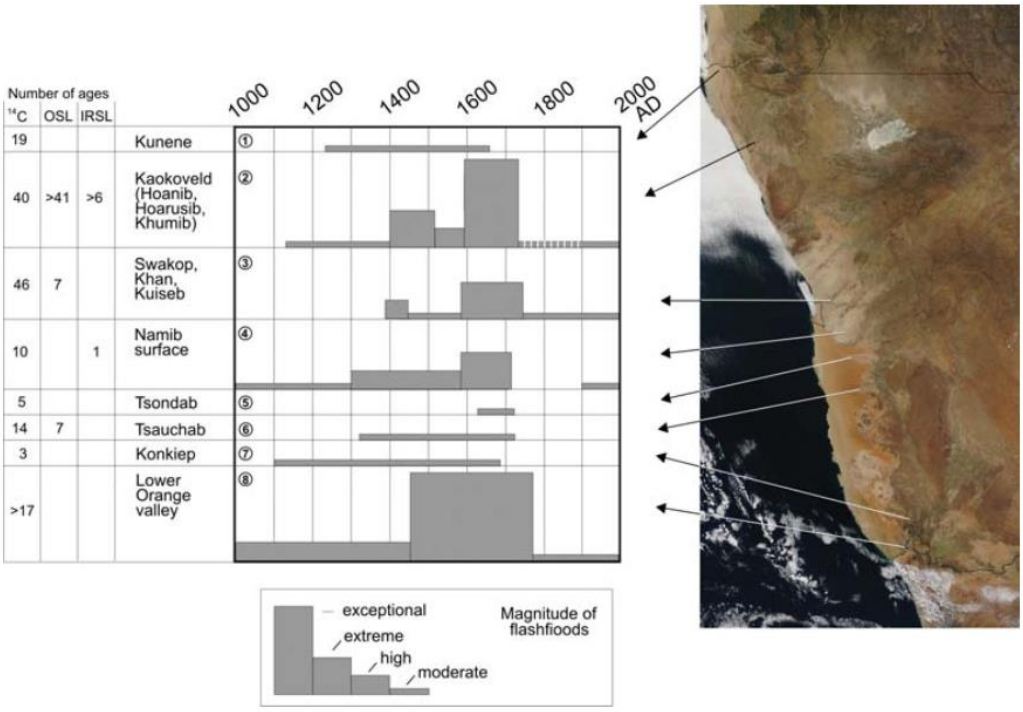


Figure 36: Slack water deposits which occurred during the LIA (Heine and Völkel 2011: 11).

Historical documentary evidence extracted from missionaries' diaries, letters, chronicles, and official reports can provide valuable information regarding precipitation from around the 19th Century. Grab and Zumthurn (2018) investigated such documentary evidence from central Namibia and compiled an extensive hydro-climate record for the period 1845-1900 cal yr CE (Table 10). Notably, 60% of all years categorised as dry followed El Niño events and 59% of all years categorised as wet coincided with La Niña years (Grab and Zumthurn, 2018).

Historical floods were documented for the period 1893-1963 near the Swakop River in Swakopmund (Stengel, 1964; Table 10). Some of these identified overlap with other historical flood records from Namibia namely 1893, 1897, 1931, 1934 and 1950 (Persendt

et al., 2015; Grab and Zumthurn 2018, Greenbaum *et al*., 2020). The years 1923, 1931 and 1934 were noted for having the largest and most frequent flood events due to large rainfall amounts (Stengel, 1964; Greenbaum *et al*., 2020).

Grodek *et al*. (2020) compiled a list of historical floods and droughts documented from 1837 to 2020 using multiple sources extracted from historical documents and records (Figure 37; Stengel, 1964; Blom, 1978; Nicholson, 2000; Grab and Zumthurn, 2018). The documentary flood data was compared to precipitation data from Windhoek (1891-2017). According to this palaeoflood record, a large flood occurred on average every 30 years (Grodek *et al*., 2020).

Table 10: Wet and dry periods (Grab and Zumturn, 2018) and flood years identified by Stengel (1964) for Namibia.

Wet Periods (Grab and Zumthurn, 2018)	Dry Periods (Grab and Zumthurn, 2018)	Flood years (Stengel, 1964)
1847-1850 CE		
	1850-1851 CE	
1851-1852 CE		
	1852-1854 CE	
1854-1856 CE		
	1858-1861 CE	
1857-1858 CE		
	1865-1869 CE	
	1865-1869 CE	
	1870-1872 CE	
	1876-1879 CE	
1880-1881 CE		
	1881-1882 CE	
	1883-1885 CE	
1886-1887 CE		
	1887-1889 CE	
1891-1893 CE		1893 CE
	1895-1896 CE	
		1897 CE
		1904 CE
		1915 CE
		1917 CE
		1918 CE
		1923 CE
		1925 CE
		1927 CE
		1931 CE
		1934 CE
		1942 CE
		1949 CE
		1950 CE
		1953 CE
		1954 CE
		1961 CE
		1963 CE

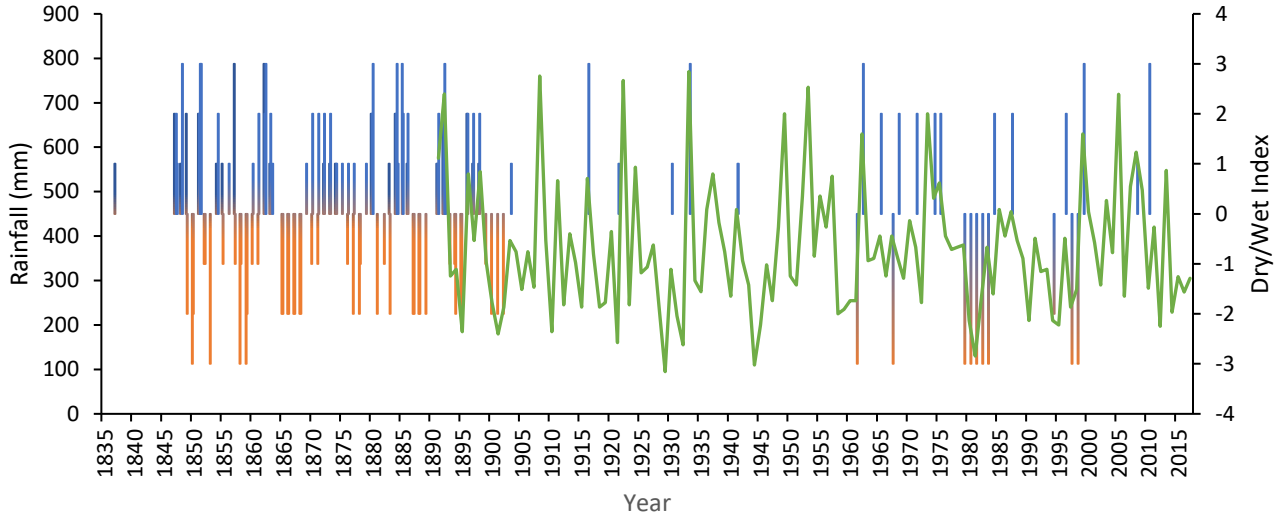


Figure 37: Historical precipitation data compiled by Grodek *et al*. (2020). Wet periods are indicated by the blue bars (3= extremely wet) and dry periods are in orange (-3 = extremely dry). The green line represents rainfall (mm) for Windhoek (Ministry of Agriculture, Water and Forestry, (MAWF), Namibia) (Adapted from Grodek *et al*., 2020).

Shikangalah and Mapani (2019) analysed tree rings from *Dichrostachys cinerea* to explore trends in precipitation during 1891-2016 in Namibia. It was noted that periods of high precipitation (>500mm) are often followed by a period of very low precipitation (<250mm).

The last millennium seems to be one of marked climatic heterogeneity in Namibia, especially in terms of precipitation (Heine and Völkel, 2011; Sletten *et al*., 2013; Grodek *et al*., 2020). The Dante Cave speleothem record indicates a dry period between 1250-1600 cal yr CE, followed by abruptly wetter conditions (1660-1690 cal yr CE) coinciding with the Maunder Minimum. Overall, the wettest period occurred between 1720-1850 cal yr CE (Sletten *et al*., 2013). Historical records from the 19th and 20th Centuries record multiple wet and dry phases which highlight precipitation variability in the region. There are no significant wetting or drying trends present in the data.

6.3 Climate during the last millennium in southern Africa

Exploring the southern Africa region more broadly, the climate was relatively cooler during the LIA, with highly spatially variable changes in precipitation (Nicholson *et al*., 2013; Nash *et al*., 2016; Hopper *et al*., 2018; Völkel *et al*., 2021). Speleothem records from Cold Air Cave (Limpopo) (Sundqvist *et al*., 2013) and Cango Cave (Western Cape) (Talma and Vogel, 1992) indicate that temperatures were around 1°C lower than present-day. Broad precipitation trends indicate that there was an increase in rainfall in the WRZ and a decrease in rainfall over the SRZ during the LIA in southern Africa (Tyson *et al*., 2000; Stager *et al*., 2012, 2013). However, precipitation is heterogeneous across southern Africa during this time (Nash *et al*., 2016). For example, the Pafuri baobab record (SRZ) indicates a period of increased rainfall between 1570-1620 cal yr CE, but the LIA was still the driest period in the last millennium (Woodborne *et al*., 2016). Many palaeoclimate records suggest that peak aridity occurred at around 1700 cal yr CE which resulted in widespread extreme droughts (Huffman, 2009; Ekblom *et al*., 2012; Sundqvist *et al*., 2013; Norström *et al*., 2018; Hannaford and Beck, 2021). Hannaford and Beck (2021) suggest a distinction within the SRZ by comparing the east (Mozambique) and west (Angola) climatic regions concerning LIA rainfall availability, their findings show opposing rainfall anomalies between the Summer Rainfall Zone East (SRZE) and West (SRZW) for the period 1500-1900 cal yr CE (Figure 40). This evidence further highlights the high level of precipitation variability within southern Africa for the LIA.

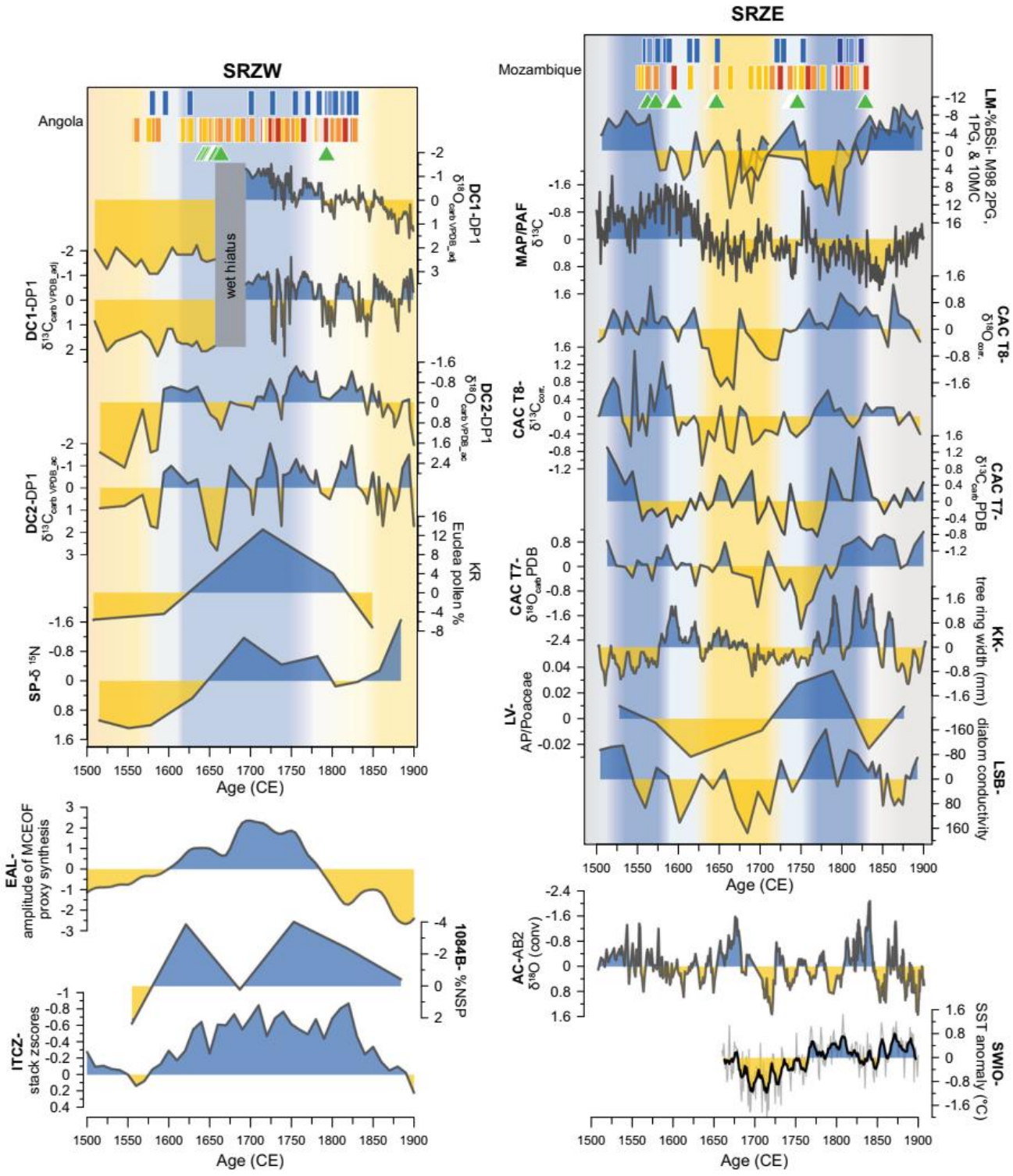


Figure 38: Palaeoclimate reconstruction for the SRZW and SRZE, blue indicates wetter conditions while yellow represents drier conditions (above or below the mean) for the period 1500-1900 (Hannaford and Beck, 2021: 15).

Towards the end of the LIA, there is an increase in the availability of both documentary evidence and rain gauge data for southern Africa (Nash *et al*., 2016). These documentary data demonstrate that the climate was highly variable across southern Africa, especially for the SRZ (Figure 41).



Figure 39: Annually resolved rainfall reconstructions for southern Africa SRZ (1850-1900) (Nash *et al*., 2019: 469).

Overall, the SRZ saw increased precipitation during the 1800s, with a drying trend beginning in the 1900s (Nash, 2017). The most notable multi-year droughts for the 19th Century occurred in 1861-1863, 1876-1879 and 1895-1897 (Nash *et al*., 2019). Wetter periods are documented for the late 1830s, early 1840s, 1855, 1870 and 1890 (Nash,

2017). The 1900s saw dry periods occurring in 1930, 1945 and the 1970s, with a wet year recorded for 1925 (Neukom *et al*., 2014).

Precipitation in the WRZ was relatively consistent in the 19th and 20th Centuries with no significant trends, although slightly elevated precipitation is noted during the 1900s in comparison to the 1800s (Neukom *et al*., 2014; Nash, 2017). Anomalously wet years were recorded for 1801, 1804 and 1850, with the 1820s being the wettest decade (Hannaford *et al*., 2015). Historical records indicate that relatively drier conditions occurred in the 1830s, and a wet period in 1890, but overall conditions were variable toward the end of the 19th Century (Neukom *et al*., 2014; Hannaford *et al*., 2015). An increase in precipitation is noted at around 1920 and 1950, with dry periods occurring in 1930 and 1965 (Neukom *et al*., 2014).

When considering southern Africa in a broader context, differences are noted for the timing of wet and dry phases relative to the SRZ and WRZ, especially during the LIA. However, conditions are highly variable and there are even notable differences between wet/dry phases when comparing the SRZ in the west and eastern parts of southern Africa between 1500 cal yr CE and 1900 cal yr CE (Hannaford and Beck, 2021). Although Namibia falls within the SRZ, the hyper-arid conditions mean that it is not a typical summer rainfall area. Inferences from broad regional patterns for the SRZ in southern Africa cannot always extend to the unique conditions of the central Namib Desert.

6.4 Long term dendroclimatic studies in southern Africa

Dendroclimatic studies in southern Africa that go back as far as the LIA are scarce. The longest dendroclimatic record was constructed through isotope analyses on multiple baobab trees (*Adansonia digitata*) which spans 1000 years (999-2009 cal yr CE). The record incorporates four baobab trees from the Pafuri region of South Africa (Limpopo), combined with five additional baobabs from Mapungubwe (Zimbabwe) (Woodborne *et al*., 2015, 2016). Both records indicate that the LIA was the driest period in the last millennium (Woodborne *et al*., 2015). A wetter period is interpreted from these records to have spanned the period 1570 to 1620 cal yr CE, but following this, dry conditions prevail until 1840 cal yr CE, with the driest period occurring from between 1650-1800 cal yr CE (Woodborne *et al*., 2016).

A second relatively long dendroclimatic record using *Breonadia salicina* spanning 1395-1995 cal yr CE provides insight into the precipitation of the Limpopo region (Norström *et al*., 2005). Dry conditions were noted for the early 1400s, 1550s, 1700s and early 1900s. Periods of increased precipitation were identified in the 1480s, and 1600s (Norström *et al*., 2005).

From the Karkloof forest in the KwaZulu-Natal Midlands (South Africa), a yellowwood tree (*Afrocarpus falcatus)* was used to produce a precipitation chronology for the period 1142-1916 cal yr CE (Hall, 1976; Vogel *et al*., 2001). The Karkloof record indicates that there was decreased precipitation before 1520 cal yr CE, this is followed by a gradual increase in precipitation peaking at around 1700 cal yr CE. Low rainfall occurred again between

1705-1800, after which very wet conditions prevailed until 1880. The end of the record is marked by a dry period until 1916 (Vogel *et al*., 2001).

For the Kalahari Desert in Botswana, an *Acacia* (*Vachellia*) *erioloba* tree was used to construct a 250-year proxy precipitation record spanning 1758-2013 cal yr CE (Woodborne *et al*., 2018). $\delta^{13}C$ and $\delta^{18}O$ analyses were used to investigate precipitation variability for the period, indicating a strong but complex relationship between precipitation and ENSO and SST anomalies (Woodborne *et al*., 2018).

Another relatively long term dendroclimatic precipitation record spanning 200 years (1796-1996 cal yr CE) was constructed for Zimbabwe using *Pterocarpus angolensis* (Therrel *et al*., 2006). The reconstructed rainfall record also demonstrated a strong correlation with ENSO. Two extreme dry periods were noted between 1859-1868 and 1882-1896, which were followed by a 6-year wet spell from 1897-1902 (Therrell *et al*., 2006).

Precipitation is more commonly reconstructed as opposed to temperature in dendroclimatic studies in southern Africa (Norström *et al.,* 2005; Trouet *et al.,* 2006; Therrell *et al*., 2007). In comparison to other long term palaeoclimate proxies such as pollen (Scott and Neumann, 2018), they can produce high resolution (annual to sub-annual) relative precipitation datasets (Loader *et al*., 2007).

6.5 The Husab isotopic time series

Qualitatively, an apparent ~30-year cycle for Husab-1 and a ~20-year cycle for Husab-2 is detected, which are similar to the ~18-year rainfall cycle which has been identified for southern Africa (Tyson *et al*., 2002; Malherbe *et al*., 2015). However, as the errors on the radiocarbon dates range from ± 29 to ± 141 ^{14}C yr BP it would not be statistically appropriate to quantitatively measure these cycles through methods such as Fourier or Spectral analysis. Further investigations into the periodicity and cyclicity of rainfall would require a higher resolution dating approach, that would provide valuable context to the spatial extent of the Tyson rainfall cycle.

Similar issues regarding the sampling frequency and errors on the radiocarbon dates apply when comparing the results of this study to records of different temporal resolutions. Given the paucity of studies for the region, tentative comparisons that are made with cognisance of these issues can potentially reveal regional patterns. A comparison between the lower temporal resolution DP1 speleothem record from Dante Cave and the Husab isotopic time series illustrated that although the general trends do not align, interestingly there are similarities between Husab-1 and the DP1 record, with the lowest isotope values aligning at around 1580-1585, 1650, 1740, 1800, 1845, 1875 and 1900 cal yr CE (Figure 38). There is less agreement when looking at higher isotope values in the records, but there are similarities between 1601-1640, 1710-1730, 1740-1790, and 1850-1890 cal yr CE (Figure 38). Although it is not good dendrochronological practice to consider only one tree, the similarities between DP1 and Husab-1 tentatively suggest that rainfall in the central Namib Desert is somewhat influenced by the same climatic drivers that influence rainfall in northern Namibia (Sletten *et al*., 2013). The disagreement

between the Husab isotope series, and the DP1 record may be due to errors in the age model, and it is important to note that rainfall is variably distributed in Namibia and that different areas receive varying levels of precipitation (Mapani *et al*., 2021). The relative role of coastal fog may also influence these differences (Kaseke *et al*., 2018). There is also the possibility that rainfall and groundwater may also interact differently over short distances, providing some trees with an advantage in accessing water due to different root placement even if they are near one another (Pierret *et al*., 2016).

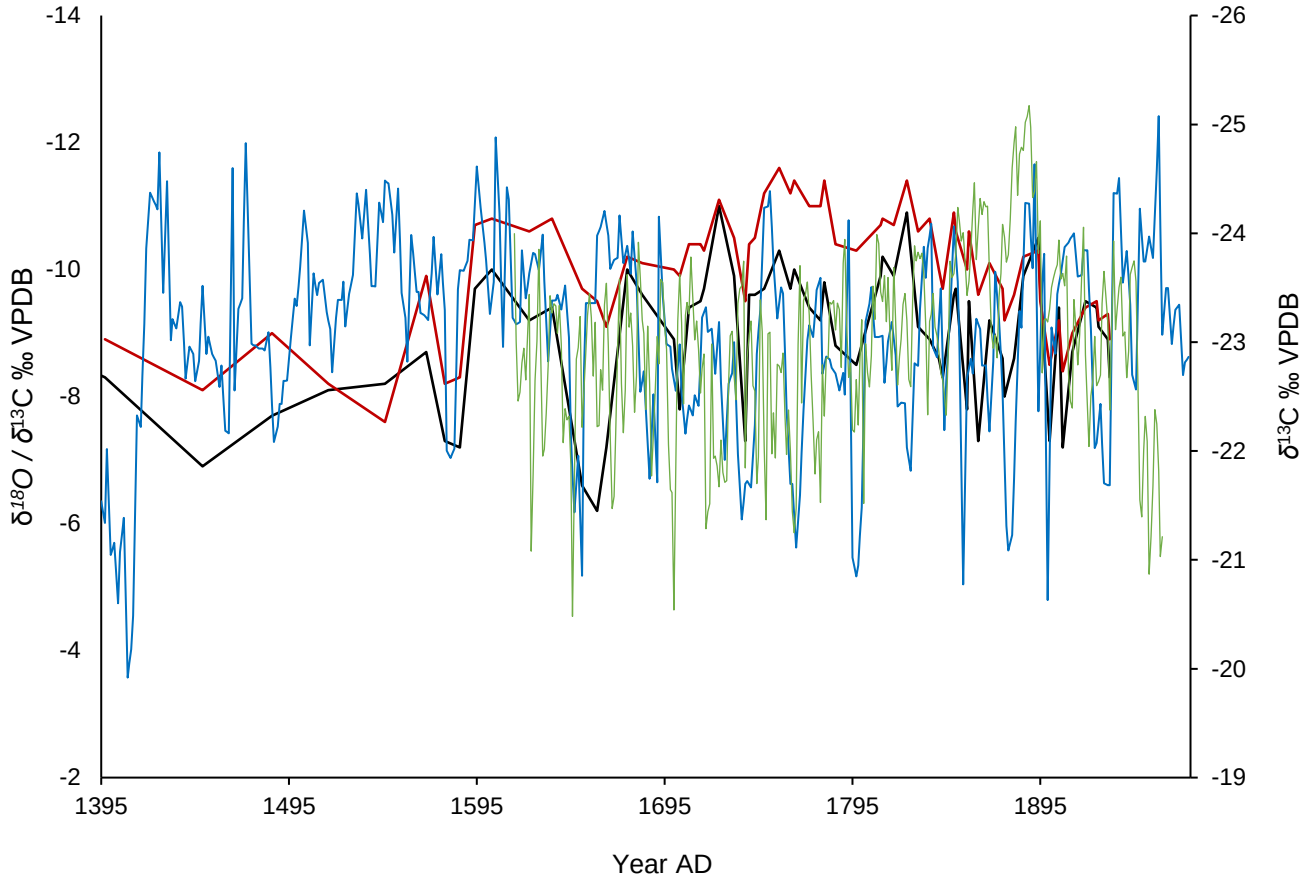


Figure 40: Comparison between Husab-1 (blue line), Husab-2 (green line) and the DP1 speleothem record with $\delta^{18}O$ in red and $\delta^{13}C$ in black (Voarintsoa *et al*., 2017).

The Husab isotopic time series indicates a slightly wetter phase from ~1421 to ~1620 cal yr CE, thereafter, mostly dry conditions prevail between ~1624 cal yr CE and ~1854 cal yr CE, and no very wet years until a peak of -24.7‰ in ~1856 cal yr CE. However, slightly wetter conditions are reflected in Husab-1 with peaks at around -24‰ between ~1662 and ~1692 cal yr CE. The DP1 speleothem record (Sletten *et al*., 2013) also indicates a declining precipitation trend from 1600-1659 cal yr CE, but following this, there are two periods of slightly increased precipitation 1664 -1700 cal yr CE, and 1708-1724 cal yr CE, in between this there is a brief period of decreased precipitation from 1700-1709 cal yr CE. These two peaks in the DP1 record, and slightly above average values for the period ~1662 to ~1692 cal yr CE indicated in Husab-1 may coincide with the occurrence of palaeofloods in Namibia suggested by the occurrence of slack water deposits noted by Heine and Völkel (2011).

Wet periods (isotope values < -24.8‰) identified from the Husab isotope record were noted for 1856, 1881-1882, 1886-1889, 1890, 1893 and 1958 cal yr CE (each of which carries an error margin relating to the accuracy of the radiocarbon dating) which tentatively align with the wet periods identified by Grab and Zumthurn (2018). Higher isotope values are also recorded at around 1932-1937 in the Husab-1 and 2 isotope records (around -24‰) which may correlate to the extreme floods that occurred in 1934 (Greenbaum *et al*., 2014). The driest years (> -21.2‰) were noted for 1854, 1878, 1880, 1899,1948-1949,1953-1954 cal yr CE and 1959-1960 cal yr CE for the Husab-1 and 2 isotope record. Only two of these years (1854, 1878) correspond exactly to dry periods noted by Grab and Zumthurn (2018), likely due to error margins on radiocarbon dating. Grab and Zumthurn (2018) indicate that the years 1876-1877 cal yr CE were relatively

dry, which was followed by two very dry years (1877-1879 cal yr CE). Notably, this is in accordance with the record for Husab-1 but not for Husab-2, $\delta^{13}C$ values for Husab-1 during 1876-1879 cal yr CE are around -21‰ whilst the values for Husab-2 are around -23‰ to -24‰. It is important to reiterate that due to the Suess effect, the age model presented is not exact, this means comparisons on an annual or even decadal scale may not be accurate.

A comparison between the Windhoek rainfall data (Grodek *et al*., 2020) and the Husab-1 isotopic time series yields a significant correlation (r=-0.27, p=0.0130) between 1891 cal yr CE and 1973 cal yr CE (Figure 41). This is notable given the high temporal resolution and temporal accuracy of ground-based meteorological records. Rainfall in Windhoek is on average much higher than the Husab study site, but notable similarities can be seen especially within the Husab-1 record. Both records indicate wet periods in ~1892 cal yr CE and ~1934 cal yr CE as well as dry conditions in ~1895 cal yr CE and ~1900-1902 cal yr CE, and from ~1925 cal yr CE to ~1930 cal yr CE.

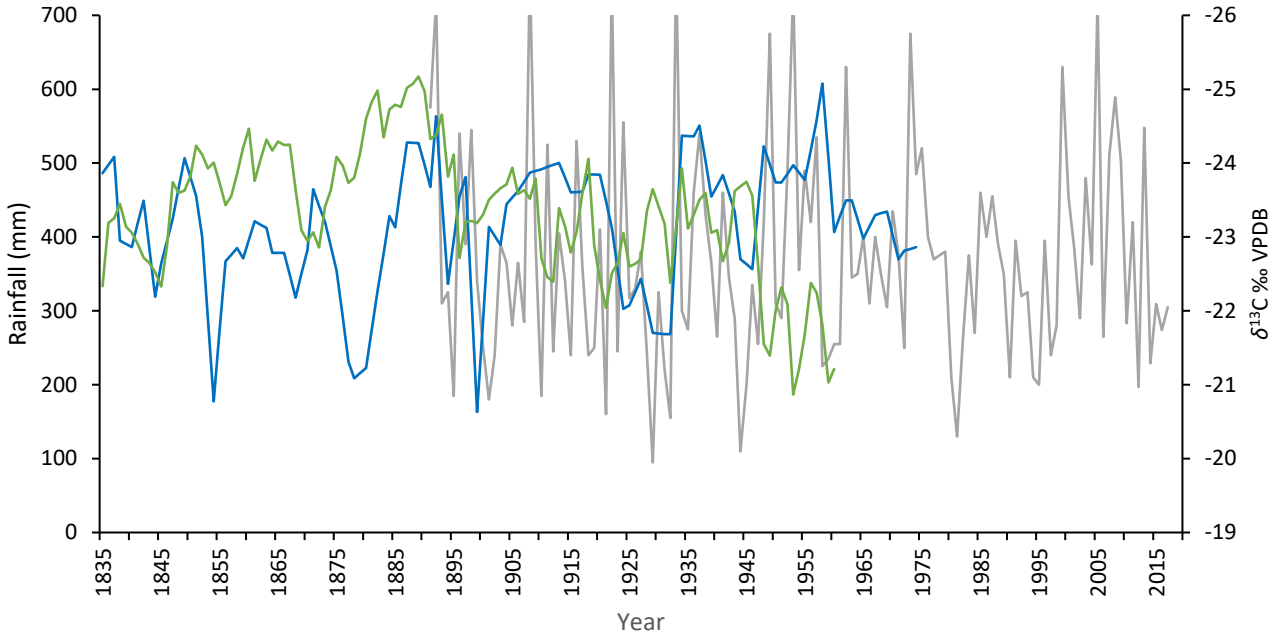


Figure 41: Comparison between Windhoek rainfall (mm) in grey (adapted from Grodek *et al*., 2020; MAWF) and Husab-1 (blue) and Husab-2 (green) isotope record between 1835-2015.

Shikangalah and Mapani (2019), noted that periods of high rainfall are often followed by periods of very low rainfall for their study sites in northern and central Namibia. A similar trend can be seen for Husab-1 between ~1791-1900 cal yr CE where a peak of -24‰ is often followed by a trough of -21‰ to -20‰. There is a decreasing rainfall trend noted for rainfall in Windhoek from 1891 to 2016 (Shikangalah and Mapani, 2019). This trend is also apparent for Husab-1 between 1941-1974 and Husab-2 between 1880-1960.

In general, there are many similarities when comparing the Husab record to historical data from Namibia for the 19th and 20th Centuries, but there are also periods where they contradict one another, which is expected in any environmental reconstructions and comparisons. Overall, Husab-1 has a greater correlation with the historical documentary and meteorological data in comparison to Husab-2.

6.6 Synoptic Drivers

Precipitation in Namibia is strongly influenced by three major climate drivers, namely the CAB, TTT cloud band and the AL (Eckardt *et al*., 2013; Grab and Zumthurn, 2018). Moisture availability in the atmosphere is also linked to SST variability in the southeast Atlantic Ocean and Benguela upwelling system (Eckardt *et al*., 2013). The majority of precipitation that occurs is a result of convective thunderstorms which are driven by day-time heating, atmospheric stability and synoptic conditions that are present (Eckardt *et al*., 2013). These conditions form a combination of multi-factorial precipitation systems which can indirectly and directly impact rainfall in the central Namib Desert (Eckardt *et al*., 2013). Other important non-rainfall forms of water include fog, humidity and dew (Henschel and Seely, 2008).

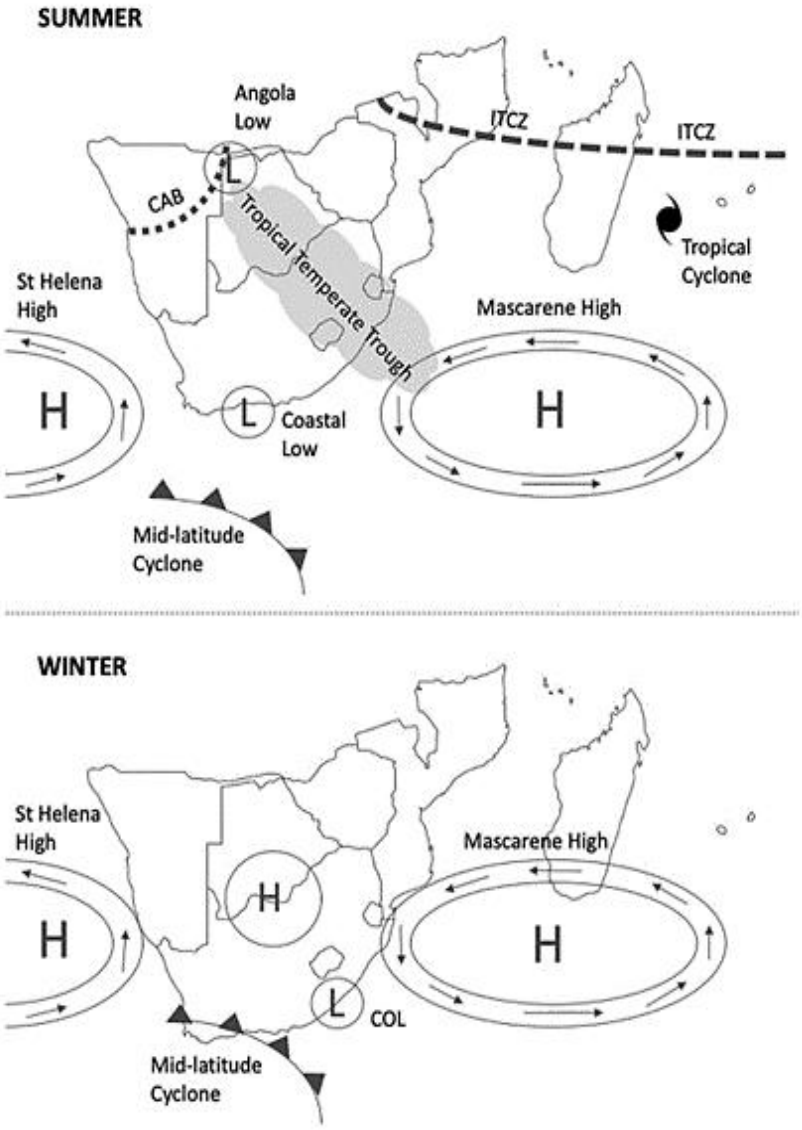


Figure 42: Synoptic climate systems of southern Africa (Saarinen *et al*., 2022: 17).

The CAB extends roughly in a westerly direction from the southern extent of the ITCZ over the southern African sub-continent to the northern extent of the Namibian coastline (Figure 42; Saarinen *et al*., 2022). It is the meeting point between warm moist air from over the Indian Ocean, and cooler dense air from over the Atlantic Ocean. The convergence of these two air masses causes uplift and the preferential formation of

convective low-pressure cells which bring about increased moisture and rainfall (Howard and Washington, 2019). The exact position of the CAB is highly variable but is more clearly defined during austral spring to early summer, and during winter it dissipates as it moves in relation to the position of the ITCZ (Howard and Washington, 2019). Depending on the location and intensity of the CAB, it has been known to influence rainfall over Namibia (Grab and Zumthurn *et al*., 2018). The CAB has also been linked to the occurrence of TTT events (Macron *et al*., 2014; Howard and Washington, 2019).

The TTT cloud band extends NW-SE from northern Namibia to the southern coast of South Africa (Figure 42; Saarinen *et al*., 2022). It is formed through the linkage of tropical easterly waves to westerly waves in the south through a trough (Eckardt *et al*., 2013; Macron *et al*., 2014; Grab and Zumthurn, 2018). It is one of the most important rainfall bearing systems for the SRZ in southern Africa contributing around 30% to 60% of total annual rainfall (Usman and Reason, 2004; Crétat *et al*., 2012). The development of the TTT is influenced by SST variability in the Atlantic and Indian Oceans, as well as the position of the Angola-Benguela Front and the strength of the AL (Saarinen *et al*., 2022).

The AL begins as a shallow heat low, which receives an influx of moisture from the Atlantic Ocean and develops into a deeper tropical low (Reason *et al*., 2006; Munday and Washington, 2017; Howard and Washington, 2018). The low-pressure cell generally develops in October and strengthens toward January/February. It is a key driver of seasonal moisture over southern Africa, and rainfall originating from this system can be attributed to up to 15% of total rainfall over Namibia and Angola (Desbiolles *et al*., 2020).

Similar to the TTT, the strength and position of the AL are influenced by SST variability, and as such, both the TTT and AL can be linked to ENSO (Howard, 2019).

Cut off lows (COLs) were also identified as possible rain-bearing systems that can bring rainfall into Namibia (Eckardt *et al*., 2013). They are formed in the westerlies when unsteady Rossby waves form troughs and extend equatorward but are interrupted by high-pressure cells forming closed cyclones (Favre *et al*., 2013; Saarinen *et al*., 2022). These isolated subtropical low-pressure systems are associated with intense precipitation over southern Africa (Favre *et al*., 2013). COLs are anomalous events in Namibia but have resulted in extreme rainfall and flooding in the past (Muller *et al*., 2008).

6.7 Climate Forcing and the Husab isotope record

Statistically significant relationships were found when comparing the Husab isotope series to SST and SAM (see chapter 5). The Atlantic, Indian and Pacific Ocean SSTs are known to influence climatic variability in southern Africa (Tyson and Preston-Whyte, 2000; Gergis and Henley, 2017; Howard, 2019). Moisture availability in the atmosphere over Namibia is strongly dependent on SST variability in the southeast Atlantic Ocean, the western Indian Ocean and the tropical Pacific Ocean (Eckardt *et al*., 2013). The correlation between the Husab isotope record is negative, and because more negative $\delta^{13}C$ values correspond to increased precipitation, increased SST is interpreted to have a positive influence on rainfall in central Namibia. Generally, cold SST along the coast of Namibia result in stable atmospheric conditions and a strong SAHP which suppress convective rainfall, contributing to the arid climate (Crétat *et al*., 2010; Eckardt *et al*., 2013;

Desbiolles, 2020). It is reasonable then that if SST had to increase, this would introduce instability, and result in increased convection and precipitation over Namibia. Fluctuations in SST in the Angola/Benguela upwelling system or Angola Benguela Front (ABF) along the Namibian and Angolan coastline have also been shown to influence precipitation in Namibia (Reason *et al*., 2006; Richter *et al*., 2010; Rouault *et al*., 2018). Anomalously warm SST events in this region have been termed Benguela Niños (Shannon *et al*., 1986), while anomalously cold events have been termed Benguela Niñas (Imbol Koungue *et al*., 2017, 2019; Koseki and Imbol Koungue, 2021). Benguela Niños are associated with the weakening of the SAHP, and increased precipitation, whereas Benguala Niñas suppress rainfall in Namibia (Koseki and Imbol Koungue, 2021). Correlation analysis yielded a significant positive relationship between SAM and the Husab isotope series (Figure 43). This means that the negative phase of SAM is associated with increased precipitation in central Namibia. A similar relationship was shown for the Western Cape WRZ, and it is suggested that this relationship may extend to other parts of the western coast of southern Africa (Reason and Rouault, 2005). When SAM is negative there is a northward displacement of the westerlies and mid-latitude cyclones, which results in increased rainfall over the western parts of southern Africa (Ibebuchi, 2021). However, a southward displacement of the westerlies during the positive phase of SAM can be associated with an expansion of the SAHP, and this would result in a decrease in moisture availability and rainfall (Sousa *et al*., 2018). Ibebuchi, (2021) notes that the SAM is also linked to ENSO, with the positive phase of ENSO (La Niña) contributing to the negative phase of SAM.

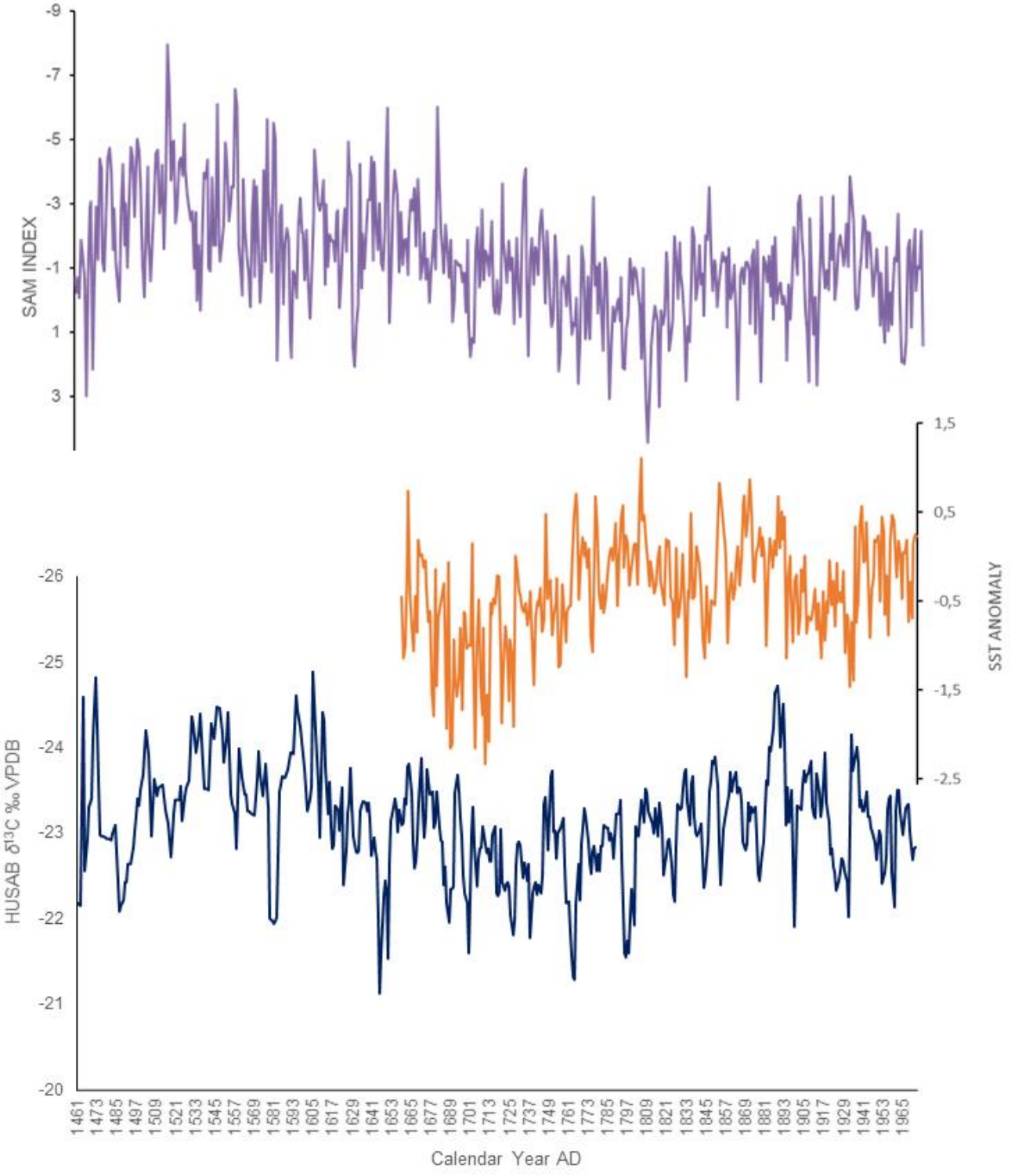


Figure 43: Composite figure showing the SAM index (purple), SST anomaly (orange) and Husab isotope record (Here Husab 1 and 2 were averaged to form one record) (dark blue).

No statistically significant relationship was found through the comparison of the SOI to the Husab record. Nonetheless, it is known to influence wet and dry periods over the Southern Hemisphere (Gergis and Henley, 2017), and has been detected in other palaeoclimate records for southern Africa (Woodborne *et al*., 2018) The El Niño phase of ENSO is typically associated with dry conditions for the SRZ, and wetter conditions for the WRZ over southern Africa, while the opposite is true for the La Niña phase (Malherbe *et al*., 2020). However, the impacts of ENSO in southern Africa is secondary through teleconnections, and the magnitude, duration, and seasonal timing of the rainfall response is variable (Grab and Zumthurn, 2018). The impacts of ENSO in southern Africa are also spatially variable, and not uniform (Harduth and Fitchett, 2020). Even though no statistically significant correlation was found when comparing the Husab isotope series to the SOI, it has been noted as a climate forcing mechanism in other climate research for Namibia (Fichtler *et al*., 2004; Neukom *et al*., 2014; Nash *et al.,* 2016; Grab and Zumthurn, 2018; Hannaford and Beck, 2021). For example, Grab and Zumthurn (2018) noted that between 1845-1900, 60% of all dry years followed El Niño events and 59% of all wet years coincided with La Niña years for central Namibia. The current La Niña year (2022) has resulted in above-average rainfall in Namibia. According to an article in Getaway Magazine, on the 16th of February 2022, the Swakop River reached the Atlantic Ocean for the first time since 2011 (also a La Niña year) (Cowley, 2022). The accuracy of the radiocarbon dates and age model may obscure the ENSO pattern in the Husab record.

The IOD is also known to impact rainfall in southern Africa. Broadly, rainfall is enhanced (reduced) over southern Africa during the negative (positive) phase of IOD (Gaughen *et al*., 2016). However, the impacts of the IOD on rainfall is spatially variable (Manatsa *et*

al., 2012; Gaughen *et al*., 2016). The correlation between the Husab record and IOD did not yield a statistical relationship, and this may be because rainfall in Namibia is more impacted by SST fluctuations in the adjacent Atlantic Ocean in comparison to the Indian Ocean (Rouault *et al.*, 2003). The positive phase of IOD is typically associated with El Niño conditions, and the negative phase is associated with La Niña conditions, although, this relationship is not always constant (Gaughen *et al*., 2016). The IOD has been proven to be a climatic driver over eastern and southern Africa (Conway *et al*., 2007; Marchant *et al*., 2007; Manatsa *et al*., 2008; Ogwang *et al*., 2015, 2020) but the relationship between the IOD and rainfall in the western parts of southern Africa is not well studied.

The Spearman's rank correlation analyses between the Husab isotope record and possible synoptic drivers indicates that fluctuations in SST and the SAM have the most influence on rainfall variability in the central Namib Desert. Significant correlations (95% confidence interval) were also found when comparing the meteorological data for the study site with SST anomalies (Pointbill station and CHIRPS gridded data) and SAM (Pointbill station). This further validates the importance of SST fluctuations on precipitation in the Namib Desert. For wet conditions to occur in the hyper-arid Namib Desert, anomalous circulation patterns are likely to be present (Muller *et al*., 2008). For example, in April 2006 a COL formed along the coast of Namibia, following this, the AL linked to a mid-latitude cyclone forming a truncated TTT just east of the COL. This system produced extreme uplift along the Namibian coastline, resulting in anomalously high rainfall (Muller *et al*., 2008). The year 2006 was also categorized as a La Niña year, and warmer than average SSTs were noted for the ABF region during 2006 suggesting a Benguela Niño event (Muller *et al*., 2008). Miller *et al*. (2021) state that TTTs which extend

from the CAB are the dominant causal factor for increased precipitation and flooding in Namibia. The likelihood of flooding is further increased when coupled with heightened SST at the ABF, as well as a strong sea breeze and an influx of air from the vegetated areas of northeastern Namibia (Miller *et al*., 2021). It is also possible that the WRZ expanded during the LIA, inducing more frequent MLCs over Namibia, as has been proposed from geomorphological flood records (Miller *et al*., 2021).

In contrast, dry periods occur in the absence of these circulation patterns, and likely with the strengthening of the SAHP. Anomalously cold SST at the ABF may also result in Benguela Niña events which suppress rainfall over Namibia (Koseki and Imbol Koungue, 2021). Furthermore, El Niño conditions are known to cause drought conditions over southern Africa including Namibia (Fichtler *et al*., 2004). In 2019, Namibia experienced the lowest recorded rainfall since 1891 and this drought period coincided with the 2018-2019 El Niño event (Shikangalah, 2020).

In southern Africa, multi-decadal trends indicate that average annual precipitation will decrease resulting in drier conditions (Gaughen *et al*., 2016). The declining rainfall trend in southern Africa coincides with a southward shift in the Southern Hemisphere storm tracks (westerlies) and the poleward expansion of the Hadley cell (Burls *et al*., 2019). Trends towards shorter wet seasons (for both the WRZ and SRZ), later wet season start dates, and an overall reduction in rainfall across the SRZ has also been linked to the expansion of the Hadley cell and a poleward shift of the mid-latitude westerlies (Roffe *et al*., 2021). The climate in Namibia is projected to become hotter and drier by 2100 (Beck *et al*., 2018), and the aridity in the region will likely be intensified with increasing drought

frequency (Luetkemeier and Liehr, 2019; van Rensburg and Tortajada, 2021). Further water scarcity in Namibia will have severe consequences such as decreased availability of drinking water for animals and humans, decreased crop yields and damage to ecosystems (Liu and Zhou, 2021).

6.8 Limitations

6.8.1 Sampling technique

Due to the rings of Husab-1 and Husab-2 being microscopic and prone to occlusion, sampling was performed at the most practical resolution (0.5mm) that could be managed by hand using a chisel. This means that the samples did not represent individual rings. The sampling of individual rings could be achieved through the use of a UV-laser microdissection microscope, a microtome, or utilising programmes that can provide digital tree-ring width analyses. However, this was not possible, as access to such a microscope or programme was hindered by the resources and funding available. The very high sampling resolution of 0.5mm, performed by hand, introduces error as it was difficult to maintain the 0.5mm resolution at all times. The consequence was that statistical approaches such as BACON age-depth modelling were not appropriate as they require exact depths against which ages and accumulation (or growth in this instance) rates are interpolated. A lower sampling resolution (such as 3mm) would have better facilitated the use of BACON, but this was not practical for a slow-growing tree with microscopic rings. Therefore, temporal resolution was prioritised, and an age model approach appropriate to the sampling resolution was used, as has been conducted in recent dendroclimatic research elsewhere in southern Africa (Woodborne *et al*., 2015, 2016, 2018).

6.8.2 Errors in the radiocarbon dates

The first selection of samples that were used for radiocarbon analyses yielded higher than usual error estimates (±69 to ±141 ^{14}C yr BP) due to technical issues with the AMS. When calibration was performed for these dates, multiple date ranges were calculated. The poor precision of the radiocarbon dates was exacerbated by the Suess effect, so obtaining accurate calibrated dates for the samples was not possible. Once the problems with the AMS were resolved, selected samples were reanalysed, which yielded lower error estimates (±29 to ±46 ^{14}C yr BP). These error margins are large in comparison to the temporal resolution afforded by the 0.5mm sampling and reduce the ability for comparison to other high-resolution records such as historical data from archival sources. This is a frequent problem found in published dendroclimatological research that includes approximately the last 300 years due to the Suess effect (Fichtler *et al*., 2003; Pazdur *et al*., 2007). This issue is usually overcome by crossdating multiple trees and wiggle matching (Andreu-Hayles *et al*., 2015; Hua, 2009; Leavitt *et al*., 2009). The use of the crossdating technique on multiple trees was not feasible within the scope of this project, but a suggestion for future work would be to analyse additional trees in the central Namib region to be able to create a more accurate isotopic chronology. The number of dates needed to wiggle matching the Husab trees is prohibitively expensive, but extensive additional analyses will be performed so that a reliable chronology is be presented when this research goes to publication.

6.8.3 Comparisons to meteorological data

There is a paucity of instrumental climatic data for Namibia, and the data that does exist is difficult to access. This study used ground-based meteorological data was from a weather station at the Rössing Uranium mine and CHIRPS gridded data accessed from the Google Earth Engine. Unfortunately, the earliest rainfall data that could be found for the study site was from 1981. Consequently, there was no overlap between the meteorological data and the Husab isotope record and comparisons between the two could not be achieved. A comparison would have allowed for insight into whether the isotope record was an accurate proxy for rainfall at the study site. In future, further efforts could focus on obtaining longer meteorological records for the central Namib desert, through avenues such as the Ministry of Agriculture, Water and Forestry in Namibia, as well as analysing more trees to bridge the gap between meteorological records and dendroclimatology.

CHAPTER 7: CONCLUSIONS

7.1 Introduction

This chapter presents a summary of the results from the application of $\delta^{13}C$ on two *Acacia (Vachellia) erioloba* trees, to create a proxy precipitation record for the central Namib Desert. The achievement of the aim and objectives of this research project is assessed. This chapter concludes with possible directions for future work regarding palaeoenvironmental research in Namibia.

7.2 Synthesis

Stable carbon isotope analysis was performed on two *Acacia erioloba* trees, namely Husab-1 and Husab-2, to construct a relative precipitation chronology for the central Namib Desert. An age model for the chronology was created using AMS radiocarbon dates on selected samples for each tree. Poor precision of radiocarbon dates and the Suess effect resulted in a high error range for the age model. The Husab isotope chronology was statistically compared with SST, IOD, SAM, and SOI indices to determine climatic forcing at the study site. The chronology was also evaluated against historical documentary findings from Namibia, meteorological data from Windhoek and other palaeoenvironmental records (DP1 speleothem record, slack water deposits, and hyrax middens).

The major findings of these analyses were: (a) Husab-1 and 2 grew during the LIA and during the beginning of the modern era until the mid-20th Century cal yr CE. (b) There

was marked rainfall variability during this period, which is consistent with other palaeoenvironmental research for the Namib region, and other regions within the SRZ of southern Africa. Although the errors in the age model mitigated against accurate comparisons, there were some similarities and differences in the comparisons between the Husab chronology and the paleoenvironmental records which highlighted climatic variability within Namibia. The significant correlation between Husab-1 and Windhoek rainfall data (1891-1973 cal yr CE) tentatively suggests that the isotope chronology is somewhat a reflection of rainfall in Namibia. Overall, Husab-1 had greater similarities with the paleoenvironmental records, in comparison to Husab-2. More precise radiocarbon dates for the trees are needed to adjust the age models and improve accuracy. (c) The Spearman's Rank Correlation analyses yielded statistically significant relationships between the Husab rainfall chronology and SST anomalies, and the SAM. These synoptic drivers are known to influence rainfall in the present, but the research presented here suggests that they also influenced rainfall during the past 600 years. Climatic systems linked to SST and SAM such as the CAB, TTT, and AL may have been drivers of rainfall variability in the central Namib Desert throughout the period 1395-1974 cal yr CE. More research is needed to better understand the influences of ENSO on the region.

7.3 Achievement of study aims

This project aimed to extend knowledge of climate and rainfall variability by constructing a high-resolution hydro-climate record for the central Namib Desert using stable carbon isotope ($\delta^{13}C$) analysis on *Acacia erioloba* trees. To achieve this aim four objectives were set, these were:

1. *To determine the age of the Acacia erioloba samples by:*
    a. *AMS radiocarbon dating on selected samples.*
    b. *Creating an age model that assigns an age to each sample aliquot by interpolating the 1-sigma ranges of the radiocarbon dates. Calculating the age-depth model to which the isotope analysis can be considered.*

Objective 1 (a) was achieved by sending selected samples to iThemba LABS for AMS radiocarbon analyses. A total of six and 11 samples were analysed for Husab-1, for Husab-2 respectively (see chapter 5, section 5.2). These dates were then calibrated using the Southern Hemisphere dataset.

Objective 1 (b) was achieved using the methods used by Woodborne *et al*. (2015, 2016). The age model suggests that Husab-1 dates to ~1395-1974 cal yr AD / CE, and that Husab-2 dates to ~1615-1960 cal yr AD / CE (see chapter 5, section 5.3). However, errors in radiocarbon dates and the Suess effect did not allow for high accuracy.

2. *To reconstruct the growth of the trees through* $\delta^{13}C$ *analysis on samples throughout the radii to create a stable isotope time series.*

A total of 334 samples and 860 samples were obtained from Husab-1 and 2, respectively. The cellulose component in these samples was analysed using the Delta-V stable light isotope mass spectrometer coupled with a CHNSO 1100 series elemental analyser by a Conflo III interface (supplied by Thermo Fisher, Bremen, Germany) housed at the

University of Pretoria Stable Isotope Laboratory to produce a $\delta^{13}C$ dataset. Methods outlined in chapter 5 following those of Woodborne *et al*. (2015) and McCarroll and Loader (2004) were used to correct the $\delta^{13}C$ values for IWUE and anthropogenic atmospheric CO_2 using the Belmecheri and Lavergne (2020) correction.

3. *To test whether the time series represents a proxy for precipitation.*

This aim could not be fully achieved due to there being no overlap between the meteorological ground-based data and CHIRPS gridded data for the study site with the Husab isotope chronology. However, based on theory, and similar records for elsewhere in southern Africa, there is good reason to believe that this does represent a proxy for precipitation and is read as such.

4. *To compare the rainfall reconstruction to driving forcing mechanisms, by evaluating it against:*
    a. *El Niño Southern Oscillation (ENSO) using the SOI index,*
    b. *Southern Annular Mode (SAM),*
    c. *Indian ocean dipole (IOD),*
    d. *sea surface temperature (SST)*

This objective was achieved using Spearman's rank coefficient correlation to investigate the relationship between $\delta^{13}C$ isotope time chronology and climate forcing datasets for periods of overlap (see chapter 5, section 5.6). The SAM and SST had a statistically

significant correlation to the Husab $\delta^{13}C$ isotope chronology for the periods 1460-1974 cal yr CE and 1667-1974 cal yr CE respectively.

7.4 Directions for future work

To mitigate the influence of the Suess effect and poor precision on radiocarbon dates Husab-1 and 2 should be cross dated with other trees from the central Namib Desert. Alternative proxy rainfall records need to be further explored for the region such as additional studies into rock hyrax middens, sedimentological analyses, and environmental archaeological records. Additionally, there is a need to investigate more thoroughly, historical documentary records such as diaries, letters, missionary reports, news reports, gazettes, and any other official reports from Namibia that may contain information relating to the weather to provide a more complete understanding of climatic variation for the past 1000 years. Further efforts should similarly focus on obtaining longer meteorological records, to bridge the gap between dendroclimatological and meteorological data and allow for better comparisons and analyses.

REFERENCES

Atlas of Namibia Project, 2002. Directorate of Environmenal Affairs, Ministyry of Environment and tourism, available from; https://www.uni-koeln.de/sfb389/e/e1/download/atlas_namibia/main_namibia_atlas.html, accessed July, 2021.

Abiodun, B.J., Makhanya, N., Petja, B., Abatan, A.A. and Oguntunde, P.G. 2019. Future projection of droughts over major river basins in Southern Africa at specific global warming levels. *Theoretical and Applied Climatology*, *137*(3): 1785-1799.

Abram, N.J., Mulvaney, R., Vimeux, F., Phipps, S.J., Turner, J. and England, M.H. 2014. Evolution of the Southern Annular Mode during the past millennium. *Nature Climate Change*, *4*(7): 564-569.

Adams, M.A., Buckley, T.N. and Turnbull, T.L. 2020. Diminishing CO_2-driven gains in water-use efficiency of global forests. *Nature Climate Change*, *10*(5): 466-471.

Anderson, W.T., Bernasconi, S.M., McKenzie, J.A., Saurer, M. and Schweingruber, F. 2002. Model evaluation for reconstructing the oxygen isotopic composition in precipitation from tree ring cellulose over the last century. *Chemical Geology*, *182*(2-4): 121-137.

Andreu-Hayles, L., Santos, G.M., Herrera-Ramírez, D.A., Martin-Fernández, J., Ruiz-Carrascal, D., Boza-Espinoza, T.E., Fuentes, A.F. and MJ, P. 2015. Matching dendrochronological dates with the Southern Hemisphere ^{14}C bomb curve to confirm annual tree rings in Pseudolmedia rigida from Bolivia. *Radiocarbon*, *57*(1), DOI: 10.2458/azu_rc.57.18192.

Angombe, S.T. and Shikangalah, R.N. 2021. Pterocarpus angolensis growth rings and precipitation: A comparison between Zambezi and Otjozondjupa region, Namibia. *International Science and Technology Journal of Namibia*, 14: 34-45.

Angula, M.N. and Kaundjua, M.B. 2016. The changing climate and human vulnerability in north-central Namibia. Jàmbá: *Journal of Disaster Risk Studies,* 8(2): DOI: 10.4102/jamba.v8i2.200.

Anthonissen, C.J. 2009. *The mid-crustal architecture of a continental arc-a transect through the South Central Zone of the Pan-African Damara Belt, Namibia*. Doctoral thesis submitted to the University of Stellenbosch, Stellenbosch.

Archer, E., Landman, W., Malherbe, J., Tadross, M. and Pretorius, S. 2019. South Africa's winter rainfall region drought: A region in transition? *Climate Risk Management*, 25, DOI: 10.1016/j.crm.2019.100188.

AWR. 2012. Biodiversity Impact Assessment at Rössing Uranium Project. (Phase 1). Unpublished report to Aurecon and SLR consulting for the Environmental Impact

Assessment of the Proposed Mining of the Z20 Uranium Deposit. African Wilderness Restoration, awr@mweb.com.na; PO Box 11997 Klein Windhoek, Windhoek Namibia.

Barnes, J.I., MacGregor, J. and Alberts, M., 2012. Expected climate change impacts on land and natural resource use in Namibia: exploring economically efficient responses. *Pastoralism: Research, Policy and Practice*, 2(1), DOI: 10.1111/j.1365-2486.2006.01140.x.

Beck, H.E., Zimmermann, N.E., McVicar, T.R., Vergopolan, N., Berg, A. and Wood, E.F. 2018. Present and future Köppen-Geiger climate classification maps at 1-km resolution. *Scientific data*, 5(1), DOI: 10.1038/sdata.2018.214

Belmecheri, S. and Lavergne, A., 2020. Compiled records of atmospheric CO_2 concentrations and stable carbon isotopes to reconstruct climate and derive plant ecophysiological indices from tree rings. *Dendrochronologia*, 63, DOI: 10.1016/j.dendro.2020.125748.

Berger, W.H. 2011. Discovery of the 5.7-year Douglass cycle: A pioneer's quest for solar cycles in tree-ring records. *The Open Geography Journal*, 4(1): 131-140.

Blackwell, P.G. and Buck, C.E. 2008. Estimating radiocarbon calibration curves. *Bayesian Analysis*, 3(2): 225-248.

Blom, L. 1978. A report on the groundwater investigations of the lower Kuiseb river (GH 2990/1). DWA-Archive 89/1316, Windhoek.

Boswijk, G. Loader, N.J., Young, G.H. and Hogg, A. 2021. Developing tree-ring chronologies from New Zealand matai (*Prumnopitys taxifolia*) and miro (*Prumnopitys ferruginea*) for archaeological dating: progress and problems. *Dendrochronologia*, 69, DOI: 10.1016/j.dendro.2021.125876.

Braconnot, P. Harrison, S.P., Kageyama, M., Bartlein, P.J., Masson-Delmotte, V., Abe-Ouchi, A., Otto-Bliesner, B. and Zhao, Y. 2012. Evaluation of climate models using palaeoclimatic data. *Nature Climate Change*, 2(6): 417-424.

Bradley, R.S. and Jonest, P.D. 1993. 'Little Ice Age' summer temperature variations: their nature and relevance to recent global warming trends. *The Holocene*, 3(4): 367-376.

Braun, K., Bar-Matthews, M., Matthews, A., Ayalon, A., Zilberman, T., Cowling, R.M., Fisher, E.C., Herries, A.I., Brink, J.S. and Marean, C.W. 2020. Comparison of climate and environment on the edge of the Palaeo-Agulhas Plain to the Little Karoo (South Africa) in Marine Isotope Stages 5–3 as indicated by speleothems. *Quaternary Science Reviews*, 235, DOI: 10.1016/j.quascirev.2019.06.025.

Brienen, R.J. and Zuidema, P.A. 2005. Relating tree growth to rainfall in Bolivian rain forests: a test for six species using tree ring analysis. *Oecologia*, 146(1), DOI: 10.1007/s00442-005-0160-y.

Briffa, K.R., Osborn, T.J. and Schweingruber, F.H. 2004. Large-scale temperature inferences from tree rings: a review. *Global and Planetary Change*, 40(1-2): 11-26.

Brook, G.A., Marais, E. Srivastava, P. and Jordan, T. 2007. Timing of lake-level changes in Etosha Pan, Namibia, since the middle Holocene from OSL ages of relict shorelines in the Okondeka region. *Quaternary International*, 175(1): 29-40.

Brooks, J.R., Flanagan, L.B. and Ehleringer, J.R. 1998. Responses of boreal conifers to climate fluctuations: indications from tree-ring widths and carbon isotope analyses. *Canadian Journal of Forest Research*, 28(4): 524-533.

Buckley, T.N. 2019. How do stomata respond to water status?. *New Phytologist*, 224(1): 21-36.

Burls, N.J., Blamey, R.C., Cash, B.A., Swenson, E.T., Fahad, A.A., Bopape, M.J.M., Straus, D.M. and Reason, C.J. 2019. The Cape Town “Day Zero” drought and Hadley cell expansion. *Npj Climate and Atmospheric Science*, 2(1), DOI: 10.1038/s41612-019-0084-6.

Chase, B.M. and Meadows, M.E., 2007. Late Quaternary dynamics of southern Africa's winter rainfall zone. *Earth-Science Reviews*, 84(3-4): 103-138.

Chase, B.M., Meadows, M.E., Scott, L., Thomas, D.S.G., Marais, E., Sealy, J. and Reimer, P.J. 2009. A record of rapid Holocene climate change preserved in hyrax middens from southwestern Africa. *Geology*, 37(8): 703-706.

Chase, B.M., Scott, L., Meadows, M.E., Gil-Romera, G., Boom, A., Carr, A.S., Reimer, P.J., Truc, L., Valsecchi, V. and Quick, L.J. 2012. Rock hyrax middens: a palaeoenvironmental archive for southern African drylands. *Quaternary Science Reviews*, 56: 107-125.

Chase, B.M., Niedermeyer, E.M., Boom, A., Carr, A.S., Chevalier, M., He, F., Meadows, M.E., Ogle, N. and Reimer, P.J. 2019. Orbital controls on Namib Desert hydroclimate over the past 50,000 years. *Geology*, 47(9): 867-871.

Chudasama, B., Porwal, A., Wilde, A., González-Álvarez, I., Aranha, M., Akarapu, U., Hirsch, M. and Becker, E. 2019. Bedrock topography modeling and calcrete-uranium prospectivity analysis of Central Erongo Region, Namibia. *Ore Geology Reviews*, 114, DOI: 10.1016/j.oregeorev.2019.103109.

Cleaveland, M.K., Stahle, D.W., Therrell, M.D., Villanueva-Diaz, J. and Burns, B.T. 2003. Tree-ring reconstructed winter precipitation and tropical teleconnections in Durango, Mexico. *Climatic Change*, 59(3): 369-388.

Conway, D., Hanson, C.E., Doherty, R. and Persechino, A. 2007. GCM simulations of the Indian Ocean dipole influence on East African rainfall: Present and future. *Geophysical Research Letters*, 34(3), DOI: 10.1029/2006GL027597.

Cook, E.R., Palmer, J.G. and D'Arrigo, R.D. 2002. Evidence for a 'Medieval Warm Period'in a 1,100 year tree-ring reconstruction of past austral summer temperatures in New Zealand. *Geophysical Research Letters*, 29(14), DOI: 10.1029/2001GL014580.

Copenheaver, C.A., Pokorski, E.A., Currie, J.E. and Abrams, M.D. 2006. Causation of false ring formation in *Pinus banksiana*: a comparison of age, canopy class, climate and growth rate. *Forest Ecology and Management*, 236(2-3): 348-355.

Corvino, A.F. and Pretorius, L.E. 2013. Uraniferous leucogranites south of Ida Dome, central Damara Belt, Namibia: Morphology, distribution and mineralisation. *Journal of African Earth Sciences*, 80: 60-73.

Cowan, D.A., Hopkins, D.W., Jones, B.E. Maggs-Kölling, G., Majewska, R. and Ramond, J.B. 2020. Microbiomics of Namib Desert habitats. *Extremophiles*, 24(1): 17-29.

Cowley, C. 2022. Awe-inspiring aerial footage of the Swakop River meeting the ocean. Getaway. [Online] Available at: https://www.getaway.co.za/travel-news/awe-

inspiring-footage-of-the-swakop-river-meeting-the-ocean-from-above/, accessed February 2022.

Craig, H. 1954. Carbon 13 in plants and the relationships between carbon 13 and carbon 14 variations in nature. *The Journal of Geology*, *62*(2), pp.115-149.

Crawford, A. and Terton, A. 2016. *Review of current and planned adaptation action in Namibia.CARIAA Working Paper no. 12*. International Development Research Centre, Ottawa, Canada and UK Aid, London, United Kingdom.

Danis, P.A., Masson-Delmotte, V., Stievenard, M., Guillemin, M.T., Daux, V., Naveau, P. and Von Grafenstein, U. 2006. Reconstruction of past precipitation $\delta^{18}O$ using tree-ring cellulose $\delta^{18}O$ and $\delta^{13}C$: a calibration study near Lac d'Annecy, France. *Earth and Planetary Science Letters*, 243(3-4): 439-448.

Daron, J. 2015. Challenges in using a Robust Decision Making approach to guide climate change adaptation in South Africa. *Climatic Change*, 132(3): 459-473.

D'Arrigo, R.D. and Jacoby, G.C. 1991. A 1000-year record of winter precipitation from northwestern New Mexico, USA: a reconstruction from tree-rings and its relation to El Niño and the Southern Oscillation. *The Holocene*, 1(2): 95-101.

De Cauwer, V., Fichtler, E., Beeckman, H., Graz, F.P., Mertens, J., Van Holsbeeck, S. and Muys, B. 2017. Predicting site productivity of the timber tree *Pterocarpus angolensis*. *Southern Forests: A Journal of Forest Science*, 79(3): 259-268.

De Mil, T., Meko, M., Belmecheri, S., February, E., Therrell, M., Van den Bulcke, J. and Trouet, V. 2021. A lonely dot on the map: Exploring the climate signal in tree-ring density and stable isotopes of clanwilliam cedar, South Africa. *Dendrochronologia*, 69, DOI: 10.1016/j.dendro.2021.125879.

Desbiolles, F. Howard, E., Blamey, R.C., Barimalala, R., Hart, N.C. and Reason, C.J. 2020. Role of ocean mesoscale structures in shaping the Angola-Low pressure system and the southern Africa rainfall. *Climate Dynamics*, 54(7): 3685-3704.

Dirkx, E. Hager, C., Tadross, M., Bethune, S. and Curtis, B. 2008. *Climate change vulnerability and adaptation assessment Namibia*. Desert Research Foundation Namibia and Climate Systems Analysis Group, Windhoek.

Du Plessis, N., Chase, B.M., Quick, L.J., Haberzettl, T., Kasper, T. and Meadows, M.E. 2020. Vegetation and climate change during the Medieval Climate Anomaly and the Little Ice Age on the southern Cape coast of South Africa: Pollen evidence from Bo Langvlei. *The Holocene*, 30(12): 1716-1727.

Dunwiddie, P.W. and LaMarche Jr, V.C. 1980. A climatically responsive tree-ring record from *Widdringtonia cedarbergensis*, Cape Province, South Africa. *Nature*, 286(5775): 796-797.

Dyer, C. 2014. New names for the African *Acacia* species in *Vachellia* and *Senegalia*. *Southern Forests: A Journal of Forest Science*, 76(4), DOI: 10.2989/20702620.2014.980090.

Eckardt, F.D., Soderberg, K., Coop, L.J., Muller, A.A., Vickery, K.J., Grandin, R.D., Jack, C., Kapalanga, T.S. and Henschel, J. 2013. The nature of moisture at Gobabeb, in the central Namib Desert. *Journal of Arid Environments*, 93: 7-19.

Eeley, H.A., Lawes, M.J. and Piper, S.E. 1999. The influence of climate change on the distribution of indigenous forest in KwaZulu-Natal, South Africa. *Journal of Biogeography*, *26*(3): 595-617.

Eide, M., Olsen, A., Ninnemann, U.S. and Eldevik, T. 2017. A global estimate of the full oceanic ^{13}C Suess effect since the preindustrial. *Global Biogeochemical Cycles*, 31(3): 492-514.

Ekblom, A. and Stabell, B. 2008. Paleohydrology of Lake Nhaucati (southern Mozambique), ~ 400 AD to present. *Journal of Paleolimnology*, 40(4): 1127-1141.

Ekblom, A., Gillson, L., Risberg, J., Holmgren, K. and Chidoub, Z. 2012. Rainfall variability and vegetation dynamics of the lower Limpopo Valley, Southern Africa, 500 AD to present. *Palaeogeography, Palaeoclimatology, Palaeoecology*, 363: 69-78.

Emori, S., Taylor, K., Hewitson, B., Zermoglio, F., Juckes, M., Lautenschlager, M. and Stockhause, M. 2016. CMIP5 data provided at the IPCC data distribution centre. Fact Sheet of the task group on data and scenario support for impact and climate analysis (TGICA) of the intergovernmental panel on climate change (IPCC), pp. 8. Available from: https://www.ipcc data.org/docs/factsheets/TGICA_Fact_Sheet_ CMIP5_data_provided_at_the_IPCC_DDC_Ver_1_2016.pdf.

Eronen, M., Zetterberg, P., Briffa, K.R., Lindholm, M., Meriläinen, J. and Timonen, M. 2002. The supra-long Scots pine tree-ring record for Finnish Lapland: Part 1, chronology construction and initial inferences. *The Holocene*, 12(6): 673-680.

Farquhar, G.D., O'Leary, M.H. and Berry, J.A. 1982. On the relationship between carbon isotope discrimination and the intercellular carbon dioxide concentration in leaves. *Functional Plant Biology*, 9(2): 121-137.

Favre, A., Hewitson, B., Lennard, C., Cerezo-Mota, R. and Tadross, M. 2013. Cut-off lows in the South Africa region and their contribution to precipitation. *Climate Dynamics*, 41(9): 2331-2351.

February, E.C. and Stock, W.D. 1998. The relationship between ring width measures and precipitation for *Widdringtonia cedarbergensis*. *South African Journal of Botany*, 64(3): 213-216.

February, E.C. and Stock, W.D. 1999. Declining trend in the $^{13}C/^{12}C$ ratio of atmospheric carbon dioxide from tree rings of South African *Widdringtonia cedarbergensis*. *Quaternary Research*, 52(2): 229-236.

February, E.C., Gagen, M. and van Wyk, A.E. 2003. A dendrochronological assessment of two South African *Widdringtonia* species. *South African Journal of Botany*, 69(3): 428-433.

February, E.C., Mader, A.D., Bond, W.J. 2006. Age determination of two South African *Acacia* species using ring counts and radiocarbon dating. *African Journal of Ecology,* 44: 417-419.

February, E.C., West, A.G. and Newton, R.J. 2007. The relationship between rainfall, water source and growth for an endangered tree. *Austral Ecology*, 32(4): 397-402.

Ferguson, C.W. 1970. Concepts and techniques of dendrochronology. In Berger, R. (ed), *Scientific methods in medieval archaeology*. University of California Press, Los Angeles, California. pp. 183–200.

Fichtler, E., Clark, D.A. and Worbes, M. 2003. Age and long-term growth of trees in an old-growth tropical rain forest, based on analyses of tree rings and $^{14}C^{1}$. *Biotropica*, 35(3): 306-317.

Fichtler, E., Trouet, V., Beeckman, H., Coppin, P. and Worbes, M. 2004. Climatic signals in tree rings of *Burkea africana* and *Pterocarpus angolensis* from semiarid forests in Namibia. *Trees*, 18(4): 442-451.

Fichtler, E., Helle, G. and Worbes, M. 2010. Stable-carbon isotope time series from tropical tree rings indicate a precipitation signal. *Tree-Ring Research*, 66(1): 35-50.

Finch, J.M. and Meadows, M.E. 2019. South African biomes and their changes over time. In *The Geography of South Africa*. Springer, Cham. pp. 57-69.

Fitchett, J.M., Grab, S.W., Bamford, M.K. and Mackay, A.W. 2017. Late Quaternary research in southern Africa: progress, challenges and future trajectories. *Transactions of the Royal Society of South Africa*, 72(3): 280-293.

Fitchett, J.M., Mackay, A.W., Grab, S.W., Bamford, M.K. 2016. Holocene climatic variability indicated by a multi-proxy record from southern Africa's highest wetland. *The Holocene*, 27 (5): 638-650.

Fritts, H.C. 1971. Dendroclimatology and dendroecology. *Quaternary Research*, 1(4): 419-449.

Friedrich, M., Remmele, S., Kromer, B., Hofmann, J., Spurk, M., Kaiser, K.F., Orcel, C. and Küppers, M. 2004. The 12,460-year Hohenheim oak and pine tree-ring chronology from central Europe—a unique annual record for radiocarbon calibration and paleoenvironment reconstructions. *Radiocarbon*, 46(3): 1111-1122.

Funk, C., Peterson, P., Landsfeld, M., Pedreros, D., Verdin, J., Shukla, S., Husak, G., Rowland, J., Harrison, L., Hoell, A. and Michaelsen, J. 2015. The climate hazards infrared precipitation with stations—a new environmental record for monitoring extremes. *Scientific Data*, 2(1), DOI: 10.1038/sdata.2015.66.

Gagen, M., McCarroll, D., Loader, N.J., Robertson, I., Jalkanen, R. and Anchukaitis, K.J. 2007. Exorcising the segment length curse': summer temperature reconstruction since AD 1640 using non-detrended stable carbon isotope ratios from pine trees in northern Finland. *The Holocene*, 17(4): 435-446.

Gagen, M., McCarroll, D., Loader, N.J., Robertson, I. 2010. Stable isotopes in dendroclimatology: moving beyond ‘potential’. In: Hughes, M.K., Swetnam, T.W., Diaz, H.F. (eds), *Dendroclimatology: Progress and Prospects*. Springer, pp. 147-172.

Gasse, F., Chalié, F., Vincens, A., Williams, M.A. and Williamson, D. 2008. Climatic patterns in equatorial and southern Africa from 30,000 to 10,000 years ago reconstructed from terrestrial and near-shore proxy data. *Quaternary Science Reviews*, 27(25-26): 2316-2340.

Gaughan, A.E., Staub, C.G., Hoell, A., Weaver, A. and Waylen, P.R. 2016. Inter-and Intra-annual precipitation variability and associated relationships to ENSO and the IOD in southern Africa. *International Journal of Climatology*, 36(4): 1643-1656.

Gebrekirstos, A., Bräuning, A., Sass-Klassen, U. and Mbow, C. 2014. Opportunities and applications of dendrochronology in Africa. *Current Opinion in Environmental Sustainability*, 6: 48-53.

Gergis, J. and Henley, B.J. 2017. Southern Hemisphere rainfall variability over the past 200 years. *Climate Dynamics*, 48(7): 2087-2105.

Geyh, M.A. and Heine, K. 2014. Several distinct wet periods since 420 ka in the Namib Desert inferred from U-series dates of speleothems. *Quaternary research*, 81(2): 381-391.

Gil-Romera, G., Scott, L., Marais, E. and Brook, G.A. 2006. Middle-to late-Holocene moisture changes in the desert of northwest Namibia derived from fossil hyrax dung pollen. *The Holocene*, 16(8): 1073-1084.

Gil-Romera, G., Scott, L., Marais, E. and Brook, G.A., 2007. Late Holocene environmental change in the northwestern Namib Desert margin: new fossil pollen evidence from hyrax middens. *Palaeogeography, Palaeoclimatology, Palaeoecology*, 249(1-2): 1-17.

Gou, X., Gao, L., Deng, Y., Chen, F., Yang, M. and Still, C. 2015. An 850-year tree-ring-based reconstruction of drought history in the western Qilian Mountains of northwestern China. *International Journal of Climatology*, 35(11): 3308-3319.

Goudie, A.S., Eckardt, F. 1999. The evolution of the morphological framework of the Central Namib Desert, Namibia, since the Early Cretaceous. *Geografiska Annaler Series A-Physical Geography*, 81A: 443-458.

Grab, S.W. and Nash, D.J. 2010. Documentary evidence of climate variability during cold seasons in Lesotho, southern Africa, 1833–1900. *Climate Dynamics*, 34(4): 473-499.

Grab, S. and Zumthurm, T. 2018. The land and its climate knows no transition, no middle ground, everywhere too much or too little: a documentary-based climate chronology for central Namibia, 1845–1900*. International Journal of Climatology*, 38: DOI: 10.1002/joc.5397.

Greenbaum, N., Schwartz, U., Benito, G., Porat, N., Cloete, G.C. and Enzel, Y. 2014. Paleohydrology of extraordinary floods along the Swakop River at the margin of

the Namib Desert and their paleoclimate implications. *Quaternary Science Reviews*, 103: 153-169.

Grodek, T., Benito, G., Botero, B.A., Jacoby, Y., Porat, N., Haviv, I., Cloete, G. and Enzel, Y. 2013. The last millennium largest floods in the hyperarid Kuiseb River basin, Namib Desert. *Journal of Quaternary Science*, 28(3): 258-270.

Grodek, T., Morin, E., Helman, D., Lensky, I., Dahan, O., Seely, M., Benito, G. and Enzel, Y. 2020. Eco-hydrology and geomorphology of the largest floods along the hyperarid Kuiseb River, Namibia. *Journal of Hydrology*, 582, DOI: 10.1016/j.jhydrol.2019.124450.

Hahn, A., Schefuß, E., Andò, S., Cawthra, H.C., Frenzel, P., Kugel, M., Meschner, S., Mollenhauer, G. and Zabel, M. 2017. Southern Hemisphere anticyclonic circulation drives oceanic and climatic conditions in late Holocene southernmost Africa. *Climate of the Past*, 13(6): 649-665.

Hahn, A., Miller, C., Andó, S., Bouimetarhan, I., Cawthra, H.C., Garzanti, E., Green, A.N., Radeff, G., Schefuß, E. and Zabel, M. 2018. The provenance of terrigenous components in marine sediments along the east coast of southern Africa. *Geochemistry, Geophysics, Geosystems*, 19(7): 1946-1962.

Hahn, A., Neumann, F.H., Miller, C., Finch, J., Frankland, T., Cawthra, H.C., Schefuß, E. and Zabel, M. 2021. Mid-to Late Holocene climatic and anthropogenic

influences in Mpondoland, South Africa. *Quaternary Science Reviews*, *261*,DOI: 10.1016/j.quascirev.2021.106938.

Hall, G., Woodborne, S. and Scholes, M. 2008. Stable carbon isotope ratios from archaeological charcoal as palaeoenvironmental indicators. *Chemical Geology*, 247(3-4): 384-400.

Hall, G., Woodborne, S. and Pienaar, M. 2009. Rainfall control of the $\delta^{13}C$ ratios of *Mimusops caffra* from KwaZulu-Natal, South Africa. *The Holocene*, 19(2): 251-260.

Hall, M. 1976. Dendroclimatology, rainfall and human adaptation in the later Iron Age of Natal and Zululand. *Annals of the Natal Museum*, 22(3): 693-703.

Hannaford, M.J., Jones, J.M. and Bigg, G.R. 2015. Early-nineteenth-century southern African precipitation reconstructions from ships' logbooks. *The Holocene*, 25(2): 379-390.

Hannaford, M.J. and Beck, K.K. 2021. Rainfall variability in southeast and west-central Africa during the Little Ice Age: do documentary and proxy records agree?, *Climatic Change*, 168(1), DOI: 10.1007/s10584-021-03217-7.

Harduth, T. and Fitchett, J.M. 2020. Climatic Deviations Across a Transect of South Africa during El Niño and La Niña Years. *Climate Change Research*, 1(4): 49-65.

Heine, K. 2005. Holocene climate of Namibia: a review based on geoarchives. *African Study Monographs. Supplementary issue.*, 30: 119-133.

Heine, K. and Völkel, J. 2011. Extreme floods around AD 1700 in the northern Namib Desert, Namibia, and in the Orange River catchment, South Africa-Were they forced by a decrease of solar irradiance during the Little Ice Age. *Geographia Polonica,* 84*:* 61-80*.*

Henschel, J.R. and Seely, M.K. 2008. Ecophysiology of atmospheric moisture in the Namib Desert. *Atmospheric Research*, 87(3-4): 362-368.

Henschel, J.R. and Lancaster, N. 2013. Gobabeb–50 years of Namib Desert research. *Journal of Arid Environments*, 93, DOI: 10.1016/j.jaridenv.2012.09.015.

Herrera-Ramirez, D., Andreu-Hayles, L., Del Valle, J.I., Santos, G.M. and Gonzalez, P.L. 2017. Nonannual tree rings in a climate-sensitive *Prioria copaifera* chronology in the Atrato River, Colombia. *Ecology and Evolution*, 7(16): 6334-6345.

Hogg, A.G., Heaton, T.J., Hua, Q., Palmer, J.G., Turney, C.S., Southon, J., Bayliss, A., Blackwell, P.G., Boswijk, G., Ramsey, C.B. and Pearson, C. 2020. SHCal20 Southern Hemisphere calibration, 0–55,000 years cal BP. *Radiocarbon*, *62*(4): 759-778.

Holmgren, K., Risberg, J., Freudendahl, J., Achimo, M., Ekblom, A., Mugabe, J., Norström, E. and Sitoe, S. 2012. Water-level variations in Lake Nhauhache, Mozambique, during the last 2,300 years. *Journal of Paleolimnology*, 48(2): 311-322.

Hopper, C., Sealy, J.C. and Dewar, G. 2018. Little Ice Age drought event reconstructed from isotopic analysis of archaeological springbok (*Antidorcas marsupialis*) teeth. *Palaeogeography, Palaeoclimatology, Palaeoecology*, 495: 105-112.

Howard, E. 2019. Southern African synoptic climate dynamics and future change: tropical lows and the Congo Air Boundary. Doctoral thesis, submitted to the University of Oxford.

Howard, E. and Washington, R. 2018. Characterizing the synoptic expression of the Angola low. *Journal of Climate*, 31(17): 7147-7165.

Howard, E. and Washington, R. 2019. Drylines in southern Africa: Rediscovering the Congo air boundary. *Journal of Climate*, 32(23): 8223-8242.

Hua, Q. and Barbetti, M. 2004. Review of tropospheric bomb ^{14}C data for carbon cycle modeling and age calibration purposes. *Radiocarbon*, 46(3): 1273-1298.

Hua, Q. 2009. Radiocarbon: a chronological tool for the recent past. *Quaternary Geochronology*, 4(5)P: 378-390.

Huffman, T.N. 2009. A cultural proxy for drought: ritual burning in the Iron Age of southern Africa. *Journal of Archaeological Science*, 36(4): 991-1005.

Humphries, M.S., Kirsten, K.L. and McCarthy, T.S. 2019. Rapid changes in the hydroclimate of southeast Africa during the mid-to late-Holocene. *Quaternary Science Reviews*, 212: 178-186.

Ibebuchi, C.C. 2021. On the relationship between circulation patterns, the southern annular mode, and rainfall variability in Western Cape. *Atmosphere*, 12(6), DOI: 10.3390/atmos12060753.

Imbol Koungue, R.A., Illig, S. and Rouault, M. 2017. Role of interannual Kelvin wave propagations in the equatorial Atlantic on the Angola Benguela Current system. *Journal of Geophysical Research: Oceans*, 122(6): 4685-4703.

Imbol Koungue, R.A., Rouault, M., Illig, S., Brandt, P. and Jouanno, J. 2019. Benguela Niños and Benguela Niñas in forced ocean simulation from 1958 to 2015. Journal of Geophysical Research: Oceans, 124(8): 5923-5951.

Info-Namibia. 2021. *Namibias geography***.** Available from: https://www.info-namibia.com/info/namibias-geography, accessed January 2021.

Inman, E.N., Hobbs, R.J. and Tsvuura, Z. 2020. No safety net in the face of climate change: The case of pastoralists in Kunene Region, Namibia. *PloS one*, 15(9), DOI: 10.1371/journal.pone.0238982.

IPCC, 2021*. Summary for Policymakers.* In: Masson-Delmotte, V., Zhai, P., Pirani, A., Connors, S. L., Péan, C., Berger, S., Caud, N., Chen, Y., Goldfarb, L., Gomis, M. I., Huang, M., Leitzell, K., Lonnoy, E., Matthews, J. B. R., Maycock, T. K., Waterfield, T., Yelekçi, O., Yu, R. and Zhou, B. (eds), Climate Change 2021: The Physical Science Basis. Contribution of Working Group I to the Sixth Assessment Report of the Intergovernmental Panel on Climate Change. Cambridge University Press.

Irish, J. 1994. The biomes of Namibia, as determined by objective categorisation. *Navorsinge van die Nasionale Museum: Researches of the National Museum*, 10(13): 550-592.

Jones, P.D., Osborn, T.J. and Briffa, K.R. 2001. The evolution of climate over the last millennium. *Science*, *292*(5517): 662-667.

Jones, P.D., Briffa, K.R., Osborn, T.J., Lough, J.M., Van Ommen, T.D., Vinther, B.M., Luterbacher, J.W.E.R.Z.F.W., Wahl, E.R., Zwiers, F.W., Mann, M.E. and Schmidt, G.A. 2009. High-resolution palaeoclimatology of the last millennium: a review of current status and future prospects. *The Holocene*, 19(1): 3-49.

Jury, M.R. 1996. Regional teleconnection patterns associated with summer rainfall over South Africa, Namibia and Zimbabwe. *International Journal of Climatology: A Journal of the Royal Meteorological Society*, 16(2): 135-153.

Jury, M.R. and Engert, S. 1999. Teleconnections modulating inter-annual climate variability over northern Namibia. *International Journal of Climatology: A Journal of the Royal Meteorological Society*, *19*(13), pp.1459-1475.

Kaennel, M. and Schweingruber, F.H. 1995. Multilingual glossary of dendrochronology. *WSL FNP, Haupt*, 133: 162-184.

Kaseke, K.F., Wang, L., Wanke, H., Turewicz, V. and Koeniger, P. 2016. An analysis of precipitation isotope distributions across Namibia using historical data. *PloS one*, 11(5), DOI: 10.1371/journal.pone.0154971.

Kaseke, K.F., Wang, L. and Seely, M.K. 2017. Nonrainfall water origins and formation mechanisms. *Science Advances*, *3*(3), DOI: 10.1126/sciadv.1603131.

Kaseke, K. F., Tian, C., Wang, L., Seely, M., Vogt, R., Wassenaar, T., & Mushi, R. 2018. Fog Spatial Distributions over the Central Namib Desert-An Isotope Approach. *Aerosol and Air Quality Research*, 18(1), 49-61.

Kelso, C. and Vogel, C. 2007. The climate of Namaqualand in the nineteenth century. *Climatic Change*, 83(3): 357-380.

Kelso, C. and Vogel, C. 2015. Diversity to decline-livelihood adaptations of the Namaqua Khoikhoi (1800–1900). *Global Environmental Change*, 35: 254-268.

Kinahan, J. 2016. Human responses to climatic variation in the Namib Desert during the last 1,000 years. *African Archaeological Review*, 33(2):183-203.

Kitagawa, H. and Matsumoto, E. 1995. Climatic implications of $\delta^{13}C$ variations in a Japanese cedar (*Cryptomeria japonica*) during the last two millenia. *Geophysical Research Letters*, 22(16): 2155-2158.

Knight, J. and Fitchett, J. 2019. Climate change during the Late Quaternary in South Africa. In: J. Knight and C.M. Rogerson (eds), *The Geography of South Africa: Contemporary Changes and New Directions*. Springer, Switzerland, pp. 37-45.

Koseki, S. and Imbol Koungue, R.A. 2021. Regional atmospheric response to the Benguela Niñas. *International Journal of Climatology*, 41, DOI: 10.1002/joc.6782.

Kress, A., Saurer, M., Siegwolf, R.T., Frank, D.C., Esper, J. and Bugmann, H. 2010. A 350 year drought reconstruction from Alpine tree ring stable isotopes. *Global Biogeochemical Cycles*, 24(2), DOI: 10.1029/2009GB003613.

Krug, J.H. 2017. Tree water potentials supporting an explanation for the occurrence of *Vachellia erioloba* in the Namib Desert (Namibia). *Forest Ecosystems*, 4(1), DOI: 10.1186/s40663-017-0107-x.

Lancaster, J., Lancaster, N. & Seely, M.K. 1984. Climate of the central Namib Desert. *Madoqua*, 14: 5-61.

Leavitt, S.W. and Bannister, B. 2009. Dendrochronology and radiocarbon dating: the laboratory of tree-ring research connection. *Radiocarbon*, 51(1): 373-384.

Leijonhufvud, L., Wilson, R., Moberg, A., Söderberg, J., Retsö, D. and Söderlind, U. 2010. Five centuries of Stockholm winter/spring temperatures reconstructed from documentary evidence and instrumental observations. *Climatic Change*, 101(1): 109-141.

Lendelvo, S.; Angula, M.N.; Mogotsi, I.; Aribeb, K. 2018. Towards the reduction of vulnerabilities and risks of climate change in the Community-Based tourism, Namibia. In: do Carmo, J.S.A., (ed), *Natural Hazards—Risk Assessment and Vulnerability Reduction*. BoD—Books on Demand: London, UK, pp. 87–105.

Leuschner, H.H., Sass-Klaassen, U., Jansma, E., Baillie, M.G. and Spurk, M. 2002. Subfossil European bog oaks: population dynamics and long-term growth depressions as indicators of changes in the Holocene hydro-regime and climate. *The Holocene*, 12(6): 695-706.

Li, J., Shi, J., Zhang, D.D., Yang, B., Fang, K. and Yue, P.H. 2017. Moisture increase in response to high-altitude warming evidenced by tree-rings on the southeastern Tibetan Plateau. *Climate Dynamics*, 48(1): 649-660.

Lilly, M.A. 1977. An assessment of the dendrochronological potential of indigenous tree species in South Africa. Department of Geographical and Environmental Studies, University of the Witwatersrand, Occasional Paper No. 18.

Lindesay, J.A. and Vogel, C.H. 1990. Historical evidence for Southern Oscillation-southern African rainfall relationships. *International Journal of Climatology*, 10(7): 679-689.

Lipp, J., Trimborn, P., Fritz, P. Moser, H., Becker, B. and Frenzel, B. 1991. Stable isotopes in tree ring cellulose and climatic change. *Tellus B*, 43(3): 322-330.

Liu, X., Shao, X., Zhao, L., Qin, D., Chen, T. and Ren, J. 2007. Dendroclimatic temperature record derived from tree-ring width and stable carbon isotope chronologies in the Middle Qilian Mountains, China. *Arctic, Antarctic, and Alpine Research*, 39(4): 651-657.

Liu, X., Shao, X., Wang, L., Liang, E., Qin, D. and Ren, J. 2008. Response and dendroclimatic implications of $\delta^{13}C$ in tree rings to increasing drought on the northeastern Tibetan Plateau. *Journal of Geophysical Research: Biogeosciences*, 113(G3), DOI: 10.1029/2007JG000610.

Liu, X. and Zhou, J. 2021. Assessment of the Continuous Extreme Drought Events in Namibia during the Last Decade. *Water*, 13(20), DOI: 10.3390/w13202942.

Liu, Y., Cai, Q., Shi, J., Hughes, M.K., Kutzbach, J.E., Liu, Z., Ni, F. and An, Z. 2005. Seasonal precipitation in the south-central Helan Mountain region, China, reconstructed from tree-ring width for the past 224 years. *Canadian Journal of Forest Research*, *35*(10): 2403-2412.

Liu, Y., Sun, J., Song, H., Cai, Q., Bao, G. and Li, X. 2010. Tree-ring hydrologic reconstructions for the Heihe River watershed, western China since AD 1430. *Water Research*, 44(9): 2781-2792.

Loader, N.J., Robertson, I., Barker, A.C., Switsur, V.R. and Waterhouse, J.S. 1997. An improved technique for the batch processing of small wholewood samples to α-cellulose. *Chemical Geology*, 136(3-4): 313-317.

Loader, N.J., McCarroll, D., Gagen, M., Robertson, I. and Jalkanen, R. 2007. Extracting climatic information from stable isotopes in tree rings. *Terrestrial Ecology*, 1: 25-48.

Longridge, L., Gibson, R.L., Kinnaird, J.A. and Armstrong, R.A. 2011. Constraining the timing of deformation in the southwestern Central Zone of the Damara Belt, Namibia. *Geological Society, London, Special Publications*, 357(1): 107-135.

Lovegrove, B. 1993. *The Living Deserts of Southern Africa*. Vlaeberg, South Africa: Fernwood Press.

Luetkemeier, R. and Liehr, S. 2019. *Integrated responses to drought risk in Namibia and Angola*. SOE Policy Brief, No. 6. ISOE – Institute for Social-Ecological Research (ed.). Frankfurt am Main, Germany.

Lüning, S., Gałka, M., Danladi, I.B., Adagunodo, T.A. and Vahrenholt, F. 2018. Hydroclimate in Africa during the medieval climate anomaly. *Palaeogeography, Palaeoclimatology, Palaeoecology*, 495: 309-322.

Luoto, T.P. and Helama, S. 2010. Palaeoclimatological and palaeolimnological records from fossil midges and tree-rings: the role of the North Atlantic Oscillation in eastern Finland through the Medieval Climate Anomaly and Little Ice Age. *Quaternary Science Reviews*, *29*(17-18): 2411-2423.

MacDonald, A.M., Calow, R.C., MacDonald, D.M., Darling, W.G. and Dochartaigh, B.E. 2009. What impact will climate change have on rural groundwater supplies in Africa? *Hydrological Sciences Journal*, 54(4): 690-703.

Macron, C., Pohl, B., Richard, Y. and Bessafi, M. 2014. How do tropical temperate troughs form and develop over southern Africa? *Journal of Climate*, 27(4):1633-1647.

Malcomb, N.L. and Wiles, G.C. 2013. Tree-ring-based reconstructions of North American glacier mass balance through the Little Ice Age—Contemporary warming transition. *Quaternary Research*, 79(2): 123-137.

Malherbe, J., Dieppois, B., Maluleke, P., Van Staden, M. and Pillay, D.L. 2015. South African droughts and decadal variability. *Natural Hazards*, 80(1): 657-681.

Malherbe, J., Smit, I.P., Wessels, K.J. and Beukes, P.J. 2020. Recent droughts in the Kruger National Park as reflected in the extreme climate index. *African Journal of Range & Forage Science*, 37(1), DOI: 10.2989/10220119.2020.1718755.

Manatsa, D., Chingombe, W. and Matarira, C.H. 2008. The impact of the positive Indian Ocean dipole on Zimbabwe droughts. *International Journal of Climatology: A Journal of the Royal Meteorological Society*, 28(15): 2011-2029.

Manatsa, D., Chipindu, B. and Behera, S.K. 2012. Shifts in IOD and their impacts on association with East Africa rainfall. *Theoretical and Applied Climatology*, 110(1): 115-128.

Mapani, B., Shikangalah, R., Mapaure, I. and Musimba, A. 2021. *Dichrostachys cinerea* Growth Rings as Natural Archives for Climatic Variation in Namibia. In: Leal Filho W., Oguge N., Ayal D., Adeleke L., da Silva I. (eds) *African Handbook of Climate Change Adaptation*. Springer, Cham. pp. 2433-2446. DOI: 10.1007/978-3-030-45106-6_257.

Marchant, R., Mumbi, C., Behera, S. and Yamagata, T. 2007. The Indian Ocean dipole–the unsung driver of climatic variability in East Africa. *African Journal of Ecology*, 45(1): 4-16.

Maxwell, R.S., Wixom, J.A. and Hessl, A.E. 2011. A comparison of two techniques for measuring and crossdating tree rings. *Dendrochronologia*, *29*(4): 237-243.

McCarroll, D. and Loader, N.J. 2004. Stable isotopes in tree rings. *Quaternary Science Reviews*, 23(7-8): 771-801.

McCarroll, D., Gagen, M.H., Loader, N.J., Robertson, I., Anchukaitis, K.J., Los, S., Young, G.H., Jalkanen, R., Kirchhefer, A. and Waterhouse, J.S. 2009. Correction of tree ring stable carbon isotope chronologies for changes in the carbon dioxide content of the atmosphere. *Geochimica et Cosmochimica Acta*, 73(6): 1539-1547.

McDermott, F. 2004. Palaeo-climate reconstruction from stable isotope variations in speleothems: a review. *Quaternary Science Reviews*, 23(7-8): 901-918.

Meadows, M.E. 2015. Seven decades of Quaternary palynological studies in southern Africa: a historical perspective. *Transactions of the Royal Society of South Africa*, 70(2): 103-108.

Mendelsohn, J., Jarvis, A., Roberts, C. and Robertson, T. 2002. *Atlas of Namibia: A portrait of the land and its people*. David Phillips Publishers, Cape Town.

Midgley, G., Hughes, G., Thuiller, W., Drew, G. and Foden, W. 2005. *Assessment of potential climate change impacts on Namibia's floristic diversity, ecosystem*

structure and function. Kirstenbosch Botanical Garden, Cape Town: South African National Biodiversity Institute.

Miller, R.M., Krapf, C., Hoey, T., Fitchett, J., Nguno, A.K., Muyambas, R., Ndeutepo, A., Medialdea, A., Whitehead, A. and Stengel, I. 2021. A sedimentological record of fluvial-aeolian interactions and climate variability in the hyperarid northern Namib Desert, Namibia. *South African Journal of Geology 2021*, 124(3): 575-610.

Mitchell, D., Henschel, J.R., Hetem, R.S., Wassenaar, T.D., Strauss, W.M., Hanrahan, S.A. and Seely, M.K. 2020. Fog and fauna of the Namib Desert: past and future. *Ecosphere*, 11(1), DOI: 10.1002/ecs2.2996.

Muller, A., Reason, C.J.C. and Fauchereau, N. 2008. Extreme rainfall in the Namib Desert during late summer 2006 and influences of regional ocean variability. *International Journal of Climatology: A Journal of the Royal Meteorological Society*, 28(8): 1061-1070.

Munday, C. and Washington, R. 2017. Circulation controls on southern African precipitation in coupled models: The role of the Angola low. *Journal of Geophysical Research: Atmospheres*, 122(2): 861-877.

Mupambwa, H.A., Hausiku, M.K., Nciizah, A.D. and Dube, E. 2019. The unique Namib desert-coastal region and its opportunities for climate smart agriculture: A review. *Cogent Food & Agriculture*, 5(1), DOI: 10.1080/23311932.2019.1645258.

Nash, D.J., 2017. Changes in precipitation over southern Africa during recent centuries. In *Oxford Research Encyclopedia of Climate Science*, DOI:10.1093/acrefore/9780190228620.013.539.

Nash, D.J. and Endfield, G.H. 2002. A 19th century climate chronology for the Kalahari region of central southern Africa derived from missionary correspondence. *International Journal of Climatology: A Journal of the Royal Meteorological Society*, 22(7): 821-841.

Nash, D.J. and Grab, S.W. 2010. “A sky of brass and burning winds”: documentary evidence of rainfall variability in the Kingdom of Lesotho, Southern Africa, 1824–1900. *Climatic Change*, 101(3): 617-653.

Nash, D., Pribyl, K., Klein, J., Neukom, R., Endfield, G., Adamson, G. and Kniveton, D. 2015a. Seasonal rainfall variability in southeast Africa during the nineteenth century reconstructed from documentary sources. *Climatic Change*, 134(4): 605-619.

Nash, D.J., Pribyl, K., Klein, J., Endfield, G.H., Kniveton, D.R. and Adamson, G.C. 2015b. Tropical cyclone activity over Madagascar during the late nineteenth century. *International Journal of Climatology*, 35(11): 3249-3261.

Nash, D.J., De Cort, G., Chase, B.M., Verschuren, D., Nicholson, S.E., Shanahan, T.M., Asrat, A., Lezine, A.M. and Grab, S.W. 2016. African hydroclimatic variability

during the last 2000 years. *Quaternary Science Reviews*, 154, DOI: 10.1016/j.quascirev.2016.10.012.

Nash, D.J., Klein, J., Endfield, G.H., Pribyl, K., Adamson, G.C. and Grab, S.W. 2019. Narratives of nineteenth century drought in southern Africa in different historical source types. *Climatic Change*, 152(3): 467-485.

Nash, S.E. 2002. Archaeological tree-ring dating at the millennium. *Journal of Archaeological Research*, 10(3): 243-275

Neukom, R. and Gergis, J. 2012. Southern Hemisphere high-resolution palaeoclimate records of the last 2000 years. *The Holocene*, 22(5): 501-524.

Neukom, R., Nash, D.J., Endfield, G.H., Grab, S.W., Grove, C.A., Kelso, C., Vogel, C.H. and Zinke, J. 2014. Multi-proxy summer and winter precipitation reconstruction for southern Africa over the last 200 years. *Climate Dynamics*, 42(9): 2713-2726.

Nhemachena, C., Nhamo, L., Matchaya, G., Nhemachena, C.R., Muchara, B., Karuaihe, S.T. and Mpandeli, S. 2020. Climate change impacts on water and agriculture sectors in Southern Africa: Threats and opportunities for sustainable development. *Water*, 12(10), DOI: 10.3390/w12102673.

Nicholson, S.E., 2000. The nature of rainfall variability over Africa on time scales of decades to millenia. *Global and Planetary Change*, 26(1-3): 137-158.

Nicholson, S.E., Nash, D.J., Chase, B.M., Grab, S.W., Shanahan, T.M., Verschuren, D., Asrat, A., Lézine, A.M. and Umer, M. 2013. Temperature variability over Africa during the last 2000 years. *The Holocene*, 23(8): 1085-1094.

Norström, E., Holmgren, K. and Morth, C.M. 2005. Rainfall-driven variations in $\delta^{13}C$ composition and wood anatomy of *Breonadia salicina* trees from South Africa between AD 1375 and 1995. *South African Journal of Science*, 101(3-4):162-168.

Norström, E., Holmgren, K. and Mörth, C.M. 2008. A 600-year-long $\delta^{18}O$ record from cellulose of *Breonadia salicina* trees, South Africa. *Dendrochronologia*, 26(1): 21-33.

Norström, E., Norén, G., Smittenberg, R.H., Massuanganhe, E.A. and Ekblom, A. 2018. Leaf wax δD inferring variable medieval hydroclimate and early initiation of Little Ice Age (LIA) dryness in southern Mozambique. *Global and Planetary Change*, 170: 221-233.

Novak, K., De Luis, M., Saz, M.A., Longares, L.A., Serrano-Notivoli, R., Raventós, J., Čufar, K., Gričar, J., Di Filippo, A., Piovesan, G. and Rathgeber, C.B, 2016. Missing rings in *Pinus halepensis*–the missing link to relate the tree-ring record to extreme climatic events. *Frontiers in Plant Science*, 7, DOI: 10.3389/fpls.2016.00727.

O'Donnell, A.J., Cook, E.R., Palmer, J.G., Turney, C.S., Page, G.F. and Grierson, P.F, 2015. Tree rings show recent high summer-autumn precipitation in northwest Australia is unprecedented within the last two centuries. *PloS one*, 10(6), DOI: 10.1371/journal.pone.0128533.

Ogwang, B.A., Ongoma, V., Xing, L. and Ogou, K.F. 2015. Influence of Mascarene high and Indian Ocean dipole on East African extreme weather events. *Geographica Pannonica*, 19(2): 64-72.

Ogwang, B.A., Ongoma, V., Shilenje, Z.W., Ramotubei, T.S., Letuma, M. and Ngaina, J.N. 2020. Influence of Indian Ocean dipole on rainfall variability and extremes over southern Africa. *Mausam*, 71(4): 637-648.

Okitsu, S. 2005. Factors Controlling Geographical Distribution in Savanna Vegetation in Namibia. *African Study Monographs*, (30): 135-151.

Oliver, G.J.H. and Kinnaird, J.A. 1996. The Rössing-SJ Dome, central zone, Damara Belt, Namibia: an example of mid-crustal extensional ramping. *Communications of the Geological Survey of Namibia*, 11: 53-64

Palakit, K., Siripattanadilok, S. and Duangsathaporn, K. 2012. False ring occurrences and their identification in teak (*Tectona grandis*) in north-eastern Thailand. *Journal of Tropical Forest Science*, 24(3): 387-398.

Pallett, J., Irish, J., Aiyambo, D., Eelu, K., Guittar, J., Henschel, J., Kavari, R., Nghiitombo, V., Shikangala, J. and Siteteka, V. 2008. Rössing Biodiversity Assessment. *Unpublished report by EAAN for Rössing Uranium Ltd*.

Patrut, A., Von Reden, K.F., Lowy, D.A., Alberts, A.H., Pohlman, J.W., Wittmann, R., Gerlach, D., Xu, L. and Mitchell, C.S. 2007. Radiocarbon dating of a very large African baobab. *Tree Physiology*, 27(11): 1569-1574.

Pazdur, A., Nakamura, T., Pawełczyk, S., Pawlyta, J., Piotrowska, N., Rakowski, A., Sensuła, B. and Szczepanek, M. 2007. Carbon isotopes in tree rings: climate and the Suess effect interferences in the last 400 years. *Radiocarbon*, 49(2): 775-788.

Pearl, J.K., Keck, J.R., Tintor, W., Siekacz, L., Herrick, H.M., Meko, M.D. and Pearson, C.L. 2020. New frontiers in tree-ring research. *The Holocene*, 30(6): 923-941.

Persendt, F.C., Gomez, C. and Zawar-Reza, P. 2015. Identifying hydro-meteorological events from precipitation extremes indices and other sources over northern Namibia, Cuvelai Basin. *Jàmbá: Journal of Disaster Risk Studies*, 7(1), DOI: 10.4102/jamba.v7i1.177.

Picas, J., Grab, S. and Allan, R. 2019. A 19th century daily surface pressure series for the Southwestern Cape region of South Africa: 1834–1899. *International Journal of Climatology*, 39(3): 1404-1414.

Pierret, A., Maeght, J.L., Clément, C., Montoroi, J.P., Hartmann, C. and Gonkhamdee, S. 2016. Understanding deep roots and their functions in ecosystems: an advocacy for more unconventional research. *Annals of Botany*, 118(4): 621-635.

Railsback, L.B., Akers, P.D., Wang, L., Holdridge, G.A. and Voarintsoa, N.R. 2013. Layer-bounding surfaces in stalagmites as keys to better paleoclimatological histories and chronologies. *International Journal of Speleology*, 42(3): 167-180.

Rasmussen, S.O., Bigler, M., Blockley, S.P., Blunier, T., Buchardt, S.L., Clausen, H.B., Cvijanovic, I., Dahl-Jensen, D., Johnsen, S.J., Fischer, H. and Gkinis, V. 2014. A stratigraphic framework for abrupt climatic changes during the Last Glacial period based on three synchronized Greenland ice-core records: refining and extending the INTIMATE event stratigraphy. *Quaternary Science Reviews*, 106: 14-28.

Reason, C.J.C. and Rouault, M. 2005. Links between the Antarctic Oscillation and winter rainfall over western South Africa. *Geophysical Research Letters*, 32(7), DOI: 10.1029/2005GL022419.

Reason, C.J.C., Landman, W. and Tennant, W. 2006. Seasonal to decadal prediction of southern African climate and its links with variability of the Atlantic Ocean. *Bulletin of the American Meteorological Society*, 87(7): 941-956.

Reid, H., Sahlén, L., Stage, J., MacGregor J. 2007. *The economic impact of climate change in Namibia: How climate change will affect the contribution of Namibia's*

natural resources to its economy. Environmental Economics Programme Discussion Paper 07-02. International Institute for Environment and Development, London.

Reid, H., Sahlén, L., Stage, J. and MacGregor, J. 2008. Climate change impacts on Namibia's natural resources and economy. *Climate Policy*, *8*(5): 452-466.

Reimer, P. 2022. Evolution of Radiocarbon Calibration. *Radiocarbon,* 64(3): 523-539.

Remane, I.A. and Therrell, M.D. 2015. Dendrochronological potential of *Millettia stuhlmannii* in Mozambique. *Trees*, 29(3): 729-736.

Reynolds-Henne, C.E., Siegwolf, R.T.W., Treydte, K.S., Esper, J., Henne, S. and Saurer, M. 2007. Temporal stability of climate-isotope relationships in tree rings of oak and pine (Ticino, Switzerland). *Global Biogeochemical Cycles*, 21(4), DOI:10.1029/2007GB002945.

Richter, I., Behera, S.K., Masumoto, Y., Taguchi, B., Komori, N. and Yamagata, T. 2010. On the triggering of Benguela Niños: Remote equatorial versus local influences. *Geophysical Research Letters*, 37(20), DOI: 10.1029/2010GL044461.

Robertson, I., Loader, N.J., Froyd, C.A., Zambatis, N., Whyte, I. and Woodborne, S. 2006. The potential of the baobab (*Adansonia digitata L*.) as a proxy climate archive. *Applied Geochemistry*, 21(10): 1674-1680.

Roffe, S.J., Fitchett, J.M. and Curtis, C.J. 2021. Investigating changes in rainfall seasonality across South Africa: 1987–2016. *International Journal of Climatology*, 41, DOI: 10.1002/joc.6830.

Rouault, M., Florenchie, P., Fauchereau, N. and Reason, C.J. 2003. South East tropical Atlantic warm events and southern African rainfall. *Geophysical Research Letters*, 30(5), DOI: 10.1029/2002GL014840.

Rouault, M., Illig, S., Lübbecke, J. and Koungue, R.A.I. 2018. Origin, development and demise of the 2010–2011 Benguela Niño. *Journal of Marine Systems*, 188: 39-48.

Rozendaal, D. and Zuidema, P.A. 2011. Dendroecology in the tropics: a review. *Trees*, 25(1): 3-16.

Saarinen, J., Fitchett, J. and Hoogendoorn, G. 2022. *Climate Change and Tourism in Southern Africa*. Routledge, London.

Santos, G.M., Linares, R., Lisi, C.S. and Tomazello Filho, M. 2015. Annual growth rings in a sample of Paraná pine (*Araucaria angustifolia*): Toward improving the ^{14}C calibration curve for the Southern Hemisphere. *Quaternary Geochronology*, *25*: 96-103.

Saurer, M., Siegenthaler, U. and Schweingruber, F. 1995. The climate-carbon isotope relationship in tree rings and the significance of site conditions. *Tellus B*, 47(3): 320-330

Saurer, M., Siegwolf, R., Borella, S. and Schweingruber, F. 1998. Environmental information from stable isotopes in tree rings of *Fagus sylvatica*. In: *The impacts of climate variability on forests* Springer, Berlin, Heidelberg, pp. 241-253.

Saurer, M., Cherubini, P., Reynolds-Henne, C.E., Treydte, K.S., Anderson, W.T. and Siegwolf, R.T.W. 2008. An investigation of the common signal in tree ring stable isotope chronologies at temperate sites. *Journal of Geophysical Research: Biogeosciences*, 113(G4), DOI: 10.1029/2008JG000689.

Schlüter, T. 2006. Namibia. In: *Geological Atlas of Africa: With Notes on Stratigraphy, Tectonics, Economic Geology, Geohazards and Geosites of Each Country*, Springer, Berlin, Heidelberg, pp. 172-175.

Schoeman, M.H., Aub, B., Burrows, J., Hall, G. and Woodborne, S. 2019. Past Climatic Conditions for Bokoni at Buffelskloof, Mpumalanga, Using $\delta^{13}C$ Analysis of *Prunus africana* and *Pittosporum viridiflorum* Tree Rings. *Journal of African Archaeology*, 17(2): 150-160.

Scott, L. 1996. Palynology of hyrax middens: 2000 years of palaeoenvironmental history in Namibia. *Quaternary International*, 33: 73-79.

Scott, L. and Neumann, F.H. 2018. Pollen-interpreted palaeoenvironments associated with the Middle and Late Pleistocene peopling of Southern Africa. *Quaternary International*, 495: 169-184.

Sealy, J., Naidoo, N., Hare, V.J., Brunton, S. and Faith, J.T. 2020. Climate and ecology of the palaeo-Agulhas Plain from stable carbon and oxygen isotopes in bovid tooth enamel from Nelson Bay Cave, South Africa. *Quaternary Science Reviews*, 235, DOI: 10.1016/j.quascirev.2019.105974.

Shannon, L.V., Boyd, A.J., Brundrit, G.B. and Taunton-Clark, J. 1986. On the existence of an El Niño-type phenomenon in the Benguela system. *Journal of Marine Research*, 44(3): 495-520.

Shanyengana, E.S., Henschel, J.R., Seely, M.K., Sanderson, R.D. 2002. Exploring fog as a supplementary water source in Namibia. *Atmospheric Research,* 64: 251-259.

Sheppard, P.R. 2010. Dendroclimatology: extracting climate from trees. *Wiley Interdisciplinary Reviews: Climate Change*, 1(3): 343-352.

Shestakova, T.A. and Martínez-Sancho, E. 2021. Stories hidden in tree rings: a review on the application of stable carbon isotopes to dendrosciences. *Dendrochronologia*, 65, DOI: 10.1016/j.dendro.2020.125789.

Sheu, D.D., Kou, P., Chiu, C.H. and Chen, M.J. 1996. Variability of tree-ring δ13C in Taiwan fir: growth effect and response to May–October temperatures. *Geochimica et Cosmochimica Acta*, 60(1): 171-177.

Shikangalah, R.N. 2020. The 2019 drought in Namibia: an overview. *Journal of Namibian Studies*, 27: 37-58.

Shikangalah, R.N. and Mapani, B. 2019. Precipitation variations and shifts over time: Implication on Windhoek city water supply. *Physics and Chemistry of the Earth, Parts A/B/C*, 112: 103-112.

Shikangalah, R.N., Mapani, B., Mapaure, I., Herzschuh, U., Musimba, A. and Tabares, X. 2020. Growth ring formation of *Dichrostachys cinerea* and *Senegalia mellifera* in arid environments in Namibia. *Dendrochronologia*, 59, DOI: 10.1016/j.dendro.2019.125661.

Skomarkova, M.V., Vaganov, E.A., Mund, M., Knohl, A., Linke, P., Boerner, A. and Schulze, E.D. 2006. Inter-annual and seasonal variability of radial growth, wood density and carbon isotope ratios in tree rings of beech (*Fagus sylvatica*) growing in Germany and Italy. *Trees*, 20(5): 571-586.

Sletten, H.R., Railsback, L.B., Liang, F., Brook, G.A., Marais, E., Hardt, B.F., Cheng, H. and Edwards, R.L. 2013. A petrographic and geochemical record of climate change over the last 4600 years from a northern Namibia stalagmite, with

evidence of abruptly wetter climate at the beginning of southern Africa's Iron Age. *Palaeogeography, Palaeoclimatology, Palaeoecology*, 376: 149-162.

Soderberg, K.S. 2010. *The role of fog in the ecohydrology and biogeochemistry of the Namib Desert*. Doctoral thesis submitted to the University of Virginia, Virginia.

Sousa, P.M., Blamey, R.C., Reason, C.J., Ramos, A.M. and Trigo, R.M. 2018. The 'Day Zero' Cape Town drought and the poleward migration of moisture corridors. *Environmental Research Letters*, 13(12), DOI: 10.1088/1748-9326/aaebc7.

Spear, D., Zaroug, M.A., Daron, J.D., Ziervogel, G., Angula, M.N., Haimbili, E.N., Hegga, S.S., Baudoin, M., New, M., Kunamwene, I. and Togarepi, C. 2018. *Vulnerability and responses to climate change in drylands: The case of Namibia. CARIAA-ASSAR Working Paper*. University of Cape Town, Cape Town, South Africa. Available online at: www.assar.uct.ac.za.

Speer, J.H. 2010. *Fundamentals of tree-ring research*. The University of Arizona Press, Tuscan, pp. 30-31.

Spurk, M., Leuschner, H.H., Baillie, M.G., Briffa, K.R. and Friedrich, M. 2002. Depositional frequency of German subfossil oaks: climatically and non-climatically induced fluctuations in the Holocene. *The Holocene*, 12(6): 707-715.

St George, S. 2014. An overview of tree-ring records across the northern hemisphere. *Quaternary Science Reviews,* 95: 132-150.

Stager, J.C., Mayewski, P.A., White, J., Chase, B.M., Neumann, F.H., Meadows, M.E., King, C.D. and Dixon, D.A. 2012. Precipitation variability in the winter rainfall zone of South Africa during the last 1400 yr linked to the austral westerlies. *Climate of the Past*, 8(3): 877-887.

Stager, J.C., Ryves, D.B., King, C., Madson, J., Hazzard, M., Neumann, F.H. and Maud, R. 2013. Late Holocene precipitation variability in the summer rainfall region of South Africa. *Quaternary Science Reviews*, 67: 105-120.

Stengel, H.W., 1964. Die Riviere der Namib und ihr Zulauf zum Atlantik. I. Teil: Kuiseb und Swakop. *Scientific Papers of the Namib Desert Research Station*, 22: 1-50.

Sundqvist, H.S., Holmgren, K., Fohlmeister, J., Zhang, Q., Matthews, M.B., Spötl, C. and Körnich, H. 2013. Evidence of a large cooling between 1690 and 1740 AD in southern Africa. *Scientific Reports*, 3(1), DOI: 10.1038/srep01767.

Svarva, H.L., Thun, T., Kirchhefer, A.J. and Nesje, A. 2018. Little Ice Age summer temperatures in western Norway from a 700-year tree-ring chronology. *The Holocene*, 28(10): 1609-1622.

Talma, A.S. and Vogel, J.C. 1992. Late Quaternary paleotemperatures derived from a speleothem from Cango caves, Cape province, South Africa. *Quaternary Research*, 37(2): 203-213.

Taylor, K.E., Stouffer, R.J. and Meehl, G.A. 2012. An overview of CMIP5 and the experiment design. *Bulletin of the American Meteorological Society*, 93(4): 485-498.

Therrell, M.D., Stahle, D.W., Ries, L.P. and Shugart, H.H. 2006. Tree-ring reconstructed rainfall variability in Zimbabwe. *Climate Dynamics*, 26(7-8): 677.

Therrell, M.D., Stahle, D.W., Mukelabai, M.M. and Shugart, H.H. 2007. Age, and radial growth dynamics of *Pterocarpus angolensis* in southern Africa. *Forest Ecology and Management*, 244(1-3): 24-31.

Thuiller, W., Midgley, G.F., Hughes, G.O., Bomhard, B., Drew, G., Rutherford, M.C. and Woodward, F.I. 2006. Endemic species and ecosystem sensitivity to climate change in Namibia. *Global Change Biology*, 12(5): 759-776.

Touchan, R., Garfin, G.M., Meko, D.M., Funkhouser, G., Erkan, N., Hughes, M.K. and Wallin, B.S. 2003. Preliminary reconstructions of spring precipitation in southwestern Turkey from tree-ring width. *International Journal of Climatology: A Journal of the Royal Meteorological Society*, 23(2):157-171.

Trouet, V. 2004. *The El Niño Southern Oscillation effect on Zambezian miombo vegetation: proxies from tree ring series and satellite-derived data*. Doctoral thesis submitted to Katholieke Universiteit Leuven, Belgium.

Trouet, V. Haneca, K., Coppin, P. and Beeckman, H. 2001. Tree ring analysis of *Brachystegia spiciformis* and *Isoberlinia tomentosa*: evaluation of the ENSO-signal in the miombo woodland of eastern Africa. *IAWA Journal*, 22(4): 385-399.

Trouet, V. Coppin, P. and Beeckman, H. 2006. Annual growth ring patterns in *Brachystegia spiciformis* reveal influence of precipitation on tree growth 1. Biotropica: *The Journal of Biology and Conservation*, 38(3): 375-382.

Trouet, V. Esper, J. and Beeckman, H. 2010. Climate/growth relationships of *Brachystegia spiciformis* from the miombo woodland in south central Africa. *Dendrochronologia*, *28*(3): 161-171.

Tyson, P.D. and Preston-Whyte, R.A. 2000. *Weather and climate of southern Africa*. Oxford University Press, Cape Town.

Tyson, P.D., Karlen, W., Holmgren, K. and Heiss, G.A., 2000. The Little Ice Age and medieval warming in South Africa. *South African Journal of Science*, 96(3): 121-126.

Tyson, P.D., Cooper, G.R.J. and McCarthy, T.S. 2002. Millennial to multi-decadal variability in the climate of southern Africa. *International Journal of Climatology: A Journal of the Royal Meteorological Society*, *22*(9): 1105-1117.

Urrego, D.H., Sánchez Goñi, M.F., Daniau, A.L., Lechevrel, S. and Hanquiez, V. 2015. Increased aridity in southwestern Africa during the warmest periods of the last interglacial. *Climate of the Past*, 11(10): 1417-1431.

Usman, M.T. and Reason, C.J.C. 2004. Dry spell frequencies and their variability over southern Africa. *Climate Research*, 26(3): 199-211.

van der Sleen, P., Zuidema, P.A. and Pons, T.L. 2017. Stable isotopes in tropical tree rings: theory, methods and applications. *Functional Ecology*, 31(9): 1674-1689.

Van Holsbeeck, S., De Cauwer, V., De Ridder, M., Fichtler, E., Beeckman, H. and Mertens, J. 2016. Annual diameter growth of *Pterocarpus angolensis* (Kiaat) and other woodland species in Namibia. *Forest Ecology and Management*, 373, DOI: 10.1016/j.foreco.2016.04.031.

Van Rensburg, P.; Tortajada, C. 2021. An Assessment of the 2015–2017 Drought in Windhoek. *Frontiers in Climate*., 3, DOI: 10.3389/fclim.2021.602962.

Villalba R. 2000. Dendroclimatology: a southern hemisphere perspective. In: Smolka PP, Volkheimer W (eds) *Southern hemisphere paleo- and neoclimates*. Springer, Berlin, Germany, pp. 27–57.

Voarintsoa, N.R.G., Brook, G.A., Liang, F., Marais, E., Hardt, B., Cheng, H., Edwards, R.L. and Railsback, L.B. 2017. Stalagmite multi-proxy evidence of wet and dry intervals in northeastern Namibia: Linkage to latitudinal shifts of the Inter-Tropical Convergence Zone and changing solar activity from AD 1400 to 1950. *The Holocene*, 27(3): 384-396.

Vogel, C.H. 1989. A documentary-derived climatic chronology for South Africa, 1820–1900. *Climatic Change*, *14*(3): 291-307.

Vogel, J.C., Fuls, A. and Visser, E. 2001. Radiocarbon adjustments to the dendrochronology of a yellowwood tree. *South African Journal of Science*, 97(3-4): 164-166.

Völkel, J., Bens, O., Eden, M., Krauß, L., Murray, A.S. and Heine, K. 2021. Fluvial sediments and playa deposits of the Naukluft Mts. foreland and Tsauchab Valley, Namibia–New insights from key sections in the Late Quaternary landscape and climate change in Southern Africa. *Zeitschrift für Geomorphologie*, 62(4): 313-350.

Wang, L., Kaseke, K.F. and Seely, M.K. 2017. Effects of non-rainfall water inputs on ecosystem functions. *Wiley Interdisciplinary Reviews: Water*, 4(1), DOI: 10.1002/wat2.1179.

Wang, L., Kaseke, K.F., Ravi, S., Jiao, W., Mushi, R., Shuuya, T. and Maggs-Kölling, G. 2019. Convergent vegetation fog and dew water use in the Namib Desert. *Ecohydrology*, 12(7), DOI: 10.1002/eco.2130.

Wassenaar, T.D., Henschel, J.R., Pfaffenthaler, M.M., Mutota, E.N., Seely, M.K. and Pallett, J. 2013. Ensuring the future of the Namib's biodiversity: Ecological restoration as a key management response to a mining boom. *Journal of Arid Environments*, 93: 126-135.

Waterhouse, J.S., Barker, A.C., Carter, A.H.C., Agafonov, L.I. and Loader, N.J. 2000. Stable carbon isotopes in Scots pine tree rings preserve a record of flow of the river Ob. *Geophysical Research Letters*, 27(21): 3529-3532.

Wils, T.H., Robertson, I., Eshetu, Z., Koprowski, M., Sass-Klaassen, U.G., Touchan, R. and Loader, N.J. 2010. Towards a reconstruction of Blue Nile baseflow from Ethiopian tree rings. *The Holocene*, 20(6): 837-848.

Woodborne, S. 2004. A water stress history of an *Acacia erioloba* (Kameeldoring) tree from the Koichab. CSIR Environmentek, Pretoria.

Woodborne, S., Hall, G., Robertson, I., Patrut, A., Rouault, M., Loader, N.J. and Hofmeyr, M. 2015. A 1000-year carbon isotope rainfall proxy record from South African baobab trees (*Adansonia digitata L.*). *PLoS One*, 10(5): DOI: 10.1371/journal.pone.0124202.

Woodborne, S., Gandiwa, P., Hall, G., Patrut, A. and Finch, J. 2016. A regional stable carbon isotope dendro-climatology from the south African summer rainfall area. *PLoS one*, 11(7): DOI: 10.1371/journal.pone.0159361.

Woodborne, S., Hall, G., Jones, C.W., Loader, N.J., Patrut, A., Patrut, R.T., Robertson, I., Winkler, S.R., Winterbach, C.W. 2018. A 250-year isotopic proxy rainfall record from southern Botswana. *Studia Universitatis Babes-Bolyai Chemia*. 63, DOI: 10.24193/subbchem.2018.1.09.

Worbes, M. 1999. Annual growth rings, rainfall-dependent growth and long-term growth patterns of tropical trees from the Caparo Forest Reserve in Venezuela. *Journal of Ecology*, 87(3): 391-403.

Worbes, M. 2002. One hundred years of tree-ring research in the tropics–a brief history and an outlook to future challenges. *Dendrochronologia*, 20(1-2): 217-231.

Worbes M. 2010. Wood Anatomy and Tree-Ring Structure and Their Importance for Tropical Dendrochronology. In: Junk ,W., Piedade, M., Wittmann, F., Schöngart J., Parolin, P. (eds) *Amazonian Floodplain Forests. Ecological Studies (Analysis*

and Synthesis), vol 210. Springer, Dordrecht. DOI: 10.1007/978-90-481-8725-6_17.

Young, G.H., McCarroll, D., Loader, N.J. and Kirchhefer, A.J. 2010. A 500-year record of summer near-ground solar radiation from tree-ring stable carbon isotopes. *The Holocene*, 20(3): 315-324.

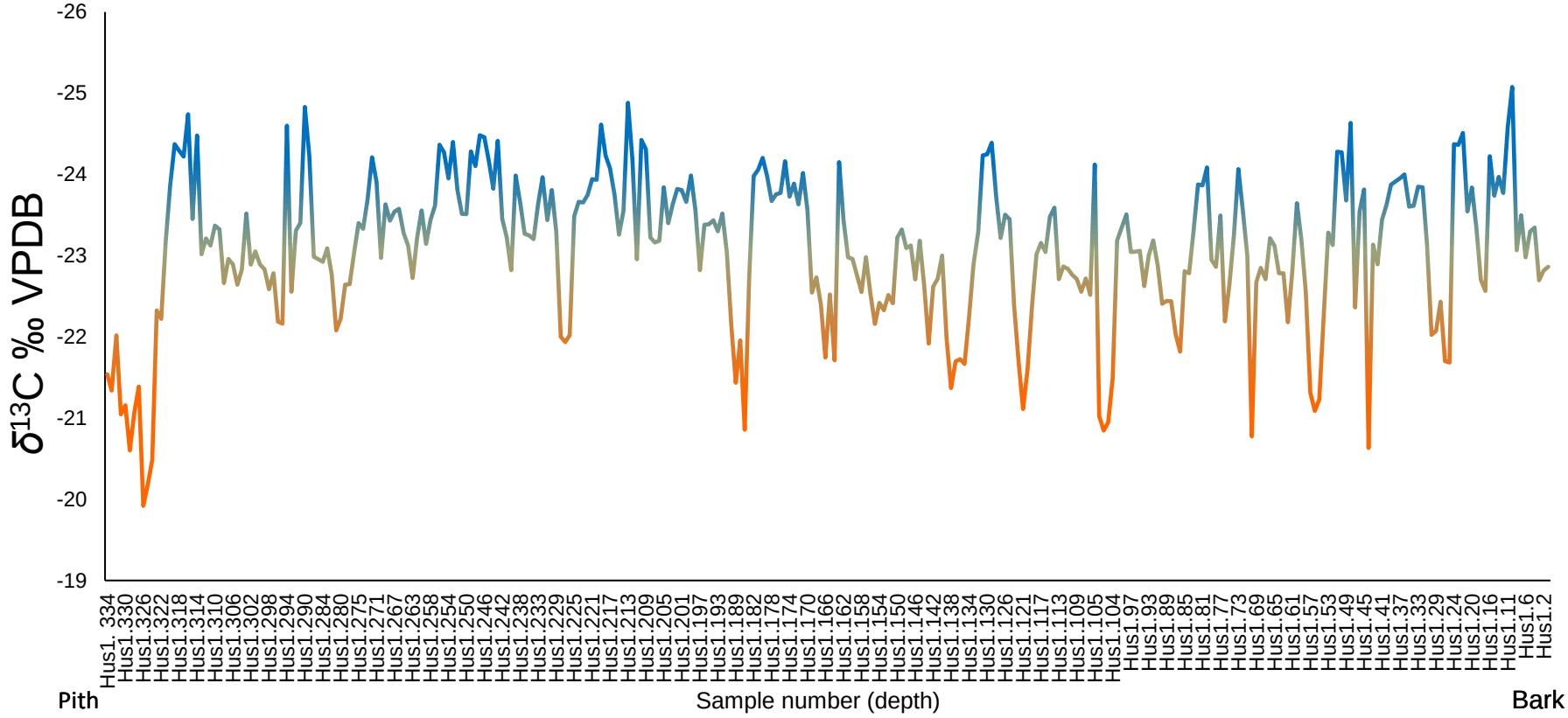
Zhao, S., Pederson, N., D'Orangeville, L., HilleRisLambers, J., Boose, E., Penone, C., Bauer, B., Jiang, Y. and Manzanedo, R.D. 2019. The International Tree-Ring Data Bank (ITRDB) revisited: data availability and global ecological representativity. *Journal of Biogeography*, 46(2): 355-368.

Zhu, B., Wang, X., Yu, J., Rioual, P., Zhang, Y. and Wang, P. 2016. Late quaternary environmental change in the Namibia of southern Africa. In: Sherman, W., (ed), *Handbook on Africa: challenges and issues of the 21st century*, Nova Science Publishers, New York, pp.119-147.

APPENDICES

Includes: Husab-1 and Husab-2 plotted against sample number, indicating wetter (blue) and drier (orange) isotope values.

8 APPENDIX 1: HUSAB-1 ISOTOPE DATA



9 APPENDIX 2: HUSAB-2 ISOTOPE DATA

